UNDERSTANDING AND QUANTIFYING CHANNEL TRANSMISSION LOSS PROCESSES IN THE LIMPOPO RIVER BASIN

A thesis submitted in fulfilment of the requirements for the degree of

MASTER OF SCIENCE

in the

FACULTY OF SCIENCE

of

RHODES UNIVERSITY

Grahamstown

South Africa

by

Vuyelwa MVANDABA

MARCH 2018

UNDERSTANDING AND QUANTIFYING CHANNEL TRANSMISSION LOSS PROCESSES IN THE LIMPOPO RIVER BASIN

by

Vuyelwa MVANDABA

SUPERVISOR

PROF D.A. HUGHES — INSTITUTE FOR WATER RESEARCH, RHODES UNIVERSITY

CO-SUPERVISORS

DR E. KAPANGAZIWIRI — COUNCIL FOR SCIENTIFIC AND INDUSTRIAL RESEARCH

DR J. MWENGE KAHINDA — COUNCIL FOR SCIENTIFIC AND INDUSTRIAL RESEARCH

DEGREE: Master of Science (HYDROLOGY)

ABSTRACT

Water availability is one of the major societal issues facing the world. The ability to understand and quantify the impact of key hydrological processes on the availability of water resources is therefore integral to ensuring equitable and sustainable resource management. A review of previous hydrological studies conducted in the Limpopo River Basin has revealed a gap in the understanding of surface water-groundwater interactions, particularly channel transmission loss processes. These earlier studies, focused largely on the Limpopo River's main stem, have attributed the existence of these streamflow losses to the presence of significant alluvial aquifers and indicated that the losses account for about 30 percent (or 1000 Mm^3 a^{-1}) of the basin's water balance.

The work conducted in this dissertation reports on the delineation of alluvial aquifers across three sub-basins of the Limpopo River Basin namely, the Mokolo (South Africa), Motloutse (Botswana) and Mzingwane (Zimbabwe) sub-basins and the estimation of potential channel transmission losses based on the alluvial aquifer properties. Additionally, an assessment of the different approaches that can be applied to simulate these channel transmission losses in the Pitman Model is presented. To delineate alluvial aquifers, general land cover classes including alluvial aquifers were produced from Landsat-8 imagery through image classification. The areal extent of the delineated alluvial aquifers was calculated using ArcMap 10.3. To quantify channel transmission losses and determine the effects on regional water resources, three approaches using the Pitman model were applied. The three approaches include an explicit transmission loss function, the use of a wetland function to represent channel-floodplain storage exchanges and the use of a 'dummy' reservoir to represent floodplain storage and evapotranspiration losses.

Results indicate that all three approaches were able to simulate channel transmission losses, although with differing magnitudes. Observed monthly flow data were used to

as a means of validating loss simulations however for each sub-basin, medium and low flows were over-simulated which accounts for water uses that were inefficiently represented due to lack of data. Knowledge of the structure of the transmission loss function dictates that it is better at representing the dynamics of channel transmission losses, as it takes into account the contribution of losses to groundwater recharge whereas the other two functions simply store water and release it back to the channel. Overall, the hydrological modelling results demonstrate the potential of each approach in reproducing the dynamics of channel transmission losses between channel and alluvial aquifer within an existing sub-basin scale hydrological model. It is believed that better quantification of losses and more efficient qualitative determination of the function which best represents transmission losses, can be attained with more reliable observed data.

In conclusion, a study of this nature can be beneficial to water resource estimation programmes as it highlights the uncertainties related with quantifying channel transmission loss processes in a semi-arid environment.

KEYWORDS: Alluvial aquifers; Channel transmission losses; Hydrological modelling; Landsat-8; Limpopo River Basin; Pitman Model

Declaration

I declare that the dissertation entitled ***Understanding and Quantifying Channel Transmission Loss Processes in the Limpopo River Basin*** which I hereby submit for the degree of MSc (Hydrology) at Rhodes University, is my own work. I also declare that this dissertation has not previously been submitted by me for a degree at this or any other tertiary institution and that all the sources that I have used or quoted have been indicated and acknowledged by means of complete references.

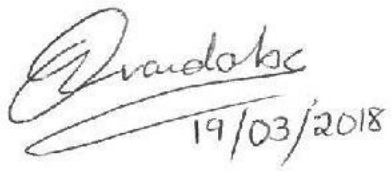

Vuyelwa MVANDABA

Acknowledgements

To my supervisor, Professor Denis Hughes and co-supervisors Drs. Evison Kapangaziwiri and Jean-Marc Mwenge Kahinda: I would like to thank you for your guidance and consistently clear and strategic advice. I value your critique and most importantly, your patience!

To my sponsors, the Council for Scientific and Industrial Research (CSIR) and Water Research Commission (WRC) in South Africa: I have benefitted immensely from being involved in the project and hope to continue contributing to this field of work. Thank you for sponsoring my MSc journey.

To my colleagues at the CSIR, Nadia Oosthuizen, Nompumelelo Mandlazi, Shirley Malema, Sabelo Madonsela: I am grateful for your moral support, assistance and friendship.

To my parents, Lineo Molingoana and Ramatedile Motseko, my grandmother Matshiliso Moji, my partner, Siviwe Vutha and my friends: Thank you for the encouragement that you have given me over the years and for understanding when I had to work over weekends!

To God: thank you for carrying me through this journey!

Table of Contents

List of Figures

List of Tables

GLOSSARY OF TERMS

Term	*Definition*
CSIR	Council for Industrial and Scientific Research
LRBMS	Limpopo River Basin Monograph Study
$Mm^3\ a^{-1}$	Million cubic metres per annum
SPATSIM	SPAtial and Time Series Information Modelling
WRC	Water Research Commission
WRSM2000	Water Resources Simulation Model 2000

CHAPTER 1
Introduction and study overview

1.1 INTRODUCTION AND BACKGROUND

Water sustains life on Earth. It is essential, not only for human and animal life, but also for the wellbeing of the natural environment. Water availability is also an integral component for sustainable growth across the world's various economies as it supports the sectors of agriculture, mining and industry (GWP, 2009; UN, 2015). In African countries, water resources are of strategic importance in achieving long-term food security and poverty eradication (SADC, 2005; UN, 2015). The quantity and quality of the world's freshwater resources are however affected by the accelerated economic and human population growth, which have seen increased water demands usually at the expense of the natural environment (GWP, 2014). Global challenges such as climate change have called for urgency in developing and establishing water conservation and management strategies to secure current and future resource availability (UN, 2015). Despite the awareness that has been raised regarding the need to use water more efficiently (GWP, 2014) and the research that has gone into 'best-practice' management of water resources (GWP, 2009), significant knowledge gaps still exist regarding the measurement and understanding of processes which affect water availability, especially in data and finance constrained regions (Hughes, 2008a). The effect of these knowledge gaps results in the substantial uncertainty regarding water resource estimates which consequently hampers progress in efficient and sustainable water resource management.

This study contributes to a project titled, *'Upstream-Downstream Hydrological Linkages in the Limpopo River Basin'* which is co-funded by the Water Research Commission (Project K5/2439/1) and the Council for Scientific and Industrial Research (Project ECHS056). The work is currently being undertaken by the Council for Scientific and Industrial Research (CSIR) in collaboration with the Institute for Water Research (IWR), Rhodes University. The project intends to contribute to the improvement of water resource management in the transboundary Limpopo River Basin by establishing, understanding and quantifying upstream-downstream hydrological linkages that impact on the availability and distribution of water in the basin. Upstream-downstream hydrological linkages consider the relationship between hydrological processes that occur in the upper regions (close to headwaters) of a river basin and the impact of such processes on water resources found along the profile of the river basin towards the lower regions (floodplain) of the basin (Nepal, 2012; Nepal *et al.* 2014). Factors which influence the type of hydrological linkages present in any river basin include environmental, socio-economic, institutional and cultural features that determine the generation, allocation and use of water resources in a basin (Nepal *et al.*, 2014). It is anticipated that the understanding of hydrological linkages in the river basin will provide valuable information on the estimation of water resources, which is essential for equitable sharing, planning for current and future socio-economic growth and maintaining ecological integrity of the basin for sustainable development. As the Limpopo River is a transboundary basin, a better understanding of the hydrological linkages in the basin is also expected to facilitate co-operation, common understanding and governance between the multiple stakeholders of the basins water resources.

The contribution of this study, to the overall project described above, is on understanding and quantification of the dynamics of channel transmission loss processes in the Limpopo River Basin. To provide context to the aim and specific objectives of the study, the introduction provides an overview of water resource management in the Limpopo River basin and reviews the understanding of key

hydrological processes in arid/semi-arid environments including a descriptive look at channel transmission loss processes.

1.1.1 Water resource management in the Limpopo River Basin

The Limpopo River Basin (Figure 1.1) is transboundary, shared by Botswana, Zimbabwe, South Africa and Mozambique. The basin extends across varying climatic and topographic zones, therefore basin characteristics are diverse and water resource availability and use differ substantially along the river from its source in South Africa to its mouth at the entrance to the Indian Ocean (LBPTC, 2010; Mohamed, 2014). Both surface and groundwater resources of the basin support a thriving population of approximately 18 million (Dlamini, 2014) and a developing economy within the sectors of agriculture, mining and industry (DWA, 2009; Dlamini, 2014; Mwenge Kahinda *et al.*, 2012; UN, 2015), making the basin one of Africa's most densely populated and urbanised river basins (Wirkus and Böge, 2006). Besides South Africa's Orange River, the Limpopo River is regarded as southern Africa's most important river in economic terms (Wirkus and Böge, 2006). Cities such as Gaborone (Botswana), Bulawayo (Zimbabwe), Pretoria and the northern portion of Johannesburg (South Africa) are the major urban water users (domestic and industrial) within the Limpopo River Basin. Rural communities, which make up 40 percent of the basin, depend largely on groundwater resources for domestic uses and subsistence farming (Busari, 2008).

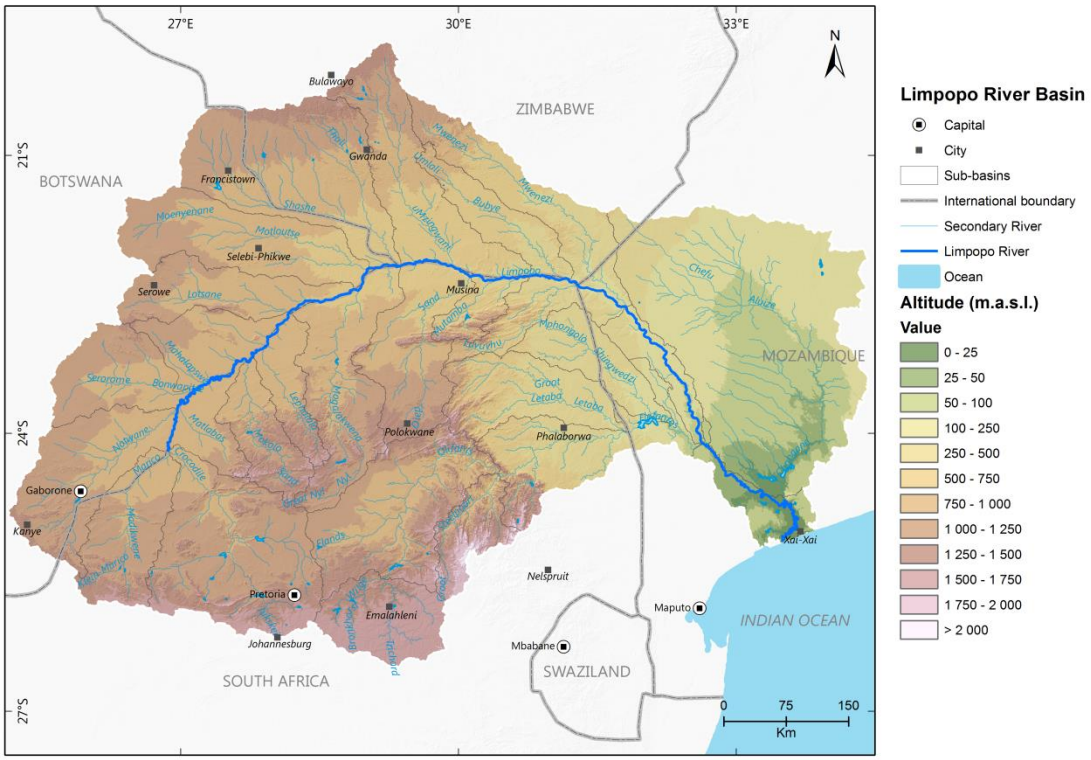

Figure 1.1. The Limpopo River Basin with the four riparian countries and the 27 delineated catchments.

Multiple studies (Görgens *et al.*, 1991; JULBS, 1991; Görgens and Boroto, 1997; LIMCOM, 2013) have been conducted in the basin in an effort to strengthen water resource management by advancing knowledge on the state of its water resources. A significant percentage of the research conducted has been documented as grey literature in the form of governmental reports on local water resource studies and peer-reviewed papers produced from projects led by multi-national socio-environmental organisations. A collection of major basin-wide studies conducted in the Limpopo over the last 25 years is indicated in Table 1.1. The majority of the basin-wide water resource management studies conducted in the Limpopo River Basin have focused mainly on highlighting issues concerning water availability and the associated socioeconomic and environmental implications (Goulden *et al.*, 2009; Zhu and Ringler, 2010; Dlamini, 2014). These studies have been carried out at different spatial and temporal scales and cover both surface and groundwater resources in the assessment

of water availability, however greater emphasis has been placed on the status of surface water resources across the transboundary basin (Goulden *et al.*, 2009). There has been limited hydrological modelling because of the general lack of hydrological data in the region (Hughes, 2004). There is therefore a need to advance understanding of the various hydrological processes in the basin that influence water resource availability.

Table 1.1. Several major hydrological studies in the Limpopo River Basin over the past 25 years.

Focus of study	**Main aspects discussed**	**Authors/Institution**
Hydrology	Surface water resources	Görgens *et al.* 1999; FAO, 2004; Alemaw *et al.* 2008; LBPTC, 2010; LIMCOM, 2013
	Hydrological monitoring systems	Görgens and Boroto, 1997; WMO, 2012;
	Wetlands	Kulawardhana *et al.*, 2007
Hydrogeology	Geology	Ferro *et al.* 1987; CSIR, 2003; FAO, 2004; Owen and Madari, 2009; Chinoda *et al.* 2009
	Groundwater resources assessment	Ferro *et al.* 1987; CSIR, 2003; FAO, 2004; Owen and Madari, 2009; LBPTC, 2010; LIMCOM, 2013;
	Hydrogeological mapping	Ferro *et al.* 1987; SADC Water Division, 2010
Climate change	Impacts on water resources	Zhu and Ringler, 2010; LIMCOM, 2013
	Drought mitigation	CSIR, 2003; FAO, 2004
	Flood forecasting	WMO, 2012
Water use, development and availability	Water use and availability	JULBS, 1991; DWA (Botswana), 1997, 2006; Boroto, 2001; Alemaw *et al.*, 2008; LBPTC, 2010; LIMCOM, 2013
	Integrated water resource management	Boroto, 2001; LBPTC, 2010
	Socioeconomic and environmental conditions	SARDC-ZERO, 2002; FAO, 2004; LBPTC, 2010; LIMCOM, 2013
Hydrological Modelling	Data Availability	LBPTC, 2010; LIMCOM, 2013
	Transmission Losses	Boroto and Görgens, 2003; LIMCOM, 2013
	Hydrological modelling	Görgens *et al.* 1991; Görgens and Boroto, 1997; Görgens *et al.* 1999; Boroto and Görgens, 2003; LIMCOM, 2013
	Water Balance	Görgens and Boroto, 1997; LIMCOM, 2013

1.1.2 Understanding hydrological processes in arid/semi-arid environments of southern Africa

Hydrological processes represent unique 'flow path mechanisms' (Lorentz *et al.*, 2004) or 'fluxes' which describe the movement of water within the hydrological cycle (Mul, 2009). The processes are a function of the characteristics of given study area including climate, topography, geology, soil cover, vegetation, anthropogenic activity, amongst others, (Riddell *et al.*, 2014) and represent the interaction between these factors in the generation and movement of water (Winker *et al.*, 2010). Therefore, identifying the key hydrological processes and their dynamics is essential for successful simulation that generates information/data for sustainable water resource management (Hughes, 2004; Lorentz *et al.* 2007 and Mul, 2009).

Several challenges limit the understanding and modelling of hydrological processes in the arid and semi-arid regions of southern Africa. These are mainly associated with the varied climatic characteristics, poor data availability, financial and technical capacity (Hughes, 2008a). Arid and semi-arid regions in southern Africa are characterised by temporally and spatially varied rainfall events that affect the magnitude and frequency of streamflow (Simmers, 2005, Hughes, 2008a) which consequently increases the complexity of hydrological modelling. Given the reliance of rural communities on groundwater for domestic use (Busari, 2008), there is a need to understand surface water-groundwater interactions and the processes which determine groundwater availability. However, as a result of the limited availability of structural geological information, such knowledge is confined to a few isolated studies (Tanner and Hughes, 2015). In addition, the limited understanding of regional groundwater processes such as discharge and recharge and surface water-groundwater interactions has affected the understanding of processes such as channel transmission loss (Hughes, 2004; Tanner and Hughes, 2015) which is evidenced by the limited number of direct studies of channel transmission loss processes in the region (Hughes, 2008a). Besides climatic factors and regional geology, variations in runoff responses in a catchment are also linked to land use patterns (Schulze, 2000; Mul, 2009) such as farm dams storing

tributary flow contributions and worsening the natural spatial and temporal discontinuity of channel flow (Hughes, 2005). Information/data on these changes as well as variations in spatial and temporal utilisation of water resources is lacking (Hughes, 2008a).

Despite the limitations discussed above, hydrological simulations have been undertaken using the Pitman model (e.g. Görgens *et al.*, 1991; Mostert *et al.*, 1993; Görgens and Boroto, 1997; Hughes and Metzler, 1998; Boroto and Görgens, 2003; Hughes *et al.* 2006) with the intention of advancing knowledge of processes operating in the basin and estimating the water resources of the basin; Chapter 5 provides a more in-depth look at the Pitman Model and the modelling approaches used to simulate channel transmission losses. Other models (e.g. SHELL (Berg *et al.* (1991); WRSM2000 (Bailey, 2008)) that have been applied in the Limpopo River Basin are indicated in Section 2.2.4.3.

1.1.3 Channel transmission losses

Channel transmission losses describe surface and groundwater interactions where streamflow is reduced by infiltration through the river bed, seepage into channel banks and flood plains (Walters, 1990). They can occur in streams that are hydraulically connected or disconnected with a groundwater system (Costa *et al.*, 2012). Losing (or influent) streams only recharge groundwater, while gaining (or effluent) streams discharge groundwater (Ivkovic, 2009) (Figure 1.2).

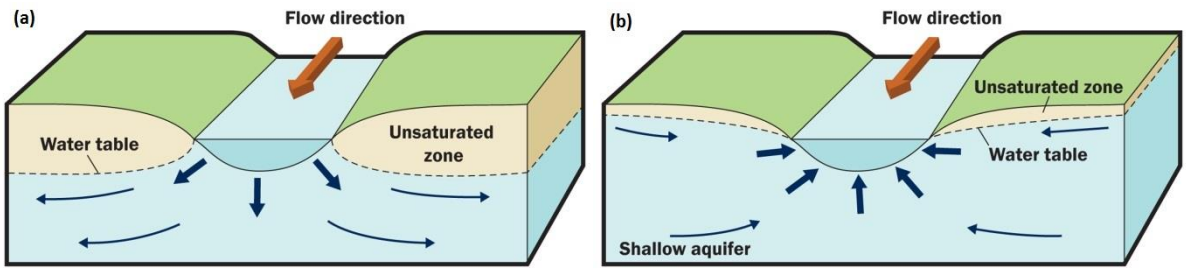

Figure 1.2. Different types of streamflow conditions. (a) When the water level in a stream, lake or wetland is higher than the groundwater level, it can lose water to the aquifer. (b) When stream flows are low and the groundwater level is higher than

the stream water level, groundwater can discharge into the stream (Spatial Vision Innovations, 2015).

Channel transmission losses along the Limpopo River represent about 30 percent (1000 Mm^3 a^{-1}) of the water balance in the system (Boroto and Görgens, 2003; Dlamini, 2014). Factors that contribute to these streamflow losses in the Limpopo River Basin include (Smakhtin and Watkins, 1997; Boroto and Görgens, 2003):

- Infiltration and extraction from bank storage,
- Recharge of storage in alluvial channel beds,
- Evaporation and evapotranspiration from the recharged beds and banks, and
- Direct evaporation from the free water surface.

Boroto and Görgens (2003), CSIR (2003) and Owen and Madari (2009) highlight that alluvial aquifers play an important role in the dynamics of transmission losses and the hydrology of the basin. The geomorphology of the Limpopo River is characterised by 100 m to 500 m wide alluvial deposits, ranging in thickness between 5 m and 10 m as well as rocky outcrops and floodplains in the upper and middle reaches and extensive floodplains further downstream (Boroto and Görgens, 2003). The aquifers comprise mainly of unconsolidated sequences of clay, sand and gravel beds (CSIR, 2003) and are sources of groundwater abstraction for multiple communities as a result of their high permeabilities (Owen and Madari, 2009) and good water quality (CSIR, 2003). Water withdrawals from alluvial aquifers are a key contributor to the direct/indirect channel transmission losses of the Limpopo River (Mwenge Kahinda *et al.*, 2012). Ultimately, channel transmission losses affect the availability of water in the river channel, hence it is imperative to understand their role in the system. To fully understand the hydrological and water resource dynamics in a drainage system, there is a need to determine the presence and distribution of these alluvial aquifers. A conceptual

understanding of the processes and the hydraulic properties of these aquifers is therefore mandatory.

1.2 PROBLEM STATEMENT AND RESEARCH JUSTIFICATION

The hydrological cycle is a broad and multifaceted system. Hydrological modelling is required to conceptualise the various components which contribute to the presence and distribution of water sources in any particular region (Xu, 2002). Although hydrological modelling has made significant strides in the understanding of hydrological processes, several other rainfall-runoff processes including channel transmission losses are relatively under-researched and therefore not well understood, which has made it challenging for such processes to be properly represented in modelling schemes (Hughes, 2004). In the Limpopo River Basin, few channel transmission loss studies have been conducted (e.g. Görgens *et al.*, 1991; Smakhtin and Watkins, 1997; Boroto and Görgens, 2003) and those available are largely based on the main stem. Consequently, there is a lack of knowledge regarding transmission loss processes in the catchments of the Limpopo River Basin beyond the main stem.

The challenges described therefore substantiate the need to conduct a study of this nature. In a region like the Limpopo River Basin where water security is threatened, it is critical to extend the knowledge on the hydrological processes which affect water availability and assess the applicability of popular simulation models in these regions, such as the Pitman Model, in representing all identified/relevant processes like channel transmission losses.

1.3 STUDY AIM AND OBJECTIVES

The main aim of this study is to understand and quantify channel transmission losses in the Limpopo River Basin. The study intends to conceptualise the dynamics of transmission losses, represent them in the Pitman model and assess their impact on

the hydrology and water resources of the Limpopo River Basin. The specific objectives therefore are:

1. To identify reaches within the Limpopo River Basin system where channel transmission losses are expected to play a major role;
2. To develop a conceptual understanding of the likely processes and dynamics of transmission losses in the basin; and
3. To assess the suitability of existing channel transmission loss modelling approaches.

The research questions developed from this set of objectives are as follows:

- *Which regions in the Limpopo River Basin indicate prevalence for channel transmission losses?*

  The occurrence of channel transmission losses in the Limpopo River Basin has been linked to the presence of notable alluvial aquifers along some of the channel reaches (e.g. Boroto and Görgens, 2003; Moyce *et al.*, 2006). Identifying these reaches, determining the extent of the alluvial aquifers and the aquifer characteristics which facilitate the occurrence of channel transmission losses is therefore essential for conceptualising and quantifying the loss processes.

- *Which processes characterise the channel transmission losses observed in the Limpopo River Basin?*

  Identifying the main processes (e.g. evaporation, evapotranspiration, groundwater recharge) that characterise channel transmission losses in the Limpopo River Basin is crucial for developing a conceptual understanding of the dynamics which influence streamflow losses. This understanding substantiates the interpretation of modelling results leading to informed quantification which, in turn, improves resource management.

- *How can channel transmission losses in the Limpopo River Basin be quantified?*

A review of 'best practices' (e.g. streamflow routing, use of hydrological budget, loss simulation using mathematical equations) applied in channel transmission loss quantification is critical to inform the loss quantification aspect of this study. Focus is particularly placed on loss quantification in semi-arid regions.

- *What are the common approaches to the simulation of channel transmission losses in the Pitman Model and how applicable are these approaches in the Limpopo River Basin?*

  Three functions of the Pitman Model are known to facilitate channel transmission loss simulation namely an explicit transmission loss function, a wetland function and a reservoir function. The channel transmission loss simulation capability of each function is assessed by comparing the simulation outputs with observed data, where available, in an effort to determine the effects of loss processes on water resource estimation.

1.4 EXPECTED OUTCOMES

The expected outcomes of the study include identification of the main river reaches where channel transmission losses are anticipated to be prevalent as well as an enhanced conceptual understanding of channel transmission loss processes in the Limpopo River Basin. The study is also expected to provide an assessment of the different approaches used in the Pitman model to simulate channel transmission losses. In the context of improving water resource management strategies, a discussion on the impact of channel transmission loss processes on water resource estimation is also anticipated.

1.5 ORGANISATION OF THE DISSERTATION

In **Chapter 1**, the introduction relates the background of the study by providing context to water resource management in the Limpopo River and the challenges concerning hydrological process understanding and modelling in southern African arid/semi-arid regions. The introduction elaborates on the relevance of the study and gives the aim and objectives of the research. **Chapter 2** provides a thorough literature review of the various themes contained in the study (i.e. channel transmission losses, alluvial aquifers and the delineation thereof, hydrological modelling) and contextualises them to the objectives of the study. **Chapter 3** provides a descriptive look at the study areas. An account of these study areas includes a description of the physiographical (geography and topography), hydro-meteorological (climate, hydrology and hydrogeology), water and land use characteristics. **Chapter 4** details the collection of data for alluvial aquifer delineation and hydrological modelling. The methodology applied in meeting the objectives of the study is also described. **Chapter 5** provides a brief description of the Pitman Model and its use in the SPAtial and Time Series Information Modelling (SPATSIM) framework. Focus is also placed on the three functions that are used to simulate channel transmission losses within the model. **Chapter 6** discusses procedures and results for alluvial aquifer delineation, alluvial aquifer capacity estimation and hydrological modelling. Commentary on the impact of channel transmission losses on water resource estimation is also provided. The overall conclusions of the study and recommendations for future work are detailed in **Chapter 7**.

CHAPTER 2
Review of Literature

2.1 INTRODUCTION

Chapter 2 provides a background review of the main themes addressed in the dissertation. Focus is placed on the definition and significance of the channel transmission loss processes as well as the estimation thereof. Considering that alluvial aquifers present a hydrological environment in which loss processes occur, the study explores the various characteristics which define an alluvial aquifer and presents the importance of such aquifers. The review looks at the technological advances in the delineation of alluvial aquifers using remote sensing techniques and geographical information systems. A general look at hydrological modelling is also considered. The review concludes with a discussion of conceptual framework development as a way of attaining a holistic understanding of the channel transmission losses in the basin.

2.2 CHANNEL TRANSMISSION LOSSES

"When flow occurs in normally dry stream channels, the volume of flow is reduced at downstream points by evaporation and infiltration to the bed, the banks, and possibly the flood plain. This flow reduction is termed transmission losses. Quantification of transmission losses yields useful information not only on surface runoff volumes, but also on groundwater recharge in some regions." (Walters, 1990)

2.2.1 Definition of channel transmission losses

Channel transmission losses are surface water and groundwater interactions where streamflow is reduced by infiltration through the river bed, seepage into channel banks and flood plains (Walters, 1990; Parsons *et al.*, 1999). Compared to other hydrological processes, information on channel transmission losses remains largely lacking. However, the dynamics between alluvial aquifers (alluvium) and channel transmission

losses have been covered by several hydrological studies across the world (e.g. Walters, 1990; Hughes and Sami, 1992; Boroto and Görgens, 2003; Lange, 2005; Hughes, 2008; Renard *et al.*, 2008; Morin *et al.*, 2009; Owen and Madari, 2010; Costa *et al.*, 2012; Jarihani *et al.*, 2015). From these studies it is understood that, as a result of their water storage capabilities, the presence of alluvial aquifers results in significant channel transmission losses in ephemeral river systems found in arid/semi-arid catchments such as the Limpopo River Basin of southern Africa (LBPTC, 2010). In such regions, factors that characterise these losses include (Smakhtin and Watkins, 1997; Boroto and Görgens, 2003):

- Infiltration and extraction from bank storage,
- Recharge of storage in alluvial channel beds,
- Evaporation and evapotranspiration from the recharged beds and banks,
- Evapotranspiration from riparian vegetation, and
- Direct evaporation from the free water surface.

The total effect of each of these factors on the magnitude of the transmission loss ultimately depends on the nature of the stream, river or irrigation canal being studied (Vivarelli and Perera, 2002).

In order to develop some comprehension of the magnitudes of transmission losses, it is essential to understand the factors that influence these losses. The most important of these factors include (Dunkerley and Brown, 1999; Vivarelli and Perera, 2002; Cataldo *et al.*, 2005; Moyce *et al.*, 2006):

- Streamflow characteristics (volume, duration, velocity): Dunkerly and Brown (1999) and Lange (2005) pointed out that the rate of transmission losses rises abruptly when overbank flow occurs, as a result of dispersion of flood waters to riverbank and floodplain areas. Additionally, small flood events have been observed to generate relatively higher channel transmission losses than major flood events

due to less antecedent moisture in channel bed/bank material (Hughes and Sami, 1992; Jarihani *et al.*, 2015).

- Channel geometry: Generally, channel transmission losses increases from upstream to downstream due to increase in channel/floodplain width and water residence time (Knighton and Nanson, 1994; Jarihani *et al.* 2015),
- Depth to water table (groundwater): A shallow water table reduces the available storage capacity of the valley alluvium, limiting the amount of streamflow that can be absorbed by the aquifer (Sharp and Saxton, 1962).
- Soil characteristics of river bed and banks: Infiltration rates depend strongly on the soil characteristics of the river bed and banks. Due to larger pore spaces and permeability, a gravely, sandy channel and valley may have much higher intake rates per day than finer soils, such as silts and loams or even less for clays (Sharp and Saxton, 1962; Renard, 1970). Typically, losses decrease progressively downstream as the material in the channel bottom became progressively finer (Cataldo *et al.*, 2005).
- Antecedent moisture of channel alluvium: Precipitation and initial flow from floods may saturate the channel alluvium and reduce storage capacity (Cataldo *et al.*, 2005; Jarihani *et al.*, 2015),
- Content and nature of sediment in streamflow: Channel transmission losses decrease with the application of silt-laden water (Cataldo *et al.*, 2005)
- Vegetation along the channels may increase the rate of transmission losses by reducing velocities of flow and increasing evapotranspiration (Sharp and Saxton, 1962).
- Anthropogenic activities and structures: Mining (Parsons, 2004; Cowie, 2014), agriculture (Smakhtin, 2001; Hancock, 2002; Siebert *et al.*, 2010), afforestation (Le Maitre *et al.*, 1999; Smakhtin, 2001; Tanner, 2013) groundwater abstractions (Smakhtin, 2001;), urbanisation (Simmons and Reynolds, 1982; Warner, 1984; Lerner, 2002) and construction of storage dams (Winter *et al.*, 1998; Vandas *et al.*,

2002; Hughes and Mantel, 2010) all contribute to reduced streamflow and therefore affect the magnitude of losses to alluvial aquifers.

Figure 2.1 illustrates the conceptual understanding of processes that occur in ephemeral channels when runoff traverses dry alluvial beds. The behaviour of channel transmission losses is summarised by Costa *et al.* (2012) as follows: "*…small sub-bank flows must firstly fill pool abstractions and channel filaments in order to propagate downstream; then bank-full flows infiltrate predominantly into bed and levees; and, at high stream discharges, overbank flows lose water for pools, subsidiary channels and floodplains, but once they become fully saturated, the most direct floodways become fully active and channel transmission losses decrease*." According to Costa *et al.* (2012) this behaviour is dependent on the seasonality of precipitation and runoff, the underlying groundwater system and flow and the layered structure of alluvial and floodplain sediments. It is important to note that channel transmission losses are not only confined to ephemeral systems. As perennial channels pass through semi-arid catchments along their course, they can discharge flow to the local aquifer system can thus recharge the local groundwater supply (Maliva and Missimer, 2012)

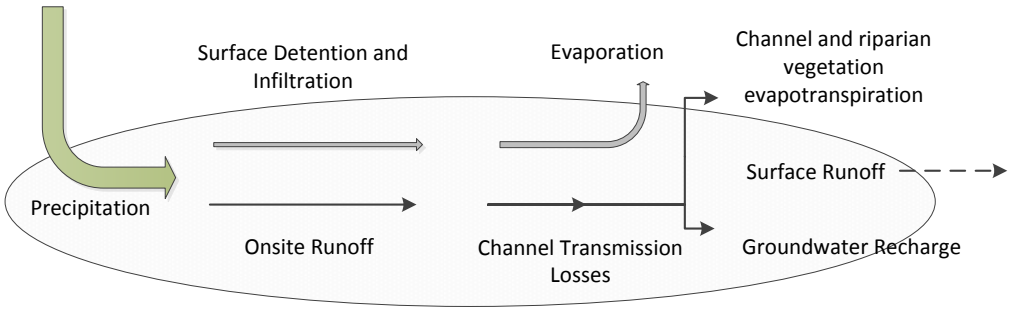

Figure 2.1. Illustration of what conceptually happens in ephemeral channels where runoff traverses dry alluvial streambeds. (Adapted from Renard *et al.*, 2008).

2.2.2 Significance of channel transmission losses

Understanding the impact of channel transmission loss processes on water resources availability is imperative for a more complete understanding of the hydrology and water resources of river basins in relevant environments. Miller *et al.* (2003) recognise the processes as an important aspect of predicting runoff rates. According to Hughes and Sami (1992), neglecting transmission losses in any modelling system designed to simulate runoff characteristics in semi-arid or arid catchments could result in severe over-estimation of the surface runoff which could impact on the effectiveness of resource planning and management. Transmission loss processes also influence the amount of groundwater recharge available in semi-arid catchments (Walters, 1990; Abdullrazzak and Sorman, 1994; Costa *et al.*, 2012) e.g. in the Shashe sub-basin (Botswana and Zimbabwe) where streamflow availability is highly intermittent and seasonal. This is highly beneficial for rural communities which depend on groundwater supply for domestic water use (FAO, 2004). When a river reach is effluent (gaining stream), groundwater discharge can effectively act as freshwater supply and thus support channel-associated ecosystems (Costa *et al.*, 2012).

2.2.3 Methods of estimating channel transmission losses

Table 2.1 gives a summary of studies that have been conducted to better understand and attempt to quantify transmission losses in rivers and streams. Most of these studies have however focused on transmission losses associated with ephemeral streams as the ratio of transmission losses to runoff volume under semi-arid conditions seems to be particularly high (Hacker, 2005) as a result of the aforementioned influencing factors. Although the methods applied have differed depending on the scale and objective of the study, Vivarelli and Perera (2002) were able to categorise the methods into five groups namely, simple regression equation, simplified differential equation, combined use of simplified differential and regression equation, flow-routing models (kinematic wave, Muskingum, and Saint-Venant equation), and hydrological balance models. Several methods of estimating transmission losses using

field-based applications are also reviewed by Shanafield and Cook (2014). The methods are classified into three groups namely:

i. Methods that monitor infiltration through the streambed (provide point estimates of infiltration) e.g. controlled infiltration experiments, monitoring changes in water content, using heat as a tracer of infiltration;
ii. Methods that are based on measurements of streamflow during flow events (provide estimates of either transmission losses or streambed infiltration over greater spatial scales i.e. 10s kms) e.g. reach length water balance, floodwave front tracking;
iii. Methods based on measurements within the groundwater underlying the ephemeral stream (provide estimates of actual groundwater recharge however represent spatial and temporal averages) e.g. groundwater mounding, groundwater dating.

Walter *et al.* (2012) investigated the estimation of aquifer recharge through visual analyses of satellite imagery, but indicated that the methods applied are best suited for explaining the spatial distribution of relative channel losses. For quantitative estimates of absolute losses, the study stipulates that in-stream flow measurements are required. According to Walter *et al.* (2012) and Shanafield and Cook (2014), streamflow losses into the underlying alluvium can be estimated by measuring discharge at two points in the channel system. If hydrometric data are available upstream and downstream of a channel reach, inflow and outflow volumes may be compared and transmission losses quantified (Tanner, 2013). Volumes of transmission loss may be related to flow and channel characteristics by means of regression analysis (Lange, 2005); however, this approach can be complicated by unknown lateral inflows (Tanner, 2013). The methods investigated by both Shanafield and Cook (2014) and Walter *et al.* (2012) do however indicate the importance of approaching transmission loss estimation holistically - "*Therefore, interdisciplinary studies linking the transmission losses (hydrology), infiltration (hydrology/soil physics), riparian response (ecology), and aquifer response (hydrogeology) would be extremely beneficial to the general, applied*

understanding of arid zone processes" (Shanafield and Cook, 2014). In deriving a volumetric estimate of potential alluvial groundwater resources, Owen *et al.* (1989) utilised the product of the volume of the saturated aquifer and the specific yield of the aquifer. Moyce *et al.* (2006) implemented the same method by using the product of the estimated saturated aquifer thickness, the aquifer area extents and specific yield.

2.2.4 Examples of estimation of transmission losses in semi-arid/arid environments

2.2.4.1 Estimation of transmission losses in the World and Africa

Multiple studies that focus on transmission loss estimation in semi-arid and arid environments have been conducted across the world; a summary of several of these has been compiled by Cataldo *et al.* (2005) and Jarihani *et al.* (2015). These have not all been conclusive in terms of exact quantification of the channel transmission loss processes, however the methods applied are beneficial for knowledge development. A collection of major studies conducted across the world over the last 60 years is presented in Table 2.1 to **Error! Reference source not found.**. The key results discussed in these studies are summarised in this section. Notably, loss estimation studies in Africa are fewer than those conducted in the USA. As stressed by Hughes (2008), research in Africa is often hindered by lack of resources and infrastructure-related data e.g. flow gauge data etc. Channel transmission loss estimation studies conducted in South Africa and the Limpopo River Basin are discussed, in detail, in Sections 2.2.4.2 and 2.2.4.3, respectively. The region is discussed separately from studies conducted in other African countries so as to expand on the details of the techniques used to estimate channel transmission losses.

Table 2.1. Summary of relevant transmission loss estimation research conducted in semi-arid and arid environments over the last 60 years in Australia

Study	Data/ Model used	Study Area/ Aquifer type	Key results
Jarihani *et al.* (2015)	Remotely-sensed data/ 2D TUFLOW model	Diamantina catchments, Lake Eyre Basin, Australia	Lateral inflow is the most important source of uncertainty in water balance calculation. Total transmission losses are high. Actual evapotranspiration is the most important component of the transmission losses followed by infiltration and terminal water storage. Hydrodynamic model can be used to estimate water balance.
Karim *et al.* (2011)	MODIS daily images and gauge data/Mike 21 model	Fitzroy River, Western Australia	Hydrodynamic model can be used to investigate ground water recharge in a topographically complex catchment. Remote sensing can be used in calibrating hydrodynamic model in ungauged catchments and improves flood discharge estimation.
Costelloe *et al.* (2003)	Gauge data / Conceptual model	Diamantina River, Lake Eyre Basin, Australia	Transmission losses are 70–98% for floods with total discharge <2300 Mm^3. Flood travel time was non-linear, increases with increasing discharge. Satellite images are used to identify the flow-paths.
Dunkerley and Brown (1999)	Direct infiltration observations/No model used	Small desert stream in western New South Wales, Australia	Transmission losses in ephemeral streams may be minimised in near bank-full flow stage, and be higher in both sub-bankfull and overbank flows. Transmission losses in sub-bank flow were (13.2% per km) more than twice the bankfull rate.
Telvari (1997)	Gauge data, Theissen method (linear and logarithmic regression equation)	Nelia Creek, New South Wales , Australia	Established relationship between overland flow and transmission loss rate.
Knighton and Nanson (1994)	Gauge data/ streamflow routing	Cooper Creek, Lake Eyre Basin, Australia	Losses varied non-linearly with stage and could be more than 75% of the initial flow rate. Evaporation and drainage diffusion were major reasons for transmission losses.

Table 2.2. Summary of relevant transmission loss estimation research conducted in semi-arid and arid environments over the last 60 years in North and South America

Study	Data/ Model used	Study Area/ Aquifer type	Key results
Costa *et al.* (2013)	Gauge data, groundwater level data, Multi-temporal satellite data/	Middle Jaguaribe River, Brazil	Use of satellite data allowed delineation of areas with transmission losses. Transmission losses calculated from delineated areas measured similarly to those derived by using streamflow and groundwater data. Seasonal changes observed in river reach i.e. changed from losing stream to gaining stream
Cataldo *et al.* (2010)	Gauge data/regression equation	Western USA	The results indicate that discharge (either as total event volume or peak flow) and hydraulic conductivity are important factors affecting transmission losses.
Osterkamp and Lane (2003)	Channel morphology data/ Transmission loss simulation model based on regression equation	Multiple sites in Al Ain, Abu Dhabi and Amargosa River Basin, USA	Computed estimates of aquifer recharge by transmission loss processes. Established that simulation model is event based but can offer inputs for larger water-budget studies.
Parsons *et al.* (1999)	Field observations	Jornada Ecological Experiment Station, New Mexico & Walnut Gulch, Arizona, USA	Found variation in transmission loss from rills and inter-rill areas. Transmission losses in sand-bedded rills were about 66% greater than those in gravel-bedded rills
Lane *et al.* (1980)	Linear regression equation, differential equation	Walnut Gunch, Arizona & Trinity River, Texas, USA	Analysis was limited to streamflow in ephemeral stream channels with infiltrating losses. Transmission losses for Walnut Gulch site (AZ) range from 1.9 to 5.9 acre-feet per mile.(~1.796 Mm^3 km^{-1})
Jordan (1977)	Simplified differential equation	Multiple sites, western Kansas and Nebraska, USA	Approach allowed for a non-linear decrease of flow and variations in distance between gauging stations. Estimated transmission losses were lower bounds because method disregarded lateral and/or tributary inflows. Average transmission losses ranged from ~0.003 Mm^3 -1.18 Mm^3 km^{-1} Transmission losses in first mile was proportional to about 2% of upstream flow volume.
Burkham (1970)	Gauge data/ Hydrologic budget	Multiple sites in the Tucson Basin, Arizona, USA	Annual variation of infiltration mainly resulted from variation in inflow Transmission losses were 30-90% of inflow.
Sharp and Saxton (1962)	Gauge data/ field observations	Multiple sites in USA	Provided a description of factors affecting seepage, and therefore transmission losses, in natural streams. Averaged 40% in transmission loss of flood flows.

Table 2.3. Summary of relevant transmission loss estimation research conducted in semi-arid and arid environments over the last 60 years in the Middle East and India

Study	Data/ Model used	Study Area/ Aquifer type	Key results
Shentsis *et al.* (1999)	Hydrologic budget	Negev, Israel	Evaporation is substantially smaller than the transmission losses (approximately 1-2% of the transmission losses). Developed a loss function that relates total inflow (estimated inflow and lateral flow) to transmission losses.
Abdullrazak and Sorman (1994)	Linear and multi-linear regression equation, hydrologic budget	South western Saudi Arabia	Results emphasised the importance of tributary inflow in these estimations and suggest that ignoring tributary inflow results in lower bound estimation of transmission losses. Initial moisture conditions, the type of bed material, its thickness, and width may have hada impact on the magnitude of transmission losses. Transmission losses range from 2529 m^3 – 4.974 Mm^3 km^{-1}
Abdullrazak (1994)	Gauge data, evaporation data/ regression equation	South western Saudi Arabia	Regression equations indirectly estimated transmission losses Transmission losses between 0.06 Mm^3-1.190 Mm^3 per event.
Sorman and Abdullrazak (1993)	Gauge data, regression equation	Tabalah basin, Saudi Arabia	Various magnitudes of transmission losses and consequent groundwater recharge may result from similar runoff hydrographs due to the influence of channel and soil characteristics. Regression equations developed the in study can be used to estimate the groundwater recharge in areas with similar hydrological and morphological characteristics.
Walters (1990)	Hydrographs/regression equations	Multiple wadi systems, Saudi Arabia	Different regression equations were needed for smaller or larger floods. Upstream flow volume and channel length are important parameters especially for smaller flows
Sharma and Murthy (1994)	Landsat images, gauge data/linear regression and differential equation	Luni Basin, India	Transmission losses reduced the runoff by 8–56%. Infiltration rate positively correlated (r_2 = 0.56) with weighed mean diameter of bed material. Landsat images were used to extract channel geometry.

Table 2.4. Summary of relevant transmission loss estimation research conducted in semi-arid and arid environments over the last 60 years in Africa

Study	Data/ Model used	Study Area/ Aquifer type	Key results
Milewski *et al.* (2009)	Gauge data and remotely-sensed TRMM, AVHRR and AMSR-E data/ SWAT	Sinai Peninsula and the Eastern Desert, Egypt	Annual runoff in sub-catchments was 9% and annual groundwater recharge was 19.6% of total precipitation. Initial losses (e.g., infiltration and actual evaporation) were 71.4% of total precipitation.
Dahan *et al.* (2008)	Field measurements of flood and groundwater levels, and river bed infiltration rate/no model used	Kuiseb River, Namibia	Average downward fluxes in the vadose zone was 10 mm/h in relatively well-sorted sandy sediments channel bed. Large floods showed larger transmission losses.
Lange (2005)	Gauge data/mathematical flow routing scheme (MVPMC4-method)	Kuiseb River, Namib Desert, Namibia	Transmission losses are minor during small to medium flows but increase during high discharge peaks. Water losses occur mostly in flooded overbank areas.

2.2.4.2 Estimation of transmission losses in South Africa

The collection of published literature focusing on channel transmission losses in South Africa was conducted through searching for the following phrases: 'alluvial aquifers in South Africa', 'channel transmission losses South Africa', 'aquifer recharge South Africa', 'river losses South Africa'. The search results were very limited, however the studies conducted by Sami (1992), Hughes and Sami (1992), Birkhead (2000), McKenzie and Craig (2001), Brown (2005), Bredenkamp and De Jager (2011) and Tanner (2013) proved relevant for this discussion.

Sami (1992) examined recharge mechanisms and salination processes in the semi-arid sedimentary Great Fish River Basin of the Eastern Cape Province by use of isotopic tracer methods. The study was part of a project that focused on estimating recharge and studying groundwater dynamics of a fractured rock aquifer system in the same region (Hughes and Sami, 1992). However, transmission losses could not be quantified due to a lack of understanding of the processes as a result of the occurrence of small

water fluxes compounded by large seasonal variability (Sami, 1992). Hughes and Sami (1992) monitored the soil moisture dynamics of an alluvial valley bottom in the region and found that transmission losses were higher for small flow events (75% of runoff) when compared to larger flow events (22% of runoff). It is understood that during small flow events high infiltration of runoff can occur before the alluvial aquifer is saturated whereas in large flow events, a smaller percentage of the runoff will saturate the alluvium due to antecedent moisture in the channel alluvium (from initial flood waters), leading to more overland flow (Cataldo *et al.*, 2005; Jarihani *et al.*, 2015).

The interaction between channel flow and bank seepage in river was investigated by Birkhead (2000) through the development and use of a computational finite-difference bank storage model called BANKFLO as well as field monitoring. The model was applied at a study site on the Sabie River in the Kruger National Park as part of an effort to determine the nature of bank storage responses to flow events in the river as well as to assess the contribution of seepage from the river in supporting transpiration losses. The study developed a simple graphical method for determining the maximum rise in phreatic surface level in response to different flow release patterns which is deemed useful in quantifying bank storage response to flow events. Birkhead (2000) confirmed that transpiration along the Sabie River depends largely on bank seepage.

McKenzie and Craig (2001) used the ISIS hydraulic model to evaluate river losses downstream of the Vanderkloof Dam on the Orange River during a study to develop a methodology for calculating evaporative losses from South African rivers. Theoretical losses were estimated from a product of measured evaporation rate, the water surface area and the riparian vegetation area. The calculated evaporation losses from the Orange River derived from the study ranged from 575 $Mm^3\ a^{-1}$ at an annual low flow release rate of 50 $m^3\ s^{-1}$ to 989 $Mm^3\ a^{-1}$ at an annual release rate of 400 $m^3\ s^{-1}$. The variation in evaporative losses was a result of changes in the surface area with flow.

Brown (2005) used a hydraulic and hydrological approach to model water losses for the lower Renoster River in the Free State Province. Hydraulic Muskingnum and

Kinematic wave routing was implemented to estimate potential flow losses for small flow events, while the Pitman Model (WRSM2000) was used to simulate long-term streamflow and associated losses. Flow losses for individual flood events along the lower Renoster River were found to vary between 3% and 17%; however for a longer term constant flow regime, losses ranged between 10% and 40%. Based on both the hydraulic and hydrologic approaches, the primary cause of flow loss was found to be surface evaporation, with negligent transpiration and channel-aquifer losses.

Channel transmission losses along the Gamagara River alluvial aquifer of the Northern Cape Province were investigated by Bredenkamp and De Jager (2011) as well as Tanner (2013). Bredenkamp and De Jager (2011) found that transmission losses in the ephemeral river occurred as a result of the impact of dewatering operations of the Sishen open cast iron ore mine and swallets (subsidence features) which capture a portion of the flood water. Smaller flood events were found to lose more water to the underlying aquifer system because they took longer to cross the dewatered section. In addition, a series of faults found in parts of the dewatered system were found to increase recharge to the aquifer significantly when compared to other areas in the dewatered zone where faults are not present. The two main recharge mechanisms of the Gamagara River alluvial aquifer were concluded to be recharge from surrounding fractured and karst rock aquifers as well as recharge from flow/flood events in the river. The recharge to the alluvium was estimated to range between 5 % and 25% of mean annual precipitation (MAP). As part of understanding and modelling surface and groundwater interaction processes, Tanner (2013) implemented the Pitman model (Hughes, 2004; Hughes *et al.*, 2006) to compare observed groundwater levels to simulated groundwater levels, which were calculated from the groundwater gradients modelled by the Pitman model. Tanner (2013) noted several uncertainties relating to the simulated stream flow, which questioned the contribution to groundwater through transmission losses, as well as the capability of the transmission loss function itself. The accepted conclusion was that the model had successfully simulated the dominant

catchment-scale processes in a behavioural manner, even though the exact quantification was uncertain.

2.2.4.3 Estimation of transmission losses in the Limpopo River Basin

In the Limpopo River Basin, hydrological modelling incorporating channel transmission losses has been conducted by the Joint Upper Limpopo Basin Study (1991), Görgens and Boroto (1997) and Boroto and Görgens (2003) and the Limpopo River Basin Monograph Study (LIMCOM, 2013). One of the first studies on channel transmission losses in the Limpopo River Basin was conducted through the Joint Upper Limpopo Basin Study (JULBS, 1991; Görgens *et al.*, 1991). The study noted that amongst other complications, major transmission losses occurred along rivers in the region and thus contributed to the non-perennial flow regime of the Limpopo River. However, the paucity of flow gauging stations meant that direct quantification of transmission losses was not possible, which made water resource analyses rather complex. Components of these losses were observed as (Görgens *et al.*, 1991):

- Recharge of storage in alluvial channel sand beds and subsequent evaporation, either directly or by riparian vegetation.
- Recharge of storage in alluvial river banks and subsequent evaporation and evapotranspiration.
- Direct evaporation from the free water surface during surface flow conditions in the river channels.
- Recharge to deeper groundwater, usually to deep sand aquifers, but also to secondary fractured rock aquifers.
- Losses of floodplain flows during extreme events, either as evaporation or as groundwater recharge of some form or another.

To account for these losses the study conceptualised an alluvial channel reach 'black-box' transmission loss sub-model to be applied in the Pitman conceptual catchment model (Pitman *et al.*, 1981) based on the assumptions that:

i. The channel and river bank behave like a 'sand' storage reservoir with dimensions equal to the total surface area measurable from aerial photos and mean depth estimated from various regional sources.
ii. Outflow can only occur after the sand bed and river banks have been saturated.
iii. Channel evaporation occurs at the potential rate during months with residual flow (after sand bed and banks have been saturated).
iv. No evaporation from or rainfall on the channel is recognised during months without residual surface flow.
v. Evapotranspiration occurs from the river banks at all times and at the potential rate.
vi. Difference between longitudinal inflow and outflow is negligible.

The study indicated that flow from upstream tributaries in the upper Limpopo River far exceeded the annual MAR recorded at the only main-stem gauging station, (A5H006) further downstream at Sterkloop, by 187 Mm^3a^{-1} (31% of MAR). The results of this 'mass balance puzzle' led to the conclusion that, since the contribution of irrigation and riparian vegetation to the reduction of flow had been considered, the unaccounted losses could be attributed to transmission losses in the area.

In investigating the flow balance of the Limpopo main stem, Görgens and Boroto (1997) utilised the SHELL monthly time-step hydrological modelling package (Berg *et al.*, 1991) which is equipped with a channel loss module that uses a sand-reservoir/ riparian consumptive use approach to estimate transmission losses. The modelling exercise covered only the Upper Reach (from Marico and Crocodile River confluence to the Shashe confluence) and Middle Reach) (Shashe confluence to Luvuvhu confluence) of the main stem. About 80% of the modelling sub-catchments were equipped with channel loss modules to quantify transmission losses. The results of the study estimated upper reach losses to amount to 6% of the expected MAR at Sterkloop which was notably different from the 31% reported by the JULBS (1991). Görgens and

Boroto (1997) indicated that through observations made during various field trips and analyses of photographic and video material, it was found that the width of the riparian zone active in recharge storage was four times greater than that assumed in JULBS (1991). A similar 6% of unaccounted losses was observed between upstream of the Shashe confluence to the Beit Bridge gauging station. As a result of the lack of gauging stations between Sterkloop and the Shashe confluence and between Beit Bridge and the Luvuvhu confluence, potential transmission losses could not be quantified in those areas.

In 2001, through an update of the hydrological model of the Limpopo River main stem (Görgens, 1999), Matji and Görgens (2001) reported that transmission losses, resulting from main stem alluvial and riparian vegetation losses, contributed to about 33.33 % of the overall main stem water balance at the border entering Mozambique based on the observed data for the period 1971 to 1995. The SHELL monthly time-step hydrological modelling package was used for estimation. In a follow up publication that focused on alternative methods that could be used to estimate transmission losses along the Limpopo River, Boroto and Görgens (2003) indicated an estimate of 30% transmission losses along the main stem.

Mansell and Hussey (2005) investigated, through field measurements and numerical modelling of the flow of ephemeral rivers in alluvium, the flows and losses in alluvial sands at four sites in the Matabeleland Province of Zimbabwe over a period of three years. The study concluded that the main factors influencing loss of flow in the alluvial aquifers was water velocity through the alluvium, which in turn was controlled by sand properties and area of the channel contributing to flow.

Channel transmission losses were also considered in the recent Limpopo River Basin Monograph Study (LIMCOM, 2013). The loss processes were simulated through a specialised channel loss feature of the WRSM2000 (Pitman (1973) model, Version of 2000) that functioned as a 'dummy dam'. Through this approach, mean annual transmission losses along the main stem were reported to be about 30 % (1000 Mm^3

a^{-1}) of the current day MAR at the mouth of the Limpopo River (Görgens *et al.*, 2014; Dlamini, 2014) using extended patched observed monthly flow data from 1920 to 2010 (Howard *et al.*, 2013). The distribution of current-day transmission losses along the Limpopo River is illustrated in Figure 2.2.

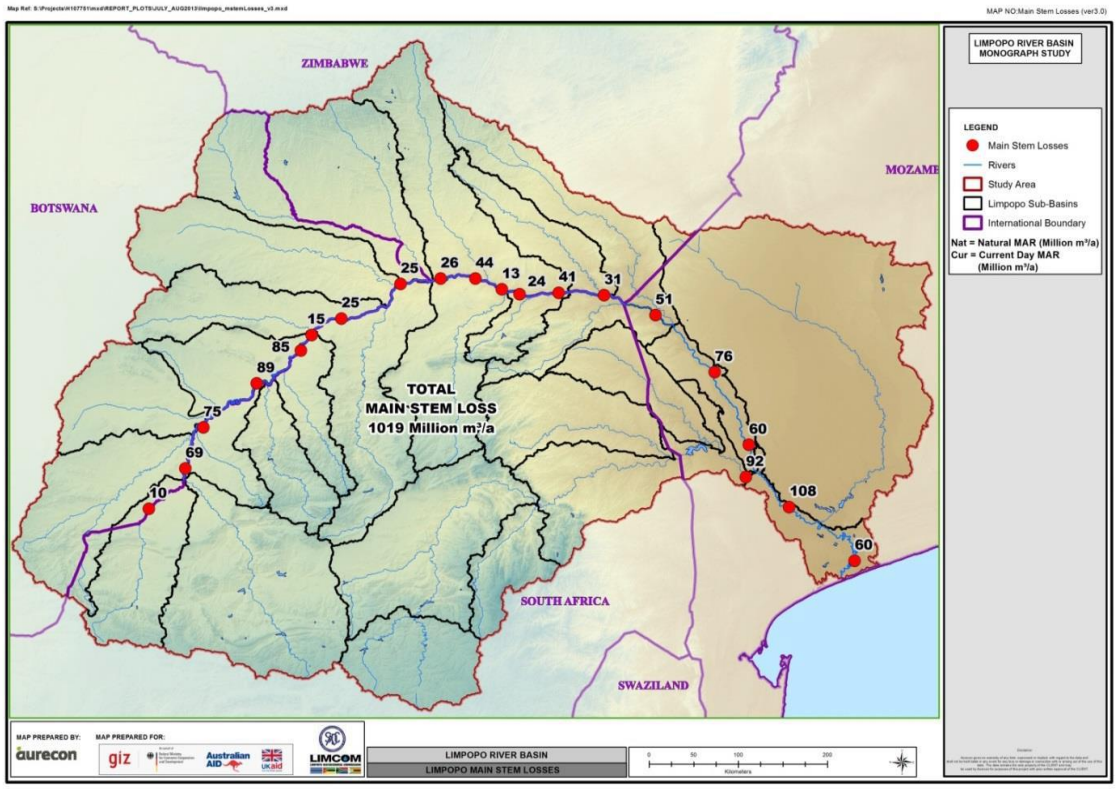

Figure 2.2. Distribution of current-day transmission losses along the Limpopo River main stem in Mm^3a^{-1} (Howard *et al.*, 2013).

2.3 ALLUVIAL AQUIFERS

2.3.1 Definition and classification of alluvial aquifers

The South African Department of Water and Sanitation Online Dictionary (DWS, 2011) describes an alluvial aquifer as "an aquifer comprising unconsolidated material deposited by water, typically occurring adjacent to rivers and buried palaeochannels." Other definitions describe it in reference to the unconsolidated material that constitutes the aquifer, its size, where it is situated in relation to the river's longitudinal and cross-sectional profile and the ecological setting within which it occurs (e.g. Moyce *et al.*, 2006). As indicated, alluvial aquifers typically comprise unconsolidated material

which can take the form of silt, sand, gravels or a mixture of these (Love *et al.*, 2007). The type of material that makes up the aquifer depends on the stream processes that eroded the bedrock to form the weathered material. Aquifer dimensions relate to the extent and thickness of the alluvial fill in the river channel and under the lateral alluvial plains and can range from a few tens to a few hundreds of metres in width and thickness (Owen and Dahlin, 2005). Alluvial aquifers can occur as isolated features measuring a few hundred metres (e.g. alluvial aquifer of Steelpoort River, South Africa (ESKOM, 2006)) to kilometre-long and continuous deposits associated with 'sand rivers' (e.g. alluvial aquifer of Shashe River, Botswana (Wikner, 1980; Botswana DWA, 1989)). The thickness and areal extent of alluvial aquifers has been associated with geological boundaries such as faults and lineaments (Owen and Dahlin, 2005; Dafalla, 2016). In terms of its position in relation to the river's cross-sectional profile, an alluvial aquifer may be characterised as a lateral accretion channel deposits, vertical accretion plains deposits, river terrace valley flat deposits and abandoned meander cut-off plain deposits (Owen, 1994). Longitudinally, deposits can be described as upper or lower catchment alluvial aquifers; however this is all relative to the catchment morphology (Moyce *et al.*, 2006). The distribution of alluvial aquifers is determined by the river gradient, geometry of the channel, fluctuation of stream power as a function of decreasing discharge downstream as a result of evaporation and infiltration losses, as well as rates of sediment input due to erosion (Moyce *et al.*, 2006). These factors are explained as:

- River gradient: Alluvial aquifers are associated with gentle topographical slopes as these facilitate deposition of eroded soil material from upstream areas (Moyce *et al.*, 2006).
- Geometry of the channel: Apart from the influences of existing (if any) fractures and faults in the strata on which the river flows, river channel patterns often indicate the evolution (age) of the river, which relates to the velocity of its flow. Young river valleys are associated with straight, fast flowing channels, while the more mature channels can be characterised by meandering and braided

patterns which are created by the slowing down of flow as soil deposits accrue (Leopold and Wolman, 1957).

- Fluctuations of stream power: As the velocity of streamflow is reduced due to increased channel transmission losses and lower rainfall during the dry season, more sediment are able to settle thus forming deeper and more extensive alluvial aquifers (Moyce *et al.*, 2006).
- Rates of sediment input due to erosion: This factor is related to fluctuations of stream power.

2.3.2 Significance of alluvial aquifers

Where there is deposition of alluvial sediments, alluvial aquifer may form. Consequently, ecological settings may range from lacustrine, deltaic and marine environments (Gonthier, 1998). Their significant water storage capabilities imply that alluvial aquifers support a multitude of ecological and anthropogenic activities. In the Luvuvhu sub-basin of the Limpopo River Basin, the Pafuri alluvial aquifer is characterised by dense, extensive natural forests which form part of the Kruger National Park (Griscom *et al.*, 2010; Kundu *et al.*, 2015). The floodplains in the sub-basin are also wetlands, therefore both the riverine and wetland ecosystems benefit from the aquifers (Pafuri River Camp, 2009).

Cultivated lands are often established on floodplains associated with extensive alluvial aquifers exploiting the fertility of the soils and the close proximity to the water source for irrigation and stock watering (Ashton *et al.*, 2001; Moyce *et al.*, 2006). Several rural and urban communities around the world depend on groundwater abstraction from alluvial aquifers for domestic water supply. Examples of alluvial aquifer systems that are used for urban water supply include the Delta Plains alluvial aquifer of eastern India (Bhattacharya *et al.*, 1997), Gascoyne River alluvial aquifer of Australia (Leonhard *et al.*, 2013), Lower Mzingwane alluvial aquifer of Zimbabwe (Love *et al.*, 2007), while the Ocheyedan River alluvial aquifer of Iowa, USA (Gannon and Voggelgesang, 2014), the

Mushawe River alluvial aquifer of Zimbabwe (Love, 2006) and several alluvial systems in Saudi Arabia (Abdullrazak, 1994) support rural communities.

The mining industry also benefits from alluvial water supply for several of its operations. To sustain its current mining operations, the Venetia Diamond Mine abstracts water from two alluvial aquifers, Greefswald and Schroda, that lie at the confluence of the Limpopo and Shashe River, located within the Mapungubwe National Park (Brown and Erasmus, 2004; Mwenge Kahinda *et al.*, 2012). The abstraction is between 2 Mm^3a^{-1} and 5 Mm^3a^{-1}. Sand mining occurs along the lower catchment bank and floodplain alluvial deposits of the Mokolo River (DWAF, 2010; De Klerk and De Klerk, 2011).

2.3.3 Hydrological processes associated with alluvial aquifers

Their shallow depth and close relationship with the river channel imply that flows in alluvial aquifers are essentially an extension of surface flows signifying interactions between surface water and groundwater (Mansell and Hussey, 2005). When describing the principal processes related to alluvial aquifers, Brenot *et al.* (2015) relate the exchanges that occur in a losing and a gaining stream, while Moyce *et al.* (2006) describe the recharge and loss processes in alluvial aquifers as being respectively a result of river flow and evaporation, transpiration, vertical seepage to bedrock and downstream flow during the dry season. These processes are also effectively a function of the river type, i.e. the duration and dominance of the processes depends on whether the river has an ephemeral, seasonal or perennial flow pattern (Tanner, 2013).

2.3.4 Alluvial aquifers in the Limpopo River Basin

The geomorphology of the Limpopo River is characterised by 100 m to 500 m wide alluvial deposits, ranging in thickness between 5 m and 10 m as well as rocky outcrops and floodplains in the upper and middle reaches and extensive floodplains further downstream (Boroto and Görgens, 2003). The aquifers comprise mainly

unconsolidated Quaternary sequences of clay, sand and gravel beds (CSIR, 2003), and are sources of groundwater abstraction for multiple communities because of their high permeabilities (Owen and Madari, 2010) and good water quality (CSIR, 2003). The alluvial aquifers along the Limpopo River have the potential for high yields, whereas those along tributaries such as the Luvuvhu River in South Africa display much lower potential because of limited aquifer extent and less than optimum hydraulic characteristics (CSIR, 2003).

Substantial investigations (Mansell and Hussey, 2005; Moyce *et al.*, 2006; Love *et al.*, 2007; De Hamer *et al.*, 2008; Love *et al.*, 2010) have taken place in an attempt to characterise the extensive alluvial aquifers of Zimbabwe, partly because those of the Mzingwane catchment are the most extensive in the Limpopo River Basin (Görgens and Boroto, 1997). Within the Mzingwane sub-basin, three main alluvial aquifers belonging to meso-catchment systems (101-103 km^2) have been identified, namely the Upper Bengu, Mnyabezi, Malala and Mushawe (Love *et al.*, 2007; Masvopo *et al.*, 2008). Moyce *et al.* (2006) looked at the distribution, properties, usage and potential expansion of alluvial aquifers in the Mzingwane sub-basin. The study used satellite imagery to locate and characterise the alluvial aquifers. The aquifers were divided into narrow and broad river channel and flood plain deposits and it was observed that the lower Mzingwane had the largest irrigation potential because of the good water quality of the river channel aquifer; however the floodplain deposits displayed high salinity. De Hamer *et al.* (2008) considered the potential of the alluvial aquifers of the upper Mnyabezi to supply water to a small reservoir but the aquifer was too small to support a large storage capacity and could only be used as a supplementary water resource.

2.3.5 Alluvial aquifer delineation techniques

Traditional methods of identifying and marking the extent of alluvial aquifers have included field observations, the use of geological and hydrogeological maps as well as

aerial photography (DWAF, 2005; Meijerink *et al.*, 2007). All these approaches rely on visual interpretation and are still applied in research, albeit more commonly as auxiliary data sources. Based on field observations, some key indicators of riparian zones associated with alluvial aquifers include low-lying, gentle slope topography which may have distinct, terraced channel morphology; prolific vegetation growth as a result of the vegetation being in close proximity to a watercourse and well-defined alluvial soils (DWAF, 2005).

More recently, the application of remote sensing techniques and mapping using geographical information systems (GIS) to hydrogeology and other scientific fields has proven more beneficial in terms of time and cost-efficiency for observing inaccessible locations, acquiring up-to-date imagery as well as covering larger geographical areas (Meijerink, 1996, Meijerink *et al.*, 2007; Campbell and Wynne, 2011; Elbeih, 2015). Succinctly put, 'remote sensing is the practice of deriving information about the Earth's land and water surfaces using images acquired from an overhead perspective e.g. satellite, using electromagnetic radiation in one or more regions of the electromagnetic spectrum, reflected or emitted from the Earth's surface.' (Campbell and Wynne, 2011). Everything in nature has its own unique distribution of reflected, emitted and absorbed radiation which is known as its 'spectral signature' (Meijerink *et al.*, 2007). Satellites use this unique spectral signature to distinguish objects from one another and use the information to relay the distribution of each object (e.g. soils, trees, water, tarred surfaces) on the Earth's surface. This ability is highly useful in land cover and land use research.

Studies that have delineated alluvial aquifers using remote sensing and GIS techniques have focused primarily on identifying groundwater recharge sites and groundwater potential development zones (e.g. Khan and Moharana, 2002; Javed and Wani, 2009;; Magesh *et al.*, 2012;), while a few others have looked at physiographical soil mapping (Afify *et al.*, 2010; Dobos *et al.* 2013) and characterising the soil, hydrogeological and physical characteristics of alluvial aquifers for water estimation purposes (e.g. Millaresis

and Argialas, 2000; Moyce *et al.* 2006). The methods employed to locate, measure and characterise alluvial aquifers through remote sensing and GIS techniques have included, amongst others, the use of multi-layer spatial analysis (e.g. Khan and Moharana, 2002), digitizing using False Colour Composite (FCC) images (e.g. Moyce *et al.*, 2006) and LiDAR-derived vegetation heights which give an indication of the extent of alluvium along river systems (Levick and Rogers, 2011).

Khan and Moharana (2002) delineated groundwater potential zones in the Sikar District of Rajasthan through use of a groundwater prospect map that was developed from integrating thematic layers generated from IRS-1D LISS-III (Indian Remote Sensing 1D Linear Imaging Self Scanning Sensor 3) false colour composite (FCC) images. Secondary data to support the mapping result included geological maps, hydrological, groundwater level and soil data. The high potential zones were confined to alluvial plains and Quaternary age valleys located in the north-western and south-eastern regions of the study area. Similarly Javed and Wani (2009) used thematic mapping to delineate groundwater potential zones in Kakund Watershed, Eastern Rajasthan, using IRS-1D LISS III FCC data in conjunction with a topographic map and field data. The FCC image was used to visually identify geomorphic units including alluvial plains plateaus, valley fill and linear ridges. Thematic maps depicting hydrogeomorphology, lineament, drainage and geology were digitized and saved as shapefiles in ArcView GIS software and superimposed to locate groundwater development zones. It was found that alluvial plains, buried pediments and valley fills possessed good to excellent groundwater prospects.

Afify *et al.* (2010) used satellite images from EgyptSat-1, topographic map and ground truth data comprising soil profiles to develop a digital physiographic soil map of a study area in Middle Egypt. The physiographic units were categorised using spectral signatures and comprised pediplains, terraced old alluvial plains, wadis, Aeolian plains, Nile River floodplain and Nile River channel alluvium. Soils samples were classified

according to the Soil Taxonomy and ranged from loamy skeletal deposits along the pediplains to sandy and coarse loamy deposits along the channel alluvium.

While the study by Levick and Rogers (2011) was focused on documenting spatio-temporal changes in woody vegetation cover dynamics using airborne LiDAR (light detection and ranging) and historical aerial photographs, it indirectly located the extent of alluvial riparian zones in the Shingwedzi catchment of South Africa. Decreases in woody cover were positively associated with the presence of alluvium, and negatively associated with the presence of clay and distance from main rivers (riparian zones). This study demonstrated that alluvial aquifers can be detected using knowledge regarding the flora that grows along alluvial regions.

Moyce *et al.* (2006) demonstrated the possibility of using Landsat TM (Thematic Mapper) imagery to identify the position of alluvial aquifers in the Mzingwane catchment of south-western Zimbabwe and distinguish channel alluvial deposits from floodplain alluvial deposits. The panchromatic image of LandSat TM and different false colour composite images (FCC345, FCC543, FCC534) were used in satellite image interpretation. On the panchromatic image channel alluvium stood out as bright white areas while on FCC345 composite, channel alluvial deposits stood out as white areas lined by green areas representing vegetated floodplain deposits. Aerial photos and geological maps were used to verify the identified alluvial deposits which were subsequently mapped, digitized and measured to determine areal extents.

2.4 HYDROLOGICAL (RAINFALL-RUNOFF) MODELLING

2.4.1 Definition and significance

Since the development of hydrological models in the 1800s (Xu, 2002) hydrological modelling has had a range of applications including runoff estimation of ungauged catchments, prediction of catchment responses to changed conditions (i.e. climate change, land use activities etc.) and water quality investigations (Džubáková, 2010).

The main objective of hydrological modelling has been to provide reliable information for water resources planning and management through an understanding of the dominant hydrological processes and the interaction of these processes within a hydrological catchment (Sawunyama, 2008). The role of the modelling process, and of the hydrological model itself, is therefore to provide a simplified representation of a real-life hydrological system, however the ability to do so is often limited by several challenges including data availability, spatial diversity between observed parameters and model parameters and differences between hydrological process scales and modelling scales (Mul, 2009). Various models have been developed in an effort to adequately model water resources, however selection depends on the modelling objective, process representation and the scale at which modelling is conducted (Vaze *et al.*, 2012).

2.4.2 Classification of hydrological models

According to Gosain *et al.* (2009), hydrological models can be broadly classified into three types namely, empirical models, conceptual models and deterministic models. Empirical models, also referred to as black-box models, rely on a mathematical account of the input and output data to predict the behaviour of a hydrological basin; physical basin processes are not generally considered, therefore parameters are used to run simulations of the hydrological system being considered (Xu, 2002; Jajarmizadeh *et al.*, 2012). Unlike empirical models, deterministic or theoretical models (also known as white box or physically-based models) rely heavily on large amounts of data and therefore offer better understanding of the hydrological system (Jajarmizadeh *et al.*, 2012). Conceptual models (grey box) are seen as an intermediate of the two and are further subdivided into lumped, distributed and semi-distributed conceptual models based on the attributes that they incorporate from either empirical or deterministic models (Xu, 2002). Lumped conceptual models (e.g. HBV model: Bergström, 1976) consider three basic processes within a river basin: the loss of water from storage to atmosphere; storage of water in soil, vegetation, aquifer, and in rivers; routing of flow

over the surface (Gosain *et al.*, 2009). A mathematical representation of hydrologic processes is used as an approximate representation of the real world therefore in the model, parameters, inputs and outputs are spatially averaged for the whole basin and do not usually have any 'true' physical meaning (Kapangaziwiri, 2007). Distributed conceptual model (e.g. SHE model: Refsgaard and Storm, 1995) consider the spatial variability that may exist in a basin (Jajarmizadeh *et al.*, 2012). In the model, the basin is regarded as a spatially variable system where the all variables and parameters can be varied spatially in response to differences in the physiographic and hydro-meteorological characteristics of the basin (Kapangaziwiri, 2007). Semi-distributed models (also called semi-lumped) are intermediate to lumped and distributed models. These models simulate the average behaviour for the entire catchment through smaller, homogenous units thus modelling the catchment as a series of lumped models (Jajarmizadeh *et al.*, 2012). The advantage of semi-distributed models is that unlike distributed models, they demand less data and can be used in data-scarce basins such as the Limpopo. The Pitman model (Pitman, 1973) was originally designed as a conceptual lumped model but in more recent versions (e.g. Hughes, 2004) the model is semi-distributed. In-depth details regarding the Pitman Model are discussed in Chapter 5.

2.4.3 Model calibration and validation

Hydrological processes can only be understood if the selected model is able to represent basin physical properties, adequately. In the case of rainfall-runoff models, model calibration involves systematically adjusting model parameter values, which represent basin physical properties, to acquire a set of parameters that provide the best estimate of the observed streamflow (Vaze *et al.*, 2012). The process is quite iterative as different values of parameters are trialled with the aim of improving the fit of the model to the observed data (Sawunyama, 2008). Calibration can be conducted either manually or automatically. Manual calibration requires an experienced user to adjust parameters interactively in successive model runs to improve results, while

automatic calibration utilises a computer algorithm to search the parameter space through performing multiple runs of the model such as the Shuffled Complex Evolution method (Duan *et al.*, 1992; Vrugt *et al.*, 2003). The main advantage with the automated approach is that the computer does much of the work of exploring parameters rather than the user and the procedure is objective (Sawunyama, 2008).

Model validation or testing or verification is a necessary step in hydrological modelling as it provides an assessment of the model's performance, as a way to ensure that modelling process produces the right results for the right reason. The model is said to be validated when there is an acceptable fit between the simulated and observed flow (Sawunyama, 2008).

2.5 CONCEPTUAL FRAMEWORK

2.5.1 Definition and significance of a conceptual framework

The hydrological cycle is a multi-faceted system that has several dominant processes e.g. precipitation, evaporation etc. that have been well documented and are well understood to exist in a state of continuum (Winter, 1985; Maser, 2015). The complexity of the system lies in its interaction with surface and subsurface landscapes as these are unique in location and scale, therefore the dominant catchment processes vary according to the hydrological basin being considered (Jajarmizadeh *et al.*, 2012;). In order to conduct a hydrological modelling exercise for a particular area, one needs to understand the interaction between the dominant hydrological processes and the surface and subsurface components of the hydrological basin being studied (Mockler, *et al.*, 2016). Development of a conceptual framework is deemed crucial as a starting point of any research as it aids the consolidation of available theoretical knowledge with the modeller's initial understanding of the research topic (Maxwell, 2005). Miles and Huberman (1994) defined a conceptual framework as a visual or written product

that explains, graphically or in narrative form, the key factors, concepts or variables to be studied and the presumed relationships among them. The framework should aim to answer questions such as:

- What do you think is going on within the system you plan to study?
- Why do think, whatever it is that is happening, is happening?
- What theories, beliefs, and prior research findings guide or inform your hypotheses?

Similar to conceptual models that are simplified representations of real-life systems (Robinson, 2006), in hydrology, conceptual frameworks are often designed to represent the hydrological basin and provide a simplified illustration of the physical components and interactions between the surface and subsurface systems, in the form of flow paths (Jajarmizadeh *et al.*, 2012; Mockler *et al.*, 2016). Figure 2.3 illustrates the flow paths occurring between water stores in the hydrological cycle. It is understood that part of the uncertainties that prevail in hydrological modelling arises from misinterpretation of the basin processes which is consequently influenced by the modeller's perception of the processes (Tshimanga, 2012), therefore the development of conceptual framework aims to improve conceptual understanding of basin dynamics and facilitate data analysis.

2.5.2 Components of a conceptual hydrological framework

As can be expected, the design of a conceptual hydrological framework is often unique to the hydrological system being researched. An integrated assessment (Letcher *et al.*, 2007) or integrated systems analysis approach (Nepal, 2014) has been suggested as a way of considering all the ecological, socioeconomic, climatic, anthropogenic and basin physical characteristics that may impact availability of water resources. Process flow diagrams (Figure 2.4) are generally used to illustrate dominant hydrological stores and the flow paths that connect stores. Alternatively a graphic diagram (Figure 2.5) can be used to convey the same hydrology setting.

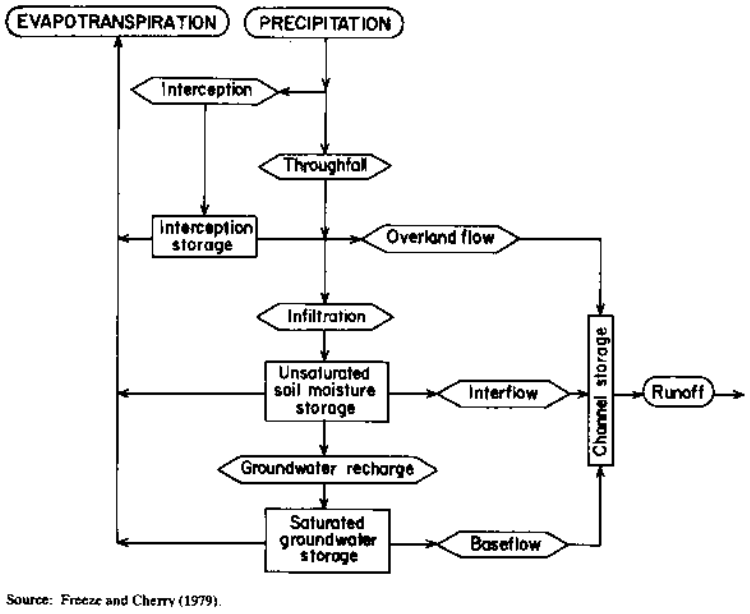

Figure 2.3. A systems representation of the hydrological cycle (Freeze and Cherry, 1979).

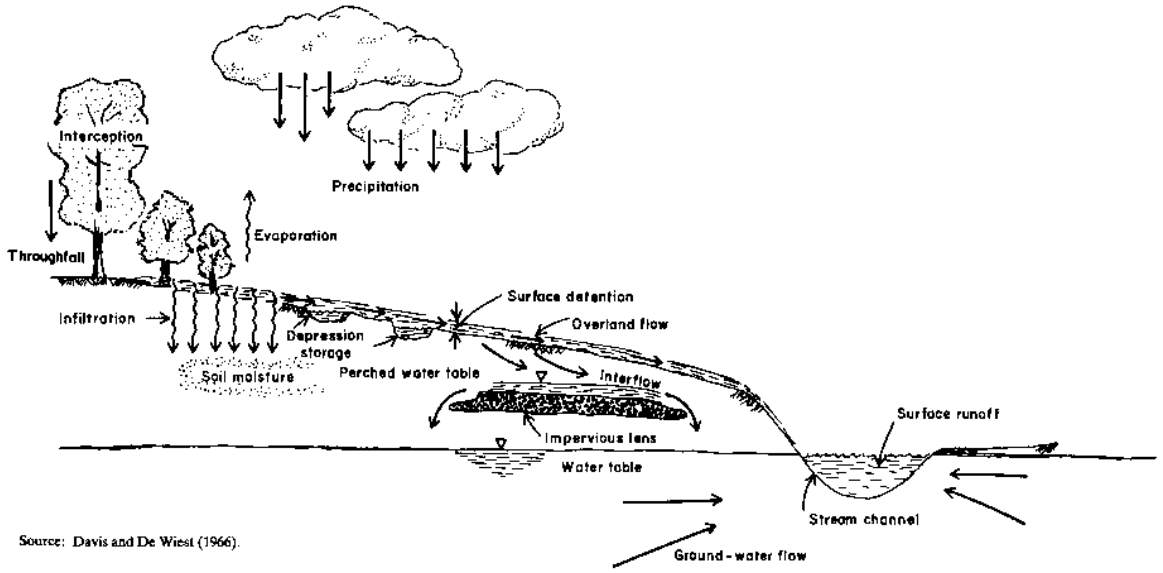

Figure 2.4. A diagrammatical representation of the hydrological cycle (Davis and De Wiest, 1966).

2.6 CLOSING REMARKS

The purpose of this literature review was to synthesise the available knowledge on the main themes discussed in the dissertation, in an effort to determine the best approach in meeting the objectives of the study. The review of channel transmission losses

indicated that there is relatively good agreement on which processes define channel transmission losses and the significance of loss processes in semi-arid regions. The methods that have been applied in estimating channel transmission losses vary from study to study however the use of remote sensing techniques and fieldwork has been beneficial in locating sites that manifest flux activity between streams and adjacent aquifers. While some studies were successful in quantifying channel transmission losses, others could only report on the behavioural impact of loss processes on available water resources. River processes and morphology determine the type of alluvial aquifer that forms. The relevance of conceptual frameworks in hydrological modelling has also been well acknowledged. It is clear from the research reviewed that a conceptual yet clear understanding of the main hydrological processes and dominant water uses operating in the study areas is imperative in understanding the role of channel transmission losses on the availability of surface water resources in each catchment.

CHAPTER 3
Study Areas

3.1 INTRODUCTION

This chapter describes the three areas selected for this study in terms of their physiographical (geography and topography), hydro-metereological (climate, hydrology and hydrogeology), water and land use characteristics. Various initiatives (FRIEND, Hydro1K, the AlcomWWF, HydroSHEDS, Water Resources Institute, LRBMS) have provided differing basin and catchments delineations for the Limpopo River Basin based on their demarcation of the basin's river morphology (Mwenge Kahinda *et al.*, 2016). For the purpose of this study, the Limpopo River Basin Monograph Study (LRBMS) delineation is used. In addition, the nomenclature used to denote lower order catchments differs from country to country i.e. in South Africa a quaternary catchment is used to denote a fourth order hydrological catchment (DWS, 2011), while Zimbabwe and Botswana refer to sub-zones and catchments, respectively. For this purpose of this study, lower order catchments (sub-divisions of sub-basins) are all referred to as catchments.

3.2 SELECTION OF CASE STUDY AREAS

The Limpopo River basin is made up of 27 sub-basins, three of which were selected for this study (Figure 3.1). These sub-basins are the Mokolo sub-basins (in South Africa), Motloutse sub-basin (in Botswana) as well as Mzingwane sub-basin (in Zimbabwe). The selection of these three study areas was dependent on the existence of alluvial deposits as well as a need to look at different parts of the basin.

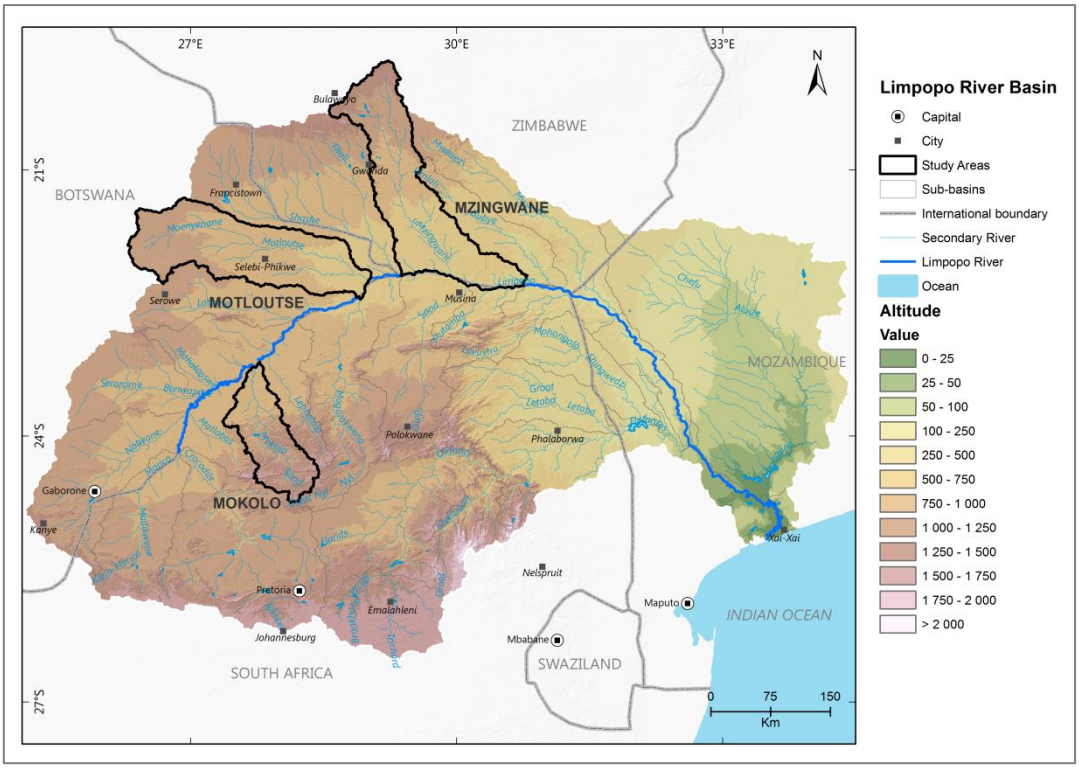

Figure 3.1. The three sub-basins chosen for the study relative to the Limpopo River Basin.

3.3 THE MOKOLO SUB-BASIN

3.3.1 Physiography of the Mokolo sub-basin

The Mokolo sub-basin (Figure 3.2) falls within the South African portion of the Limpopo River Basin and covers an area of 8 417 km^2 (Howard *et al.*, 2013). In South Africa the Mokolo sub-basin forms part of the Limpopo Water Management Area (DWS, 2016) and comprises 9 catchments, namely A42A to A42J.

The Mokolo sub-basin has vast flat open areas across much of its area with several small hills and steep gorges lining the path of the Mokolo River from the southern end of the sub-basin, which is marked by the Waterberg Mountains (RHP, 2006). Limpopo River Awareness Kit (2011) gives the highest elevation in the sub-basin as 1,833 m with 782 m being the lowest.

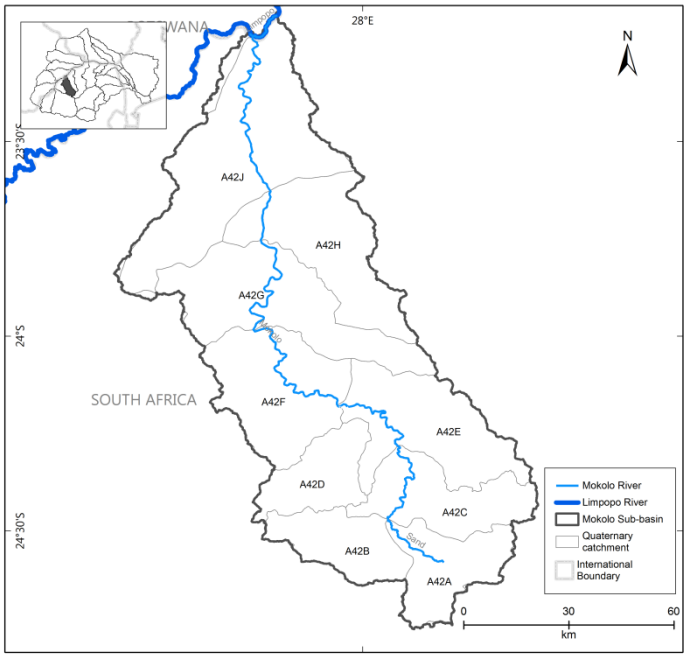

Figure 3.2. The Mokolo sub-basin and its 9 quaternary catchments.

3.3.2 Geology and soils of the Mokolo sub-basin

In the upper and middle Mokolo sub-basin (Figure 3.3), sandstones, conglomerates and diabase of the Waterberg Group and Glentig Formation are prevalent (RHP, 2006; Prucha *et al.*, 2016). The geology of the lower sub-basin is characterised by sandstones and mudstones of the Karoo Supergroup of Permian to Triassic age (Esterhuyse, 2012; Prucha *et al.*, 2016). Quaternary alluvial deposits are found along the length of the river and are characterised as medium to deep coarse-grained sandy-clay loam along the upper reaches, while moderately deep sandy loam soils dominate the lower floodplains (Midgley *et al.*, 1994; Ashton *et al.*, 2001). Batjies (2004) provides a more detailed classification of the soil types in Figure 3.3 which shows the distribution of other soil types across the sub-basin. Hydraulic investigations conducted by DWS (2010) have described the riverbed alluvium as having a thickness varying between 5 m to greater than 25 m.

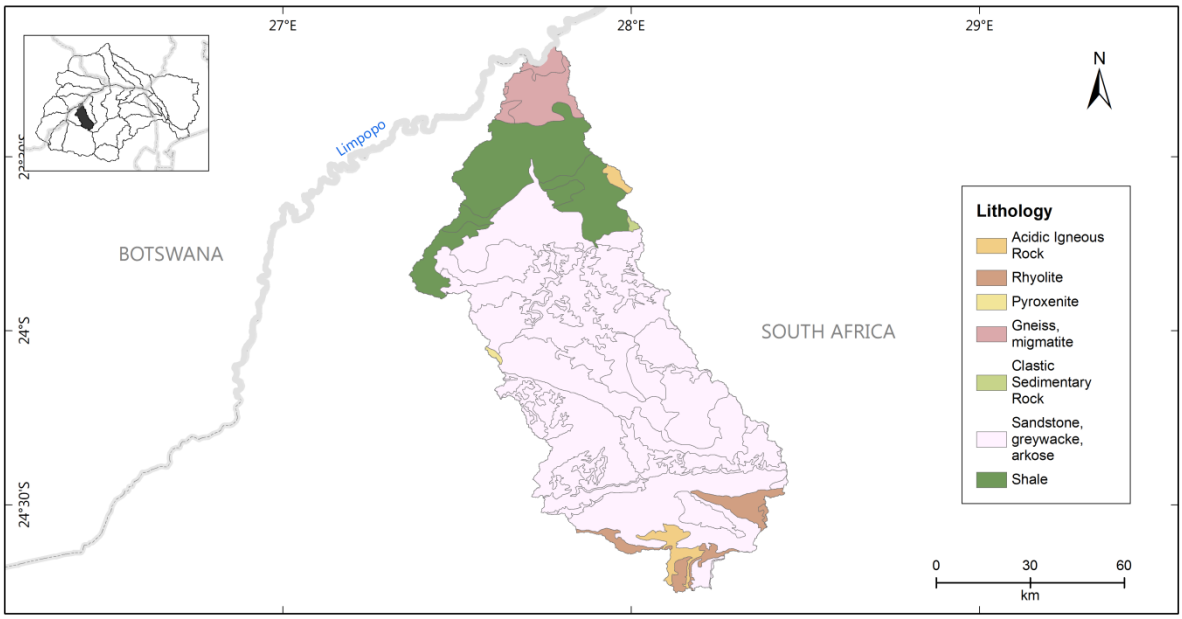

Figure 3.3. Geology of the Mokolo sub-basin (Batjies, 2004).

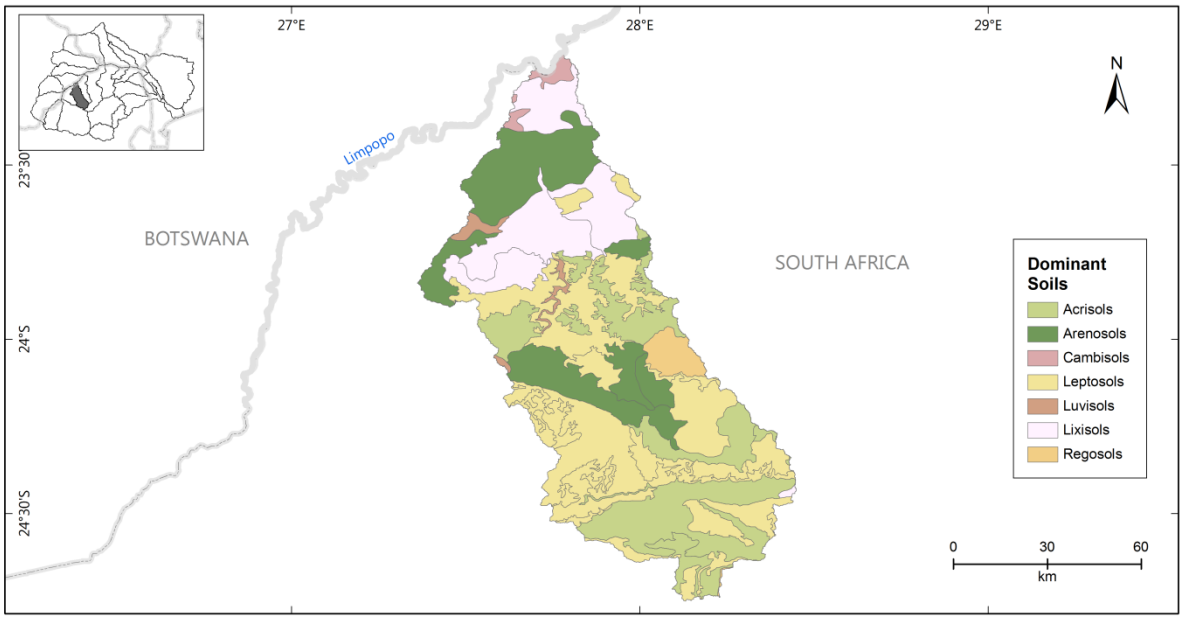

Figure 3.4. Distribution of soil types across the Mokolo sub-basin (Batjies, 2004).

3.3.3 Climate and hydrology of the Mokolo sub-basin

The Mokolo sub-basin is characterised by an arid to semi-arid climate (DWA, 2014). Average air temperatures vary between 14°C in the south and 22°C in the north (RHP,

2006). Rainfall, which occurs mainly during the summer months, decreases in a gradient from 700 mm in the mountainous Waterberg area to 400 mm in the low-lying Limpopo Plain (RHP, 2006). The mean potential evaporation recorded in the area is 1 900 mm a^{-1} which far exceeds the average rainfall (Howard *et al.*, 2013).

The Mokolo River rises in the Waterberg Mountains and flows north-easterly towards the Limpopo River. The flow of the Mokolo River and its tributaries is largely perennial, except for its lower reach and other lower order streams, which respectively display ephemeral (summer flow) and episodic characteristics (Boroto and Görgens, 1999). The inconsistent flow of the Mokolo has resulted in several oxbows and isolated off-channel sand pools along the lower reach of the river (RHP, 2006). According to the Limpopo River Basin Monograph Study (Howard *et al.*, 2013), the natural MAR of the Mokolo River is 210 Mm^3a^{-1}. The river flow is however highly regulated by the Mokolo Dam which has a total full storage capacity of 145 Mm^3 (DWS, 2017). The hydrogeology of the Mokolo sub-basin comprises of fractured and intergranular secondary aquifers of the Karoo Sequence, Waterberg Formation and Archaean Basement Complex as well as quaternary alluvium which constitutes primary alluvial aquifers along the bed of the river and some of its tributaries (Titus and Rossouw, 2008).

3.3.4 Water and land use in the Mokolo sub-basin

Land use in the Mokolo sub-basin is dominated by agriculture, game farming and recreational private reserves (RHP, 2006). Mining of sand along the lower reaches of the Mokolo has led to the removal of vegetation along these reaches, destabilising the river banks and beds and leading to increased erosion during periods of high flow and flooding (RHP, 2006). About 87% of the water is used for agricultural activities while the remainder contributes to the industrial, mining, power generation and domestic water supply service sectors (municipalities) (DWA, 2012). The Mokolo Dam plays a major role in the hydrology of the sub-basin. Along with providing water for irrigation of commercial agriculture and domestic use for the town of Lephalale, the water stored

in the dam is used to supply the Matimba Power Station and Grootgeluk coal mine (Lombaard *et al.*, 2015).

3.4 THE MOTLOUTSE SUB-BASIN

3.4.1 Physiography of the Motloutse sub-basin

The Motloutse sub-basin is situated in the Botswana portion of the Limpopo Basin on the left-hand bank of the main river, covering an approximate area of 19,393 km^2 (Howard *et al.*, 2013). The sub-basin is sub-divided into 5 catchments as mapped in Figure 3.5 (LIMCOM, 2013).

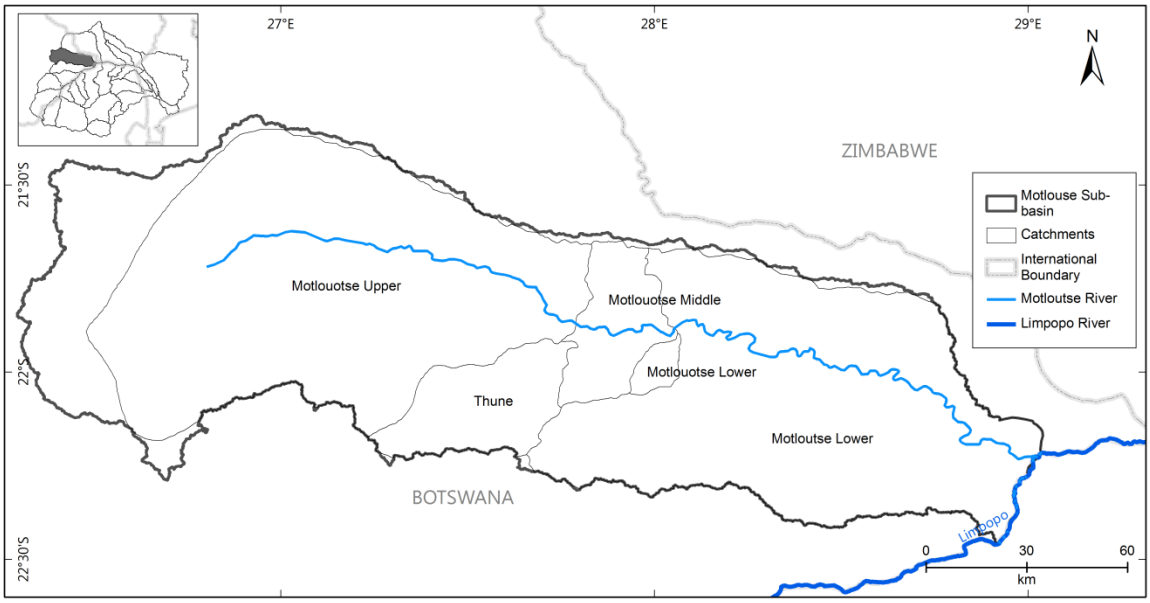

Figure 3.5. The Motloutse sub-basin and its five catchments.

3.4.2 Geology and soils of the Motloutse sub-basin

The geology of the Motloutse sub-basin (Figure 3.6) is characterised by rock types belonging to the Kalahari Craton which includes Gaborone and Mahalapye granites. Other rock formations include the Palapye Suite which comprises mainly of clastic sedimentary rock and the basaltic and coal-rich sedimentary Lebung Formation of the

Karoo System (Ashton *et al.*, 2001; Haddon, 2005). A significant characteristic of the Motloutse River is the presence of deep sand deposits on the channel bed, which has earned the river and several others in Botswana, the classification of 'sand river' (Wikner, 1980; Botswana DWA, 1989). The alluvial deposits range from 4 - 9 m in depth over the length of river from about 20 km upstream of Mmadinare to the Limpopo confluence; however, localised rock bars confine the depth in places (Botswana DWA, 1989). The soils (Figure 3.7) found in the sub-basin include moderately shallow, coarse-grained feldspathic to kaolinitic sands, sandy loams as well as clay- and sodium-rich soils (Ashton *et al.*, 2001; Batjies, 2004). Aquifer types found in the Motloutse sub-basin are similar to those in the Shashe, namely primary alluvial aquifers and secondary fractured aquifers (Meyer and Hill, 2013). Extensive alluvial aquifers are noted in the lower Motloutse River and these are attributed to palaeochannel formed when the Okavango system was connected to the Limpopo drainage (CSIR, 2003).

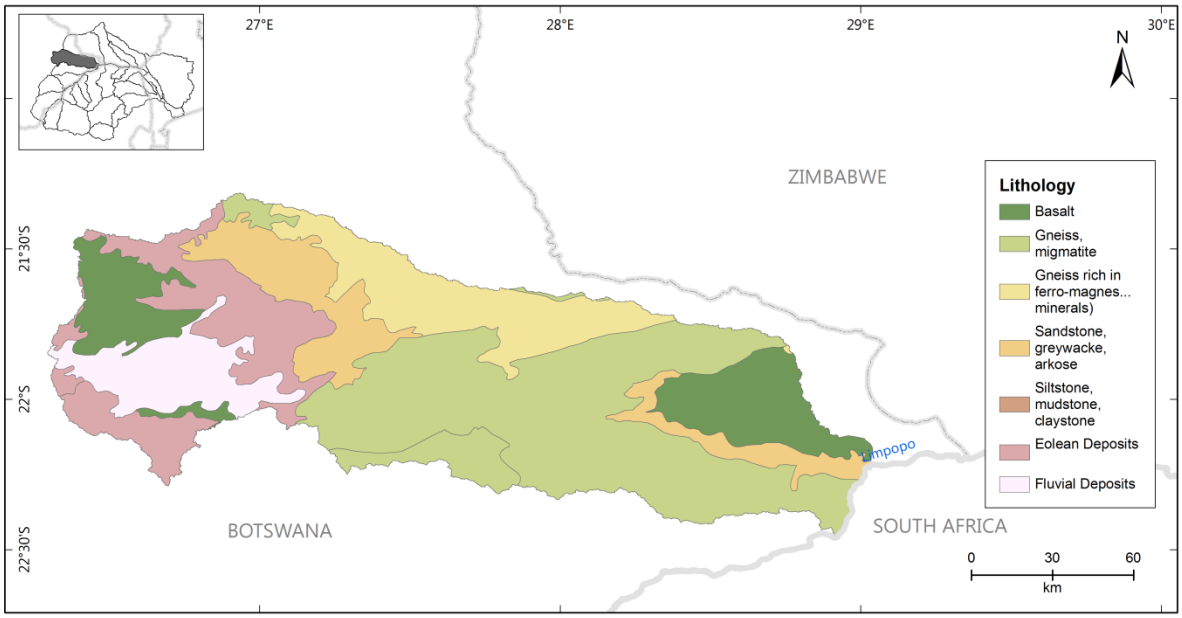

Figure 3.6. Geology of the Motloutse sub-basin (Batjies, 2004).

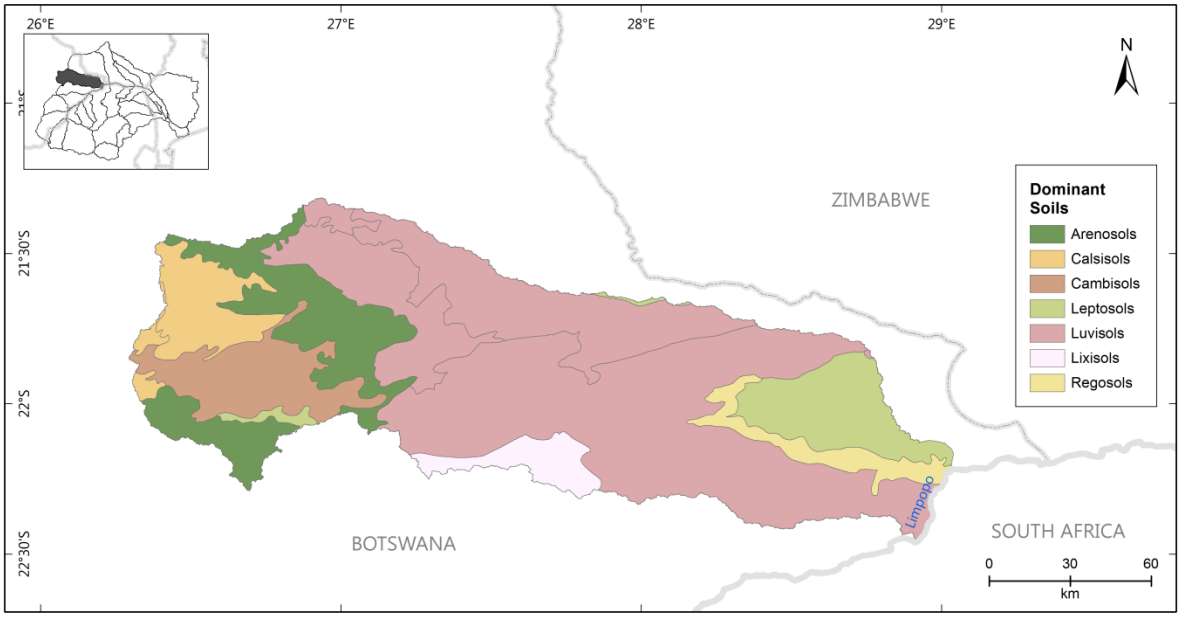

Figure 3.7. Distribution of soil types across the Motloutse sub-basin (Batjies, 2004).

3.4.3 Climate and hydrology of the Motloutse sub-basin

A semi-arid climate dominates the Motloutse sub-basin (Mafa, 2008). 90% of the MAP falls between November and March and it varies from around 450 mm a^{-1} in the upper sub-basin to below 350 mm a^{-1} near the confluence with the Limpopo; severe droughts are a frequent occurrence in the sub-basin. Maximum temperatures frequently exceeding 30°C (Kapangaziwiri *et al.*, 2017) occur in the summer months of October to February. In the winter months, mean minimum temperatures fall as low as 4°C. Potential evapotranspiration rates exceed rainfall across all the months (Botswana DWA, 1989).

The Motloutse River arises from a range of low hills at the eastern edge of the Kalahari Desert and flows to the south-west of Francistown before joining the Limpopo River some 40 kilometres upstream of the confluence of the Shashe and Limpopo rivers (Ashton *et al.*, 2001). The river flows mainly during summer rainfall and has an approximate natural MAR of 125 Mm^3 (Ashton *et al.*, 2001; Howard *et al.*, 2013) which however, is extremely variable and fluctuates widely from year to year (Botswana DWA, 1989). By 1990, the surface-water resource of the Motloutse sub-basin was fully developed to the limit of its naturalised mean annual runoff (CSIR, 2003).

3.4.4 Water and land use in the Motloutse sub-basin

Land use consists mostly of small-scale subsistence farming of drought resistant crops as well as livestock rearing of goats and donkeys. Most irrigation water use is based on water pumped from local boreholes (Ashton *et al.*, 2001). The alluvial deposits of the Motloutse River are an important local source of water and raw material for the copper-nickel mine at Selebi–Phikwe (Botswana DWA, 1989). The growing water shortage in Botswana prompted the construction of the North-South Carrier, a pipeline system that transports water from the Motloutse River southwards to the City of Gaborone (Ashton *et al.*, 2001).

3.5 THE MZINGWANE SUB-BASIN

3.5.1 Physiography of the Mzingwane sub-basin

The Mzingwane sub-basin (Figure 3.8) is situated in the Zimbabwe portion of the Limpopo River Basin on the left-hand bank of the Limpopo River, covering an approximate area of 19 393 km^2 (Howard *et al.*, 2013). It is sub-divided into ten hydrological zones namely: BUZ4, BNC, BIK, BIN2, BIN1, BUZ3, BUZ1, BL1 AND BL2 (Howard *et al.*, 2013). The physiography of the Mzingwane sub-basin is characterised by low-lying bushveld along the Limpopo River Valley which rises to a flat central plateau before reaching the northern highlands (GCBP-SRK, 2002).

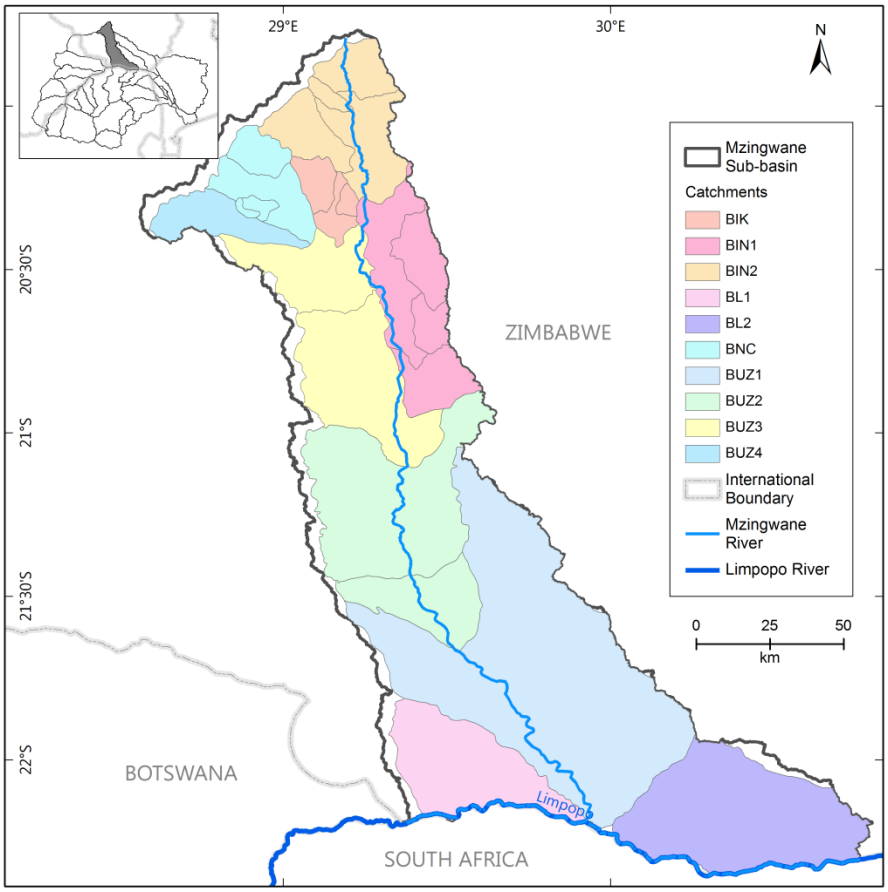

Figure 3.8. Mzingwane sub-basin and its sub-catchments.

3.5.2 Geology and soils of the Mzingwane sub-basin

The geology (Figure 3.9) of the northern half of the Mzingwane sub-basin comprises lithology belonging to the Zimbabwe Craton which includes formations such as the Bulawayo, Gwandana, Filabusi Greenstone Belts as well as granitic outcrops; the southern end is characterised by Limpopo Belt gneisses as well as Karoo Basalts and other sedimentary rocks (Ashton *et al.*, 2001). The aquifers in the Mzingwane sub-basin comprise both secondary fractured and primary alluvial aquifers (CSIR, 2003). Extensive work (Mansell and Hussey, 2005; Moyce *et al.*, 2006; Love *et al.*, 2007; Masvopo *et al.*, 2008) has been done in characterising the alluvial aquifers of the Mzingwane which are regarded as the most extensive of any of the tributaries of the Limpopo Basin (Görgens and Boroto, 1997). The alluvial deposits are described as 'clean-washed

sands' (Owen and Dahlin, 2005); Batjies (2004) provides a more detailed classification in Figure 3.10. According to Love *et al.* (2007), the alluvial aquifers are generally less than 1 km in width with areal extents ranging from 1km2 to 2.55 km in the channels and 0.85 km^2 to 4.3 km^2 on the flood plains. Moyce *et al.* (2006) reported that individual alluvial aquifers have been measured with areal extents ranging from 0.45 km^2 to 7.23 km^2 in the channels and 0.75 km^2 to 21.96 km^2 on the floodplains. When characterising the sand thickness of the Malala alluvial aquifer, a downstream aquifer found along the Mzingwane River, Masvopo *et al.* (2008) described sand thickness of between 5m and 25m, with an average porosity of 39%. Owen and Dahlin (2005) and Moyce *et al.* (2006) have respectively reported porosities of the order 35% and 30% along the Mzingwane River. Owen and Dahlin (2005) based their porosity values on direct measurements which were conducted at Bwaemura and on values obtained from other alluvial channels in the region (Nord, 1985, Owen, 1994). Moyce *et al.* (2006) conducted their study at various sites including J.Z. Moyo School, Bwaemura Village and Mtetengwe Village.

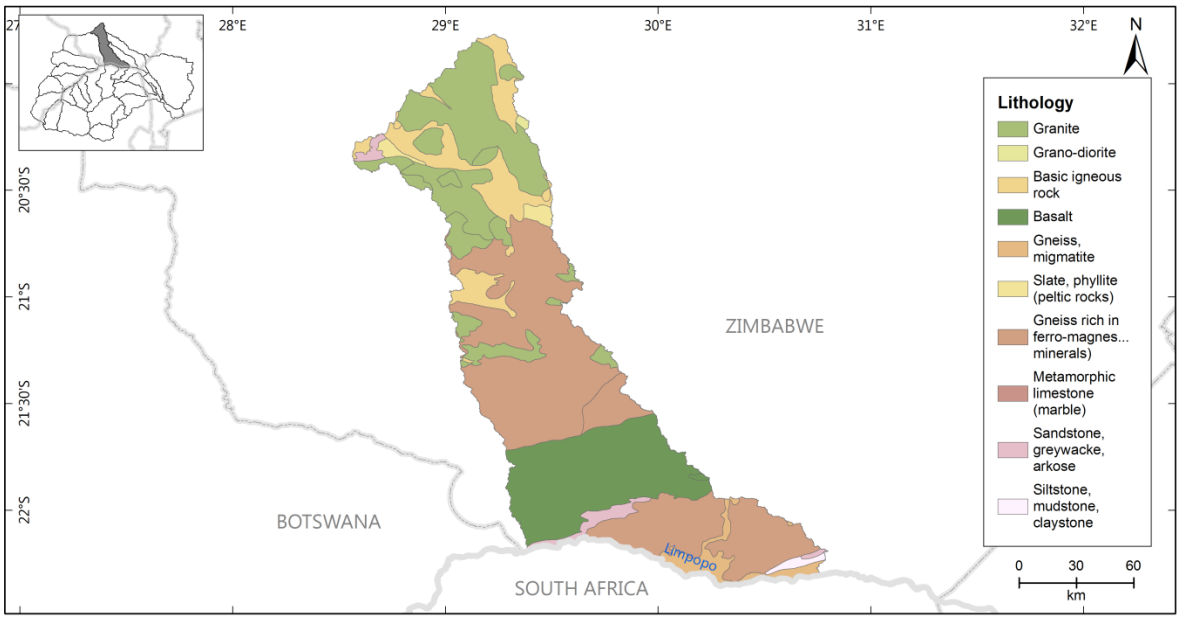

Figure 3.9. Geology of the Mzingwane sub-basin (Batjies, 2004).

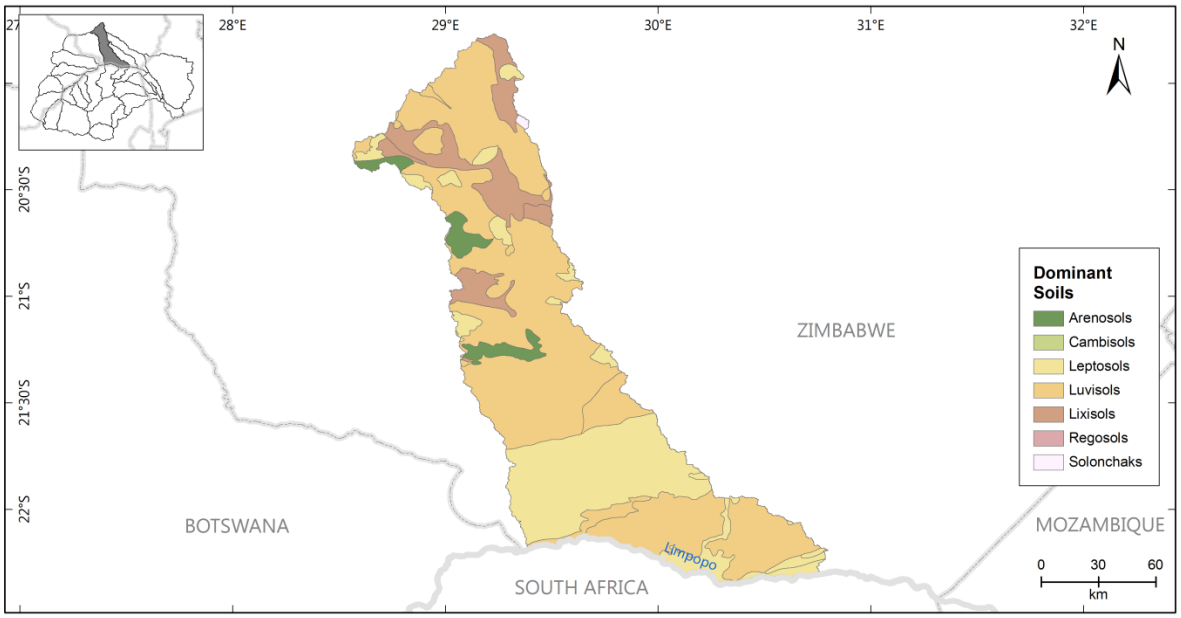

Figure 3.10. Distribution of soil types across the Mzingwane sub-basin (Batjies, 2004).

3.5.3 Climate and hydrology of the Mzingwane sub-basin

The Mzingwane sub-basin experiences a semi-arid climate with areas in the upper reaches of the sub-basin receiving an MAP as high as 800mm a^{-1}, while those in the lower reaches have an MAP as low as 300mm a^{-1} (Love *et al.*, 2007). Similar to the other sub-basins, the mean potential evaporation of over 1800 mm far exceeds the MAP in the sub-basin (Howard *et al.*, 2013).

The Mzingwane River (uMzingwane or Umzingwani River) arises near Bulawayo and flows south into the Limpopo River near the town of Beitbridge. It is an ephemeral river with flow generally restricted to the rainy season (November to March) and the natural MAR recorded is 437.8 Mm^3a^{-1}. However, the 'current day' MAR is reported as 262.6 Mm^3a^{-1}, indicating that the river is highly developed (Howard *et al.*, 2013). Two of the larger dams built in the Mzingwane sub-basin include the Insiza Dam (with capacity of 173.4 Mm^3) on the Insiza River and Zhovhe Dam (130.4 Mm^3) on the Mzingwane River (Howard *et al.*, 2013).

3.5.4 Water and land use in the Mzingwane sub-basin

Major water uses in the sub-basin are domestic, industrial, mining and agricultural (Mabiza *et al.*, 2007). Wildlife farming and horticulture are also practiced with wildlife farming carried out usually in conjunction with the tourism industry (Kapangaziwiri *et al.*, 2017). Commercial agriculture in tobacco, maize, wheat, and livestock is also carried out in other different parts of the sub-basin. Land use in the upper reaches comprises mainly commercial farming, private and resettlement land, while lower reaches consists mainly of game farms, communal lands and irrigated citrus estates (Ashton *et al.*, 2001; Moyce *et al.*, 2006).

3.6 CLOSING REMARKS

The description of each sub-basin provides knowledge that supports the conceptual understanding of the dominant processes such as channel transmission losses that may influence the hydrology and water resource availability in these areas. Additionally, this provides insight into the setting up of parameters for hydrological modelling. Further detail regarding the ranges of climatic data and hydraulic properties of the alluvial aquifers used in the hydrological modelling objective of the study is provided in Chapter 4.

CHAPTER 4
Methodology, data collection and analysis

4.1 INTRODUCTION

Chapter 4 describes the approaches applied in collating and processing the data for the study. The chapter is structured in a manner that depicts the order in which data were collected and processed for both aquifer delineation and hydrological modelling. It details the type of data and respective sources used for the collection of satellite imagery, hydrogeological maps and spatial datasets required for aquifer delineation as well as the literature which informed the determination of the hydraulic properties of the alluvial aquifers. Similarly the data collected for hydrological modelling, including climatic and hydrological data, are described. The methods applied in delineating the alluvial aquifers and estimating potential transmission losses as well as the use of the Pitman Model (Hughes, 2004) for simulating channel transmission losses are also discussed.

4.2 DATA COLLECTION FOR ALLUVIAL AQUIFER DELINEATION

One of the objectives of the study was to identify reaches within the Limpopo River Basin where channel transmission losses are expected to be prevalent. To identify these alluvial aquifers, land cover classification was applied through use of remote sensing and geographical information systems (GIS) techniques. Land cover describes the visible physical features which cover the Earth's surface; examples of said features include vegetative cover, whether naturally-occurring or cultivated, bare ground, water surfaces and man-made infrastructure including buildings and roads (Campbell and Wynne, 2011). The role of land cover classification and mapping is therefore essential

in resource and land-use management as it can provide an analysis of land cover changes over time and can thus help in monitoring urban expansion, identifying agricultural developments and assessing the extent of natural vegetative habitats (Horning, 2004). Conventionally, land cover classification is conducted with the help of aerial photography and topographical maps; however with the advancement of satellite technology, data acquisition and processing is more rapid and remotely-sensed data have proven to be more adequate in providing detailed information regarding the spatial, spectral and temporal properties of objects on the Earth's surface, which assists with precise identification (Horning, 2004). Along with satellite imagery, ancillary data comprising literature and hydrogeological GIS spatial datasets from previous studies conducted in the region are used to verify and validate the location and extent of the identified alluvial aquifers.

4.2.1 Satellite imagery

The primary data used for alluvial aquifer delineation comprised georeferenced multispectral Landsat-8 Operational Land Imager (OLI) imagery and Shuttle Radar Topographic Mission (SRTM) Digital Elevation Model (DEM). Both datasets have global coverage, are well calibrated and processed and are available freely from reliable sources. Landsat-8 imagery was accessed from the United States Geological Society (USGS) Global Visualization Viewer (GloVis) (https://glovis.usgs.gov/) download portal. The multispectral Landsat-8 sensor which captures the imagery comprises nine spectral bands (Table 4.1) with a spatial resolution of 30 m for Bands 1 to 7 and 9; the resolution for Band 8 (panchromatic) is 15 m. Additional thermal bands 10 and 11, from the Thermal Infrared Sensor, are collected at 100 m. Table 4.1 summarises the band specifications of landsat-8 OLI. A spectral band refers to a defined portion of the electromagnetic spectrum; the length and location of that portion along the electromagnetic spectrum is characterised by the range of wavelength with which it is associated (Campbell and Wynne, 2001). The resolution refers to the spatial detail the satellite is able to capture i.e. Landsat-8 has a spatial resolution of 30 m which means

that a 30 m pixel represents an area that is 30 m on the ground. The coverage of the Earth's surface which is captured by the sensor is called a scene and the approximate size for the each Landsat-8 scene is 170 km north-south by 183 km east-west (USGS, 2016).

Table 4.1. Landsat-8 OLI and TIRs band specifications (Barsi *et al.*, 2014)

Bands	**Wavelength (µm)**	**Resolution (m)**
Band 1 - Ultra Blue (coastal/aerosol)	0.431 - 0.451	30
Band 2 - Blue	0.452 - 0.512	30
Band 3 - Green	0.533 - 0.590	30
Band 4 - Red	0.636 - 0.673	30
Band 5 - Near Infrared (NIR)	0.851 - 0.879	30
Band 6 - Shortwave Infrared (SWIR) 1	1.566 - 1.651	30
Band 7 - Shortwave Infrared (SWIR) 2	2.107 - 2.294	30
Band 8 - Panchromatic	0.503 - 0.676	15
Band 9 - Cirrus	1.363 - 1.384	30
Band 10 - Thermal Infrared (TIRS) 1	10.60 - 11.19	100 * (30)
Band 11 - Thermal Infrared (TIRS) 2	11.50 - 12.51	100 * (30)

** TIRS bands are acquired at 100 meter resolution, but are resampled to 30 meter in delivered data product.*

Twenty six scenes (Table 4.2) were collected for the Limpopo River Basin. Several of the alluvial deposits on the plains of the Limpopo River Basin are used for agricultural purposes (Ashton *et al.,* 2001; Moyce *et al.*, 2006), therefore dry season Landsat-8 scenes (Figure 4.1) were used in order to maximize the spectral distinction between naturally-occurring and irrigated vegetation.

Table 4.2. List of Landsat-8 scenes collected for the Limpopo River Basin. Suitable dry season images captured between 2015 and 2016 were chosen for the delineation.

Path	Row	Date Acquired	Path	Row	Date Acquired
172	74	12/07/2015	170	77	14/07/2015
172	75	12/07/2015	170	78	14/07/2015
172	76	12/07/2015	169	75	08/08/2015
172	77	12/07/2015	169	76	08/08/2015
172	78	12/07/2015	169	77	05/06/2015
171	74	05/07/2015	169	78	05/06/2015
171	75	05/07/2015	168	75	16/07/2016
171	76	05/07/2015	168	76	16/07/2016
171	77	05/07/2015	168	77	16/07/2016
171	78	05/07/2015	167	75	09/07/2015
170	74	12/06/2015	167	76	09/07/2015
170	75	12/06/2015	167	77	09/07/2015
170	76	12/06/2015			

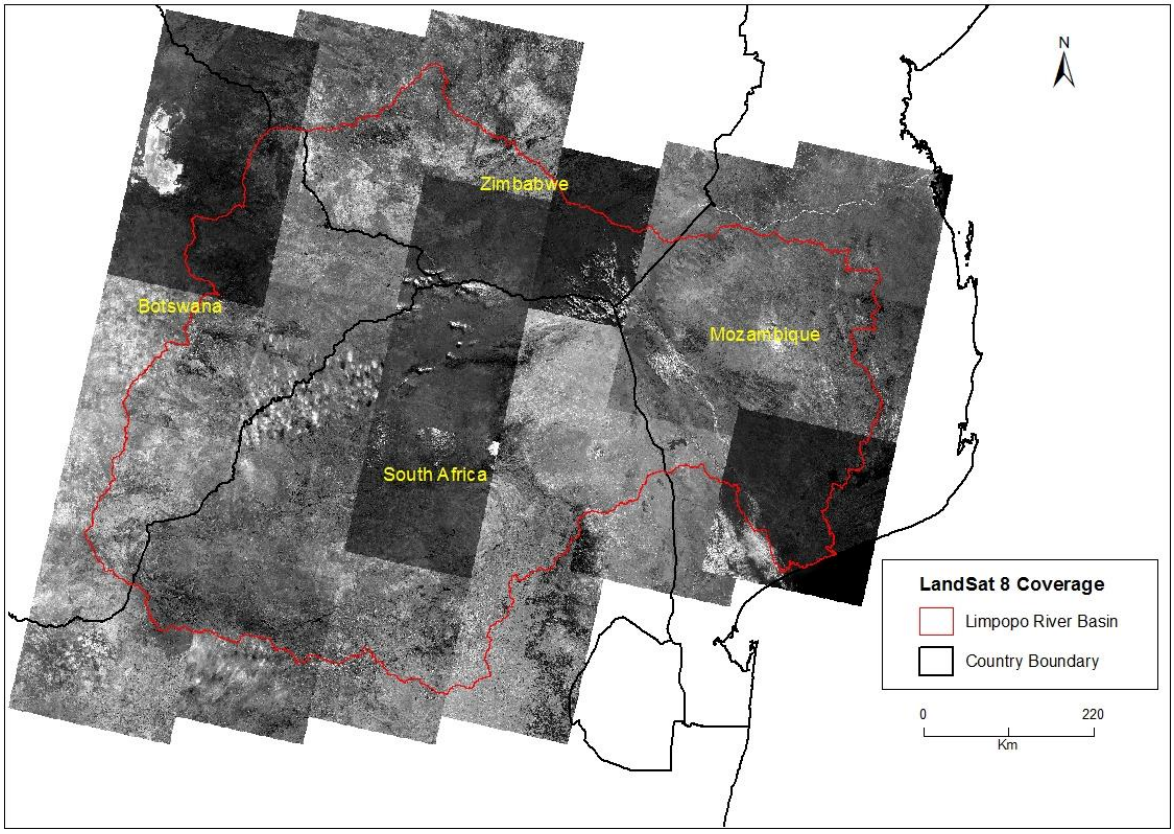

Figure 4.1. Landsat-8 OLI coverage of the Limpopo River Basin. Each individual scene was atmospherically corrected and classified before being mosaicked with the rest.

The 30 m resolution SRTM DEM data was downloaded from the Remote Pixel geospatial website (https://remotepixel.ca/) which hosts DEM data from the National Aeronautics and Space Administration (NASA) elevation radar data project (NASA, 2017). One hundred and thirteen tiles (113) were collected between the latitudes 19°-24° S and longitudes 24°-34° E (Figure 4.2) and mosaicked to create one large DEM that covers the entirety of the Limpopo River Basin, including the extent of each Landsat-8 scene .

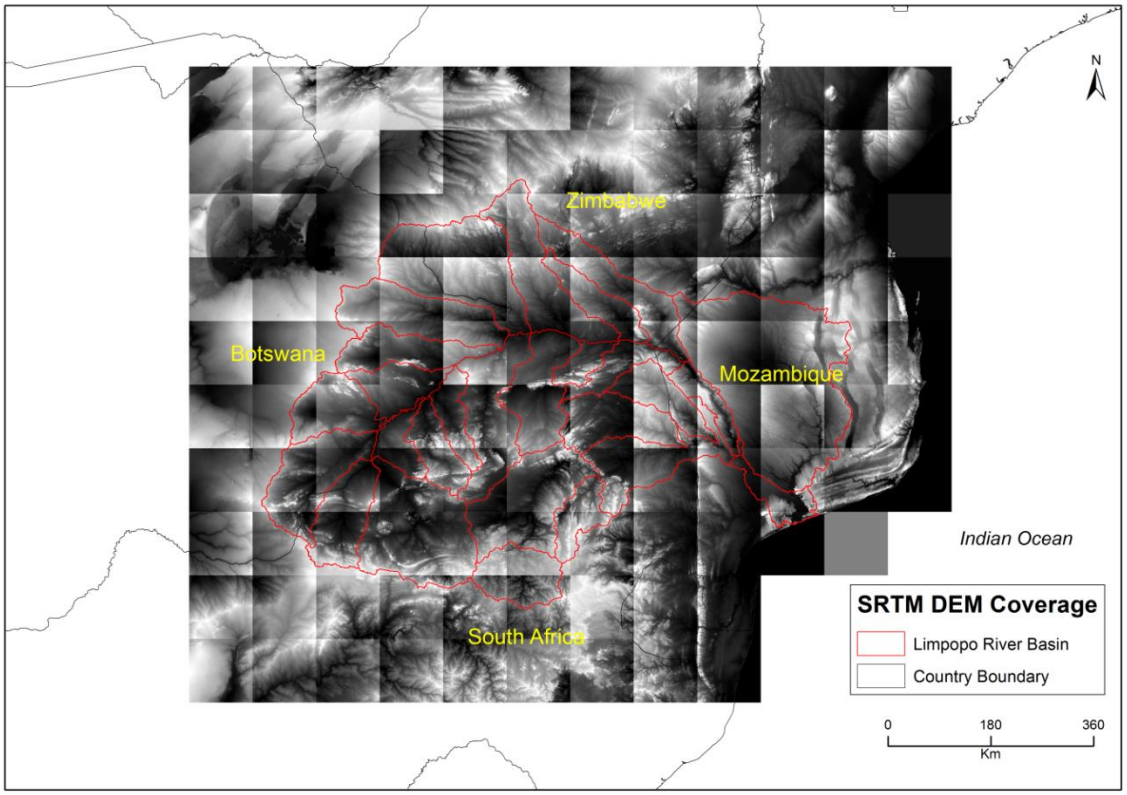

Figure 4.2. SRTM DEM coverage of the Limpopo River Basin.

4.2.2 Land cover, land use and river network

While the Landsat-8 imagery does provide detail regarding the land cover and land use activities in the study area, its resolution of 30 m is quite coarse making it difficult to identify land covers and uses occurring in localised small extents; therefore Google Earth coverage, which can be zoomed to beyond 30 m, was additionally used to

ascertain the extent of alluvium occurring along the tributaries as well as to identify the other physical features of a region.

To pinpoint the location of the various tributaries of the Limpopo river system and confirm their extent on the remotely-sensed datasets, the Limpopo River Basin Monograph Study (LIMCOM, 2013) delineation of the river network was used. The spatial dataset occurs in GIS format at a resolution of 1:5 000 000 and comprises a basin-wide shapefile of the main tributaries of the Limpopo River.

4.2.3 Soil Coverage

Soil data are useful in process modelling as they give an indication of the hydraulic properties that may influence the type and prevalence of hydrological processes present in a particular setting (Tshimanga, 2012). Mapped soil type and distribution in the study area were used to determine the effective porosity and aquifer depth associated with particular alluvium. Data were collected from the Soil and Terrain Database for Southern Africa (SOTERSAF) (ISRIC, 2003) which comprises, amongst other datasets, the SOTER-GIS shapefiles for southern Africa (SOTWIS-SAF) (Batjies, 2004). The SOTWIS-SAF dataset provides spatial classification of various soil, lithology and landforms in the southern Africa region. More specific parameter estimates relating to the soil coverage includes available water capacity, bulk density, soil drainage and the relative area of the dominant soil unit.

4.2.4 Geology and hydrogeology

Gaining knowledge of the type and distribution of geology in the Limpopo River Basin was essential to the study as that information provided insight into the type and distribution of aquifers prevalent in the region. A significant and detailed account of the geology and hydrogeology of the Limpopo River Basin has been documented within a few regional studies (e.g. CSIR, 2003; FAO, 2004; Owen and Madari, 2009;

SADC-HGM, 2010) as well as several other site-specific ones such as Love *et al.* (2007). With regards to this study, data relating to dominant lithology was collected from the SOTWIS-SAF (Batjies, 2004) spatial dataset as it provides a basin-wide coverage of the geology, although it is represented on a rather low resolution (Table 4.3). Similar to the soil coverage, the dataset occurs as GIS shapefiles. The distribution of aquifers across the basin was mapped using data retrieved from the SADC Hydrogeological Mapping Project (SADC-HGM, 2010) which focused on mapping the various hydrogeological environments across southern Africa and the extent and type of aquifers occurring in this region. The same dataset was used by the LIMCOM (2013) to illustrate the distribution of aquifers across the Limpopo River Basin (Figure 4.3). For the South African sub-basins, the Department of Water and Sanitation 1: 500 000 hydrogeological map datasets (DWAF, 2002) which cover portions of the Limpopo River Basin were also utilised to further validate the presence of alluvium along the relevant South African tributaries.

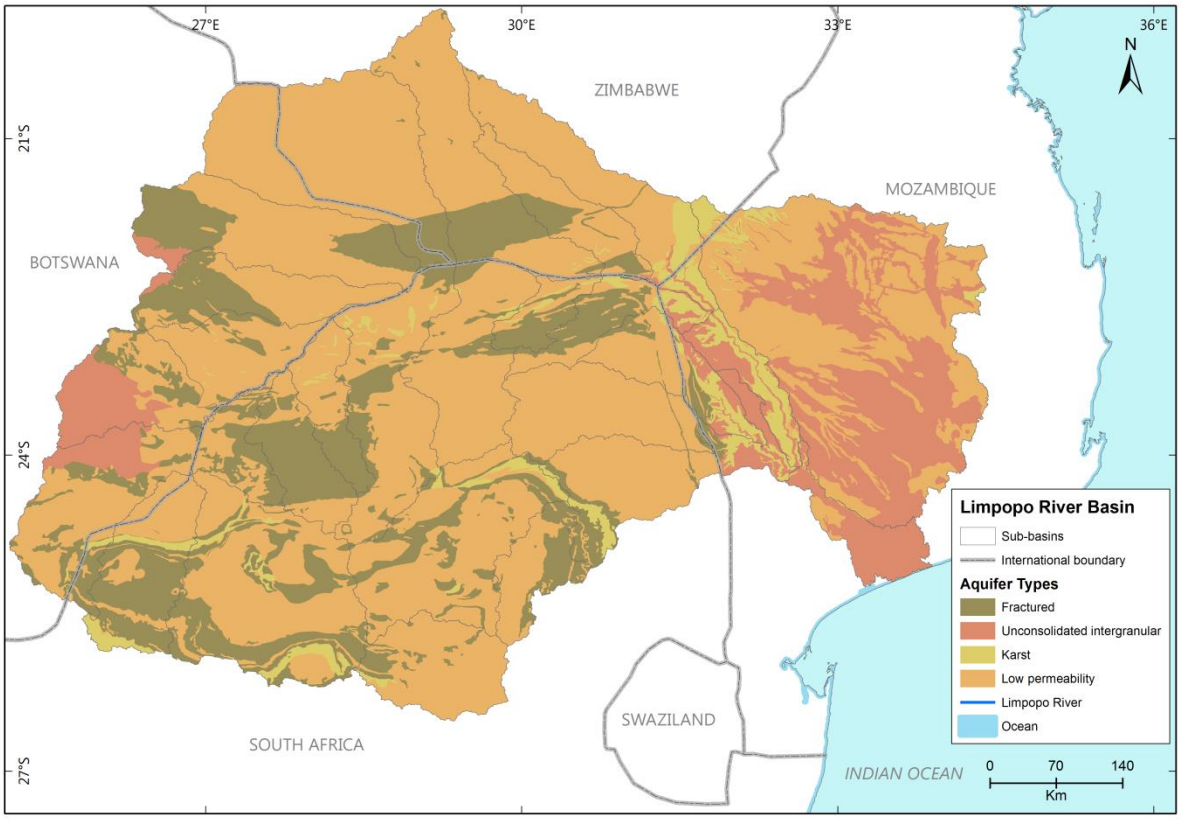

Figure 4.3. Distribution of aquifers across the Limpopo River Basin (LIMCOM, 2013).

Table 4.3. Spatial data collected and used in the study

Data set	Description	Spatial Resolution	Source
Satellite imagery	Landsat-8 OLI[a] coverage of study area	30 m, 15 m	USGS, 2015
Elevation	SRTM[b] digital elevation model	30 m	Jarvis, 2008
Terrain slope	SRTM digital elevation model	30 m	Jarvis, 2008
Soil types	Regional soil classification	1:2 000 000	Batjies, 2004
Dominant lithology	Regional geology	1:2 000 000	Batjies, 2004
River Network	Delineation of Limpopo River Basin river network	1:5 000 000	Howard *et al.*, 2013
Land cover and use	Google Earth coverage of study area	30 m	Google Earth, 2016

[a]*OLI Operational Land Imager*
[b]*SRTM Shuttle Radar Topographic Mission*

4.3 DATA PROCESSING FOR ALLUVIAL AQUIFER DELINEATION

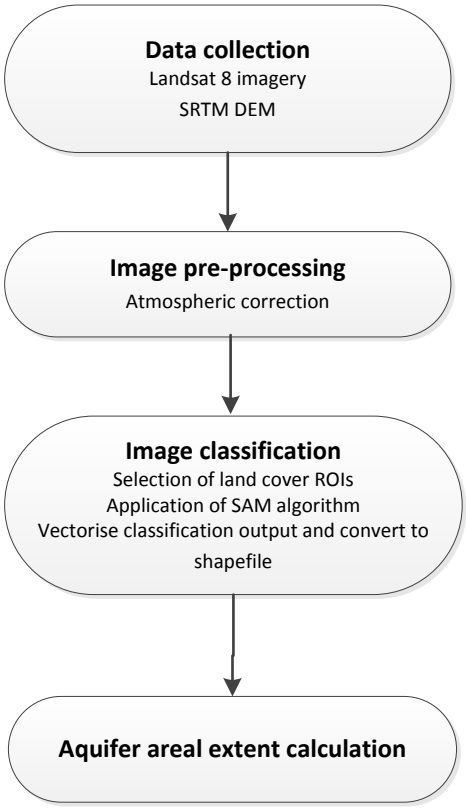

Figure 4.4. Approach applied to delineating alluvial aquifers in the Limpopo River Basin.

4.3.1 Image pre-processing

When a satellite sensor captures a multispectral image of the earth, it captures all of the Earth's physical properties including cloud cover and atmospheric haze. This modifies the surface reflectances processed by the sensor, creating errors that influence the quality of the remote information extracted by the satellite (Hadjimitsi *et al.*, 2010). Atmospheric correction is therefore applied to minimise this error by removing the atmospheric effects. In this study, atmospheric correction was conducted using the ATCOR-3 software. The process involved initially defining the sensor type (i.e Landsat-8), the dominant terrain in the particular Landsat-8 scene (i.e. flat or mountainous) and the aerosol type (i.e. rural or urban atmosphere). With regards to mountainous scenes, the DEM data was incorporated in the correction process in order to account for slope features that can cause shadows to form on the image. Further processing involved selecting the atmospheric feature to be corrected e.g. haze removal, shadow, cirrus cloud etc. The correction is automated and delivers a processed output image that is clearer and more illuminated.

4.3.2 Image interpretation and classification

To interpret the atmospherically-corrected image and conduct land cover classification, ENVI 4.8 software was used. Image interpretation included an analysis of the panchromatic Band 8 image and a false colour composite image produced from Bands 4, 5 and 6 (FCC 456). Descriptions of the band combination used are detailed in Table 4.4. A similar study by Moyce *et al.* (2006), which used a similar band combination, describes the use of the panchromatic and false colour composite images to distinguish channel alluvial deposits from floodplain alluvial deposits. Alluvial deposits stand out as bright white areas within the extent of the river channel on a panchromatic band (Figure 4.5a). In the FCC RGB 456 image, the dry alluvial deposits are also white with moist sands reflecting an off-white pink hue. Sands that are more saturated reflect a brighter pink and regions where surface flow is prominent are a bright to deep red (Figure 4.5b). The floodplain alluvial deposits are identified by

the green riverine zone that lines the channel boundary, representing naturally vegetated floodplain deposits. This visual interpretation is then used to isolate the location and extent of the alluvial aquifers within the catchment/ sub-basin of interest.

Table 4.4. Landsat-8 spectral band combination description (Horning, 2004).

Band	Description
Band 4	Water absorbs nearly all light at this wavelength therefore water bodies appear very dark. This contrasts with bright reflectance for soil and vegetation therefore it is a good band for defining the water/land interface.
Band 5	This band is very sensitive to moisture and is therefore used to monitor vegetation and soil moisture.
Band 6	This band is primarily used for geological applications.

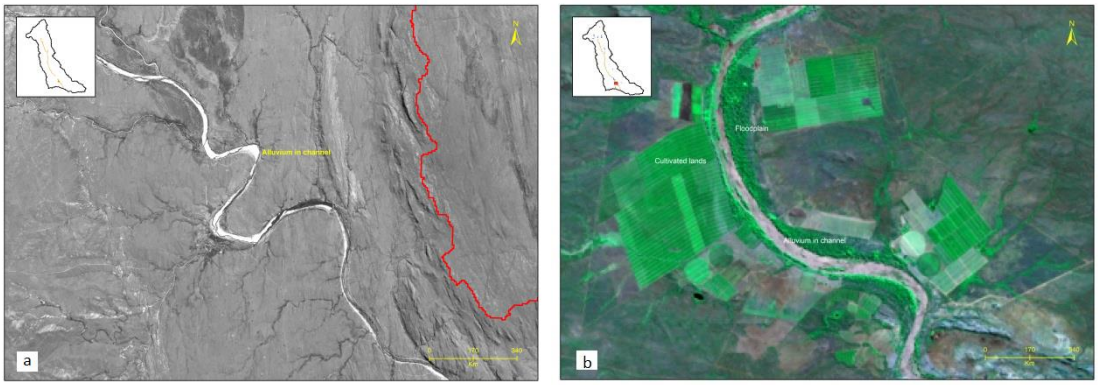

Figure 4.5. An example of the process of delineating alluvial aquifers of the Mzingwane Sub-basin. (a) On the panchromatic image, channel alluvium stands out as bold white deposits within the extent of the river channel. An example of the Mzingwane sub-basin is shown. (b) On the false colour composite image (RGB 456), the contrast between channel alluvium and vegetated floodplain deposits can be observed.

Land cover classification involved the identification of 8 land cover classes and collection of regions of interest (ROIs) in each Landsat scene covering the Limpopo River Basin (Table 4.5); an average of 33 pixels was assigned to each ROI. The chosen land cover classes were based on land cover and land use characteristics verified with existing land cover studies (Kundu *et al.*, 2015) and 2016 Google Earth image. Each class was assigned 40 ROIs that were used for training the automated supervised classification algorithm, namely Spectral Angle Mapper (SAM). Essentially, SAM is a similarity measure that computes the level of similarity between two spectra; a high

angle between spectra indicates that the two objects are spectrally separable (Keshava, 2004). The algorithm was applied with a pixel angle of 0.15 to obtain the land cover classification results.

Table 4.5. Description of classes chosen for land cover classification

Class name	**Description**
Channel alluvial deposits	Alluvial deposits confined within the boundary of the river channel; river bed alluvium
Vegetated floodplain deposits	Naturally vegetated riverine zone that lines the river channel
River	Areas indicating streamflow within the river channel
Dams	Artificial (man-made) water bodies
Built-up areas	Urban residential areas and industrial sites including shopping complexes, mines/quarries
Rural settlements	Open cleared fields with isolated buildings
Cultivated areas	Irrigated and non-irrigated agricultural lands, centre pivots and forest plantations
Open grassland	Bare land with no fences/boundaries

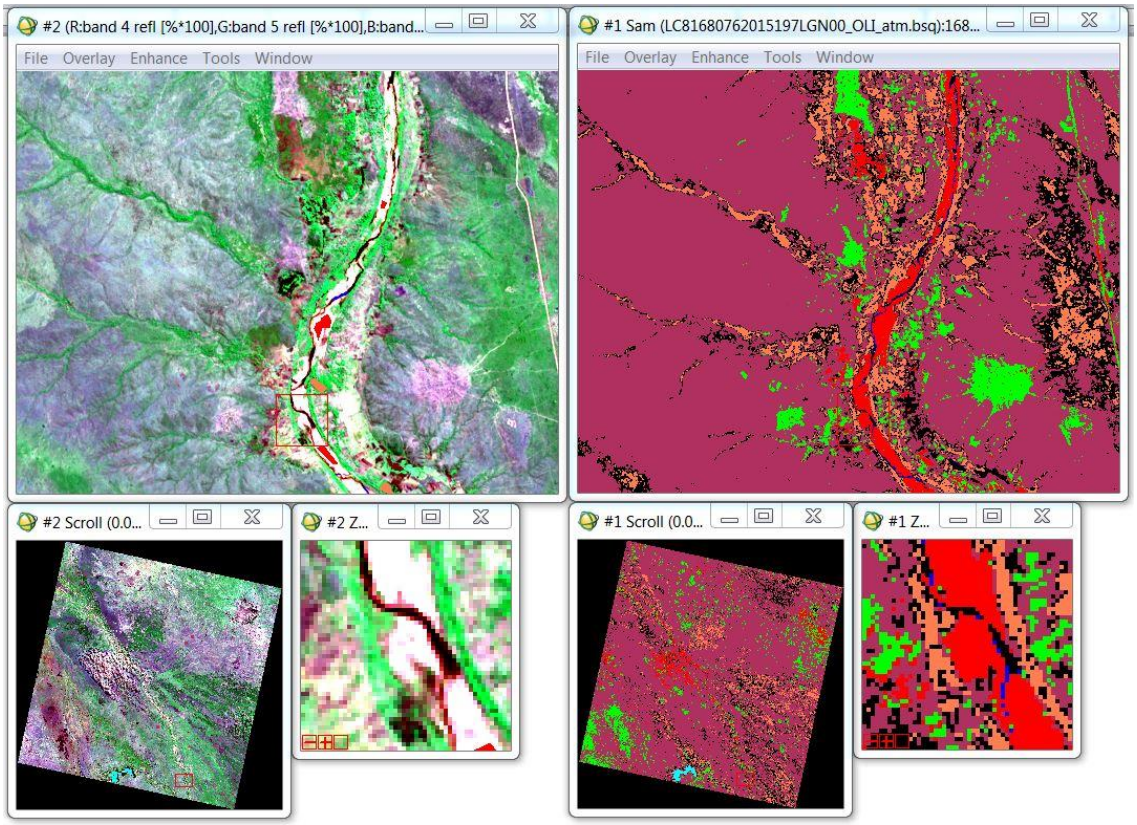

Figure 4.6. Land cover classification output images in ENVI 4.8. The group of images on the left indicates the collection of ROIs (coloured polygons) across Landsat-8 scene (Path 176, Row 076) (FCC 456) which covers part of the Mzingwane sub-basin. The group of images on the right indicates the land cover classification output using the SAM algorithm. The main classes of interest are indicated as: channel alluvium (red), vegetated floodplain alluvium (coral), river (blue). Within the scene, unclassified pixels are marked as black.

4.3.3 Map creation and alluvial aquifer areal calculation

Post image classification, three classes i.e. channel alluvial deposits, vegetated floodplain deposits and river which define alluvial aquifers were vectorised and converted to shapefiles for the areal extent to be determined using the GIS software, ArcMap 10.3. In ArcMap 10.3, the areal extent of identified alluvial deposits was calculated by manually digitizing the boundary determined by the classification. This process was implemented to ensure that misclassified or missing pixels (unclassified) within the boundary of alluvial deposits could be accounted for.

4.4 ESTIMATION OF SATURATED AQUIFER VOLUME

The volume of water that can be stored in the alluvium was estimated from the average saturated aquifer thickness, the derived areal extents of the alluvium and the effective porosity of the soil material of the alluvial deposit. The method applied is similar to the one used by Masike (2007) who used it in the Khurutshe area of Botswana when estimating the volume of water that could be stored by intergranular aquifers, mainly sandstones. The equation used is as follows:

$$V_w = A \times b \times \tilde{n} \qquad \text{Equation 4.1}$$

Where: V_w *= Aquifer Capacity [Mm^3], A = Area [km^2], b = Estimated Aquifer Thickness [m] and* $\tilde{n}$ *= average effective porosity [Dimensionless]*

Masike (2007) indicates though that estimation of aquifer capacity comes with great uncertainty as a result of the high variability of aquifer properties. The estimated saturated aquifer thickness and effective porosity (Table 4.6) used in this study are based on previous hydrogeological work conducted in the Limpopo River Basin for similar alluvial aquifer environments in neighbouring catchments. Where applicable, the effective porosity was also estimated from observations made by regional hydrogeological studies; however, in cases where hydraulic properties from neighbouring catchments could not be sourced (e.g. Motloutse), the effective porosity used was an average derived from the range of 25% to 50% given by Freeze and Cherry (1979) for unconsolidated sand deposits.

Table 4.6. Average alluvial aquifer thicknesses and effective porosities used for aquifer capacity estimation

Catchment	Alluvium thickness range (m)	Average effective porosity (%)
Mokolo	5-25	37
Motloutse	4-9	37
Mzingwane	1-25	35

4.5 DATA COLLECTION FOR HYDROLOGICAL MODELLING

The collection of data for hydrological modelling was based on the input requirements of the Pitman Model, which is discussed in Chapter 5. Most of the data used in this study was sourced from the recent Limpopo Monograph Study (LIMCOM, 2013) which used patched input data for the 1920-2010 simulation period. According to the Monograph Study report (Howard *et al.*, 2013), patching of almost all of the rainfall and runoff time series was conducted using the ClassR/PatchR suite of programmes, which are incorporated in the South African Department of Water and Sanitation Rain Water Resources Information Management System software package. The Monograph Study data were preferred over other data as they represent the most recent database collected from the riparian states and accepted hydrological 'state of affairs' of the basin.

4.5.1 Rainfall data

For the Mokolo (Table 4.7) sub-basin, monthly rainfall data from the Water Resources of South Africa of 2012 (WR2012) study (Bailey and Pitman, 2015) were used as provided and accessible from http://waterresourceswr2012.co.za/. The Monograph Study (LIMCOM, 2013) used the same data in configuring the South African catchments of the Limpopo River Basin. The rainfall data cover the period from 1920 to 2010.

Monthly rainfall data for the Motloutse sub-basin were collected from the Monograph Study (LIMCOM, 2013), which collected historical records from 40 rainfall stations in Botswana from the following sources:

- Botswana Department of Water Affairs
- WR2005 Study (Middleton and Bailey, 2009)
- Limpopo River Hydrological Model Study (Boroto and Görgens, 1999)
- Limpopo River Hydrological Model Update Study (Matji and Görgens, 2001)

The data were then patched and the records extended to cover the 1920-2010 period.

Table 4.7. Catchment area (km^2), MAP (mm) and MAE (mm) of the catchments of the Mokolo sub-basin. The MAE data were taken from the WR2005 database.

Catchment	Catchment Area (km^2)	MAP (mm)	MAE (mm)
A42A	573	640	1700
A42B	522	660	1700
A42C	698	656	1700
A42D	497	667	1700
A42E	1007	605	1700
A42F	1022	577	1800
A42G	1207	551	1900
A42H	1057	518	1900
A42J	1812	428	1950

For the Zimbabwean part, monthly rainfall data, collected from 32 rainfall stations, were obtained from the Zimbabwe Meteorological Services Department and the Zimbabwe National Water Authority (ZINWA) (Howard *et al.*, 2013). Additional data for 21 stations were obtained from a previous hydrological modelling study by Boroto and Görgens (1999).

Table 4.8. Catchment area, mean annual precipitation (MAP) and mean annual evaporation (MAE) for the Mzingwane catchment (Howard *et al.*, 2013).

Zone	Catchment	Catchment Area (km^2)	MAP (mm)	MAE (mm)
BUZ4	BUZ-B30	446.9	629	1878
	BUZ4-B40	82.4	629	1878
BNC	BNC-B11	244.9	633	1852
	BNC-B1	389.8	633	1852
	BNC-B3	103.2	633	1852
BIK	BIK-B60	206.2	618	1836
	BIK-B61	72.7	618	1836
BIN2	BIN2-B75	393.0	617	1865
	BIN2-B74	76.0	617	1865
	BIN2-UpperNsiza	64.5	617	1865
	BIN2-B89	485.9	617	1865
	$BIN2_{-Rest}$	543.2	617	1865
BIN1	BIN1-NsizaDam	303.0	572	1862
	BIN1-B52	119.3	572	1862
	BIN1@B13	432.4	572	1862
	BIN1@B69	255.8	572	1862
	BIN1@B66	253.9	572	1862
	$BIN1_{-Rest}$	485.5	572	1862
BUZ3	BUZ3@B20	867.2	547	1874
	$BUZ3_{-Rest}$	1387.9	547	1874
BUZ2	BUZ2@B62	2408.2	506	1927
	$BUZ2_{-Rest}$	694.4	506	1927
BUZ1	BUZ1@B91	552.1	477	1977
	$BUZ1_{-Rest}$	3142.1	477	1977
BL1	BL1	1497.6	416	2020
BL2	BL2	2732.0	453	2034

4.5.2 Evaporation data

The Pitman Model requires evaporation data expressed as a percentage of the annual total evaporation. Evaporation data for the Mokolo sub-basin were based on calibrations conducted in the Water Resources of South Africa 2005 (WR2005) study (Middleton and Bailey, 2009).

LIMCOM (2013) used A- and S-pan evaporation data collected from three evaporation stations based in northern, central and southern Botswana. The Botswana Department of Water Affairs provided monthly data from 1971 to 2000 while Boroto and Görgens (1999) supplied daily data from 1958 to 1994. The data were patched and averaged as indicated in Table 4.9.

Table 4.9. Botswana evaporation stations (Howard *et al.*, 2013)

Station name	Country	Gauge Type	Location	Record length	MAE (mm)
033-FRAN	Botswana	A-pan	21°10'00"S, 27°31'00"E	1957-2000	2585 (A)
037-GABO	Botswana	A-pan	24°40'00"S, 25°55'00"E	1960-1993	2311 (A)
106-MAHA	Botswana	S-pan	23°07'00"S, 26°50'00"E	1966-1999	2176 (S)

For the Zimbabwe catchments, the LRBMS (LIMCOM, 2013) collected evaporation data from 9 American Class A Pan evaporation stations located in close proximity of major dams and operated by ZINWA. The raw data were subsequently patched and converted to regional monthly evaporation values using the mean monthly evaporation from a selected station or group of station.

4.5.3 Observed flow data

Observed streamflow data were used in the study to help assess the performance of the model. Gauge station A4H010 (Mokolo River at Mokolo Nature Reserve) was used for the Mokolo sub-basin. Monthly flow data, covering the time period from 1980 to present day, was collected from the South African Department of Water and Sanitation online data repository (DWS, 2017).

For the Motloutse catchment, only one gauge station was used, namely 4131/4121 which are located on the Motloutse River at Tobane (Howard *et al.*, 2013). Observed monthly streamflow data for the Botswana catchments comprised patched flow data from the LRBMS (Howard *et al.*, 2013) which were collected from the following sources:

- Botswana Department of Water Affairs
- WR2005 Study (Middleton and Bailey, 2009)
- Limpopo River Hydrological Model Study (Boroto and Görgens, 1999)
- Limpopo River Hydrological Model Update Study (Matji and Görgens, 2001)

Observed streamflow data for the Zimbabwe catchments comprised patched monthly flow data from the LRBMS (Howard *et al.*, 2013) which were sourced from ZINWA and Boroto and Görgens (1999). Additional data were sourced from the updated 'Blue Book' (Mazviwavi, 2006). The flow gauge stations used in this study are indicated in Table 4.10.

Table 4.10. Flow gauge data (MAR, Mm^3) used for the Mzingwane catchment

Station	MAR (Mm^3)	Record length
B20	6.884	1952-2009
B60	0.649	1965-2010
B75	0.516	1968-2009
B22	27.560	1953-1962
B62	23.871	1966-2012
B91	16.148	1977-2001
B90	1.819	1975-2007

4.6 CLOSING REMARKS

Chapter 4 has provided a detailed account of the methodology applied in meeting the objectives of the study. Land cover classification, using Landsat-8 imagery and DEM data, was employed for alluvial aquifer delineation. To determine the potential amount of water that could be 'lost' between aquifer and river channel, the aquifer capacity was estimated by calculating the product of the aquifer areal extent, aquifer saturated thickness and effective porosity of the alluvium. Hydrological data comprising MAP, MAE and available flow gauge data was collected for hydrological modelling. The setup of the Pitman Model for hydrological modelling and the three loss simulating functions are described in Chapter 5.

CHAPTER 5
The PITMAN model

5.1 INTRODUCTION

This chapter provides a description of the SPAtial and Time Series Information Modelling (SPATSIM, Hughes, 2005; Hughes and Forsyth, 2006) version of the Pitman Model (Pitman, 1973; Hughes, 2004) and a discussion of the three possible approaches that are used to simulate channel transmission losses with the model.

5.1.1 The Pitman Model

The Pitman (Pitman, 1973; Hughes *et al.*, 2006) is a conceptual, monthly time-step and spatially semi-distributed rainfall-runoff simulation model. Similar to other conceptual models, the Pitman model consists of storages linked by functions designed to represent the main hydrological processes prevalent at the basin scale (Hughes *et al.*, 2006). It was originally developed in 1973 by W.V. Pitman as a conceptual lumped model and has now become one of the most extensively used models within southern Africa (Hughes, 1997; IHP, 1997; Mazvimavi *et al.*, 2004; Tshimanga *et al.*, 2011). Its main application has been as an estimation tool for basin-wide water resource assessments and planning (Hughes, 2004; Kapangaziwiri *et al.*, 2011). The original version of the model (Pitman, 1973) has undergone several modifications (Hughes, 1997; Hughes, 2004; Sami, 2006) to improve its functionality as a tool for integrated water resource assessment. One of the most significant revisions to the model has been the incorporation of groundwater recharge and discharge functions as a means to improved understanding of surface water-groundwater interactions at the model application scale (Hughes, 2004; Kapangaziwiri, 2011). The model originally incorporated groundwater components in an overly simplistic manner which rendered

it inadequate to simulate several important processes necessary for integrated water resource management (Hughes, 2004; Tanner, 2013). Consequently, the model was revised by Hughes (2004) and Sami (2006) by integrating more explicit groundwater routines; both new versions are based upon similar concepts and simulate the major groundwater processes (Figure 5.1) and both approaches have been included the South African Department of Water and Sanitation (DWS) official version of the model that forms part of the WR2005 (Water Resources of South Africa) national database and analysis tools (Bailey, 2007). The version of the Pitman Model used in this study was developed by Hughes (2004) at the Institute for Water Research, Grahamstown, South Africa. It has under gone several other improvements including the addition of a transmission loss function (Hughes *et al.*, 2013) – an explicit model routine designed to account for riparian evapotranspiration losses and losses from storage due to sub-surface outflow to downstream areas. Given the paucity of data in southern Africa and the impact of this on modelling processes, detailed routines were developed to directly estimate parameters from the physical attributes of a basin and therefore circumvent the need for calibration (Kapangaziwiri and Hughes, 2008) which can be used in an uncertainty framework (Kapangaziwiri *et al.*, 2012). The routines attempt to translate expected errors in the available physical basin property data into uncertainty in the resulting estimates of parameter values which could be used to generate ensembles of model outputs as opposed to single, lower confidence values. Human-engineered impacts on natural streamflow, such as small farm dams, large dams, abstractions and return flows, are also included in the modelling structure (Hughes and Mantel, 2010; Hughes *et al.*, 2010) as well as a wetland component which accounts for the effectss of both wetlands and large natural lakes (Hughes *et al.*, 2013).

According to Tanner (2013), the model inherently represents a compromise between physically-based distributed models and simple empirical approaches. It has been designed to utilise existing databases of regional hydrological information and many of the input parameters can be derived from maps or by field work. Where historical data are available however calibration is possible; however these data are typically

residual because of anthropogenic water uses, which are generally poorly quantified, in the basins (Hughes, 2008; Kapangaziwiri and Hughes, 2008). The model outputs are assessed based on either comparison with observed data (if available), outputs from other models that have already been tested or, at the very least, against our conceptual understanding of reality (Tanner, 2013).

5.1.2 Structure of the revised Pitman Model

Table 5.1 provides a list of the parameters and brief explanations of their purpose, while Table 5.2 indicates the typical field data required to estimate some of the parameters. Additional compulsory data requirements that are not illustrated include basin area, a time series of basin average rainfall, seasonal distributions of evaporation (fractions), irrigation water demands (mm) and other non-irrigation water demands (fraction). Optional data requirements include time series of basin average potential evaporation, upstream and transfer inflows.

The Pitman Model (Hughes, 2004) is applicable through an integrated modelling software package called SPATSIM (Hughes, 2005) that links spatial data with other data types (e.g. parameter tables and time series) and includes a variety of data input, output and analysis routines as well as links to hydrological and water resource simulation models (Hughes, 2004). The Pitman model operates over four equal time steps within a month in order to approximately represent variations in the rainfall, and to avoid excessively large changes in any one component of the water balance. This is considered necessary in a coarse time-step model given that natural processes occur concurrently, while the model simulates them sequentially. The model simulates upstream and downstream catchments simultaneously with a routing of the surface water and groundwater between catchments (Tanner, 2013). A detailed description of the structure of the model, including the surface water component of the model, is found in (Hughes, 2004; Hughes *et al.*, 2006; Kapangaziwiri, 2008 and Tanner, 2013).

Kapangaziwiri (2008) provides detailed descriptions of the parameters of the model, their conceptual meanings and how they are generally estimated in a typical model application.

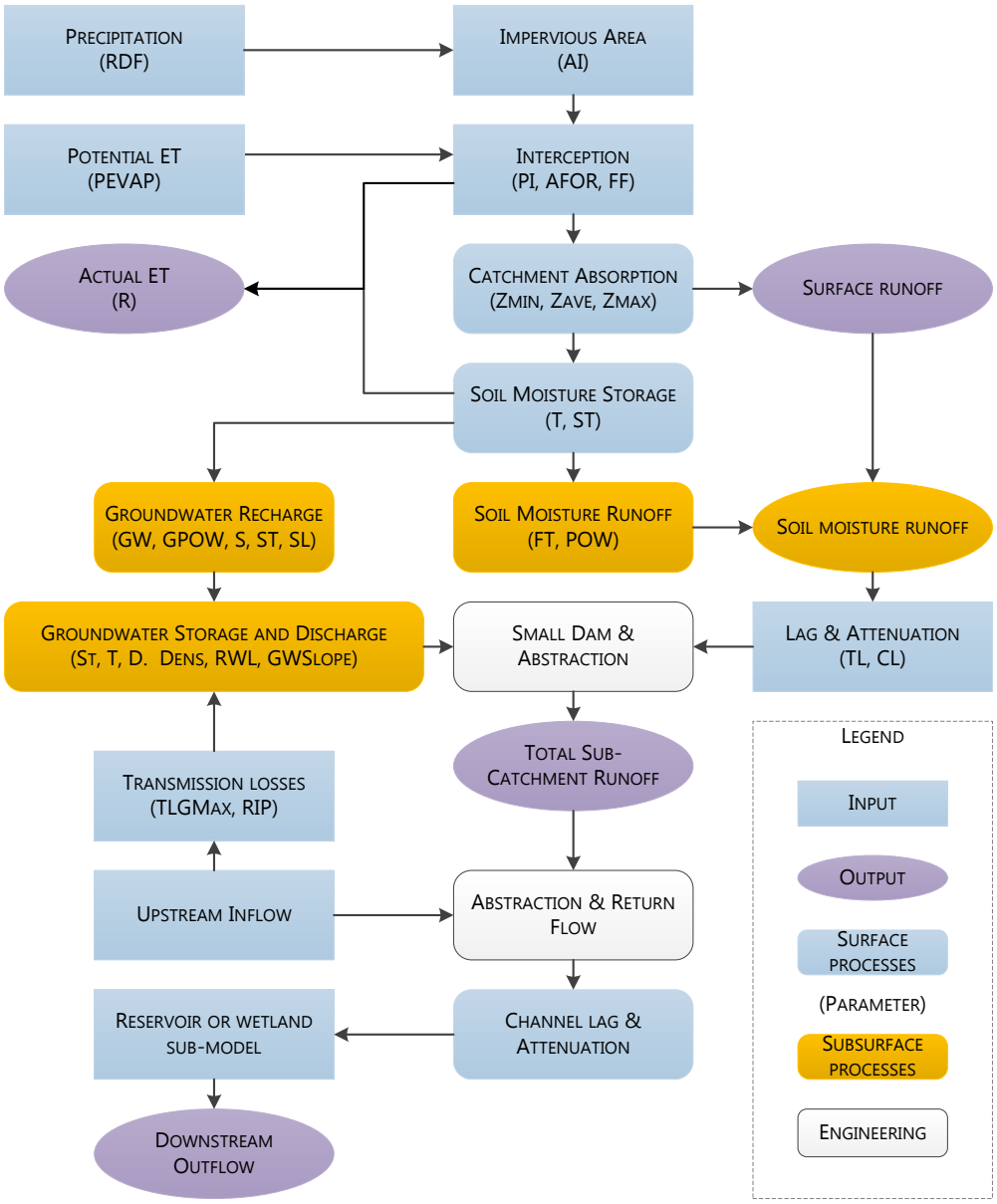

Figure 5.1. A flow diagram of the revised Pitman Model (Hughes, 2004), indicating the main components of the model including the parameters (adapted from Hughes *et al.*, 2006; Kapangaziwiri *et al.*, 2012; Tanner, 2013)

Table 5.1. The revised Pitman Model surface and groundwater parameters (adapted from Tanner, 2013)

Parameter	Units	Parameter description
Surface water parameters		
RDF	-	Rainfall distribution factor. Controls the distribution of total monthly rainfall over four model iterations
AI	fraction	Impervious fraction of catchment
PI1s	mm	Summer Interception storage for vegetation type 1
PI1w	mm	Winter Interception storage for vegetation type 1
PI2s	mm	Summer Interception storage for vegetation type 2
PI2w	mm	Winter Interception storage for vegetation type 2
AFOR	%	% area of catchment under vegetation type 2
FF	-	Ratio of potential evaporation rate for Veg2 relative to Veg1
PEVAP	mm	Annual basin potential evaporation
ZMINs	mm $month^{-1}$	Summer minimum basin absorption rate
ZMINw	mm $month^{-1}$	Winter minimum basin absorption rate
ZAVE	mm $month^{-1}$	Mode of distribution of absorption rates
ZMAX	mm $month^{-1}$	Maximum basin absorption rate
ST	mm $month^{-1}$	Maximum moisture storage capacity
SL	mm	Soil moisture below which there is no recharge
POW	-	Power of the moisture storage runoff equation
FT	mm $month^{-1}$	Runoff from moisture storage at full capacity
R	-	Evaporation-moisture storage relationship parameter
TL	months	Lag of surface runoff
Groundwater parameters		
GW	mm $month^{-1}$	Maximum recharge depth at maximum moisture capacity
TLGMax	mm $month^{-1}$	Maximum channel loss
GPOW	-	Power of the moisture storage recharge equation
DD	km km^{-2}	Effective drainage density for groundwater inputs to streamflow
T	m^2 day^{-1}	Groundwater transmissivity
S	-	Groundwater storativity
RG	-	Initial groundwater drainage slope
Rest RWL	m (below surface)	Rest Water Level; aquifer depth
RSF	%	Riparian Strip Factor. Controls riparian evaporation losses from groundwater storage
GW Abstraction U&L	Ml y^{-1}	Groundwater abstraction Upper and Lower slopes

Table 5.2. Typical field data required to populate the parameters

Parameter	Data required from basin physical characteristics
ST	soil depth, texture, porosity, geological formation
FT	soil texture & hydraulic conductivity, permeability, transmissivity, slope
POW, GPOW	geology, topography, vegetation cover, soil type & texture
GW	groundwater recharge
ZMIN/ZAVE/ZMAX	vegetation cover, soil texture, hydraulic conductivity, rainfall, raindays, storm duration
PI	vegetation type & density (interception loss), Leaf Area Index

5.1.3 The groundwater components of the Pitman Model

The order of all the processes detailed below is given by Hughes *et al*. (2007) who outlined the progression within each model iteration step (4 per month) as follows:

- The recharge is calculated and the associated volume of water added to the upper and lower wedge storage volumes.
- The groundwater gradient from the previous iteration step is used to estimate outflow from the upper slope component to the lower slope component, the outflow from the lower slope component to the channel and the regional groundwater gradient (RG) is used to calculate the groundwater outflow to the downstream basin. The riparian evapotranspiration losses are calculated, as are any channel transmission loss inputs to groundwater and any abstraction losses from groundwater.
- The new volumes of groundwater in the two slope elements are then used to estimate the slope gradients for the next time step.
- It is assumed that the lower slope end point is fixed at the river channel and the gradient calculated from 40% of the width and the volume.
- From the previous calculations, the upper slope end point, where it joins the lower slope element can be determined and therefore so can the gradient of the upper slope element from the upper slope volume and simple geometry.

5.1.3.1 Soil moisture storage function (ST)

The model assumes that water draining from the soil has two directional components – a vertical component that contributes directly to groundwater recharge and a lateral one represented by soil interflow or re-emergence as springs, occurring at elevations above the groundwater level (Tanner, 2013). The soil moisture content of the model is controlled by the parameter ST, representing the maximum storage capacity of the soil in mm. The moisture storage of a soil (S) increases due to infiltration and is depleted by evaporative losses (including evapotranspiration through plants), runoff and recharge to the groundwater store (Kapangaziwiri, 2008). A further assumption made in the model is that S can represent moisture stored not only in the soil (ST_{soil}) but also within the unsaturated zone (ST_{unsat}) above the groundwater table (Kapangaziwiri, 2008). Although the values for ST_{soil} and ST_{unsat} are estimated separately – ST_{soil} can be estimated from some knowledge of the soils or geology and climate of an area, while ST_{unsat} is influenced by the storativity (S) of the underlying geological formation and depth to the water table - both are represented in the model under the parameter ST (Kapangaziwiri, 2008; Kapangaziwiri and Hughes, 2008).

5.1.3.2 Soil moisture runoff function (FT, POW)

Within the soil moisture runoff function, runoff generated from the soil/ unsaturated moisture store (interflow) is assumed to be regulated through a non-linear relationship between discharge and soil moisture (Tumbo, 2014); Equation 5.3 determines the generation of runoff from soil moisture storage, while Figure 5.2 illustrates the relationship assumed between the parameters of the soil moisture runoff function. The parameter FT represents the maximum interflow generated when the moisture level (S) is at its maximum value (i.e. when soil is saturated and S=ST) and is therefore the maximum possible runoff (mm) per month from both the soil moisture and unsaturated zone storage (Kapangaziwiri, 2008; Tanner, 2013). The parameter POW is a simple power function which represents the shape of the relationship between discharge and soil moisture storage (Pitman, 1973).

$$Q = FT * \left(\frac{S}{ST}\right)^{POW} \qquad \text{Equation 5.1}$$

Where: *Q= Discharge (runoff) [$m^3 s^{-1}$], FT = Runoff from moisture storage at full capacity [mm $month^{-1}$], S= Storativity [Dimensionless] and ST = Maximum moisture storage capacity [mm $month^{-1}$]*

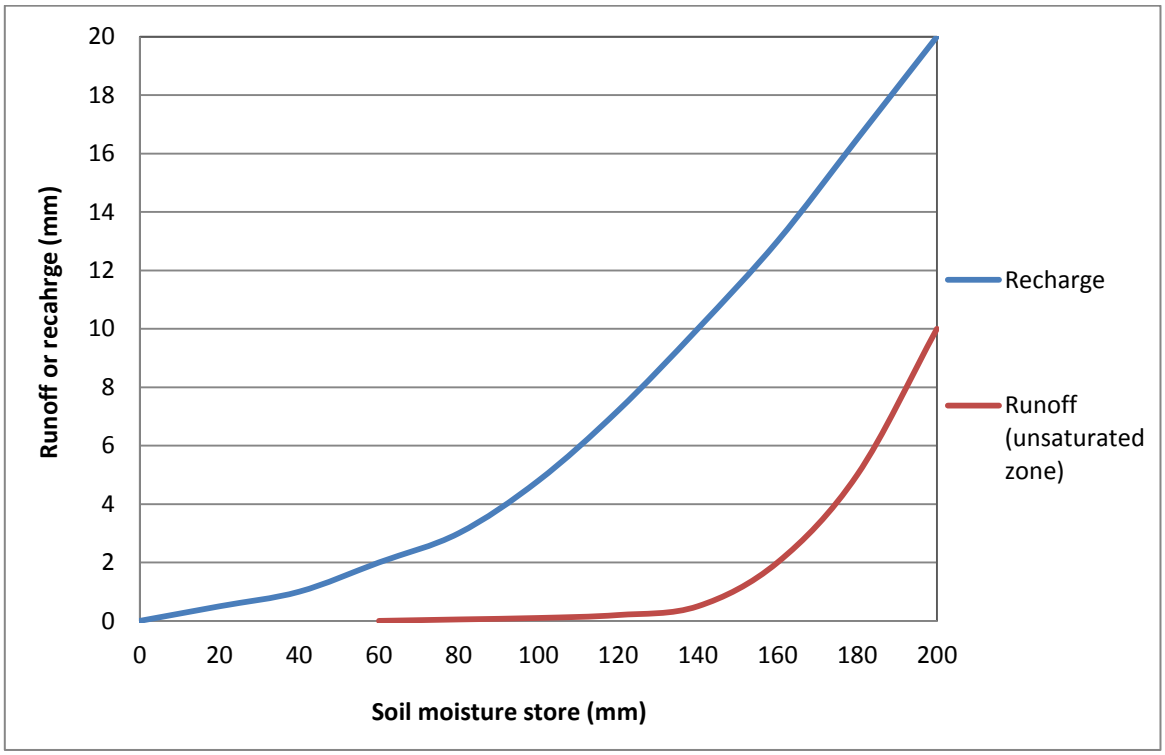

Figure 5.2. Illustration of the soil moisture runoff function (with parameter ST=200, SL-0, FT=20 and POW=2) and the recharge-moisture state relationship with parameter SL=100, GW=10 and GPOW=3 (Tanner, 2013).

5.1.3.3 Groundwater recharge function (GW, GPOW, SL)

The groundwater recharge is directly influenced by four parameters namely, ST, SL, GW and GPOW. SL represents the lower limit of soil moisture storage below which no recharge is expected to occur. Because the rates of recharge at low soil moisture are small and have little influence on the total water balance of the basin, the value of SL is usually set to zero (Hughes and Parsons, 2005). GW is defined as the maximum amount of recharge (at a moisture status equal to ST) and GPOW determines the form of the relationship between the volume of recharge and moisture stored in the unsaturated zone S, similar to the relationship illustrated for soil moisture runoff

function in Figure 5.2. A similar non-linear relationship (Equation 5.4) is used to estimate the depth of recharge, using a ratio of current storage to the maximum recharge:

$$RE = GW \frac{\mathrm{S} - \mathrm{SL}}{\mathrm{ST} - \mathrm{SL}}^{\mathrm{GPOW}} \qquad \text{Equation 5.2}$$

Where: *RE = monthly recharge rate [mm];], GW = Maximum recharge depth at maximum moisture capacity [mm month^{-1}] and S = current soil moisture storage level [mm].*

GPOW is very similar to POW and expected to reflect similar physical relationships (Kapangaziwiri, 2008).

5.1.3.4 Groundwater storage and discharge function (DD, T, S, RWL, RSF, GWSlope)

The quantification of groundwater storage and discharge is dependent on six parameters, namely DD, T, S, RWL, RSF and GWSlope. Conceptualising the processes of sub-surface flow and the aquifer is the starting point of defining the groundwater components of the model. In terms of channel transmission losses, defining the groundwater slope determines whether water is 'lost' from the aquifer to the channel or vice versa. Simple geometry comprising a rectangle and parallel lines is used to represent the basin and channels respectively and these are separated by drainage slopes which consist of the two areas between the edges of the rectangle and the outermost 'channels', plus two between each 'channel' line (Figure 5.3). Drainage is assumed to be one-dimensional for simplicity. The number, length and width of each drainage slope are determined from the basin area and the effective drainage density. The channels included in the estimation of effective drainage density are those assumed to likely receive groundwater discharge – this assumption could exclude smaller tributaries that only flow during storm events (Hughes, 2004).

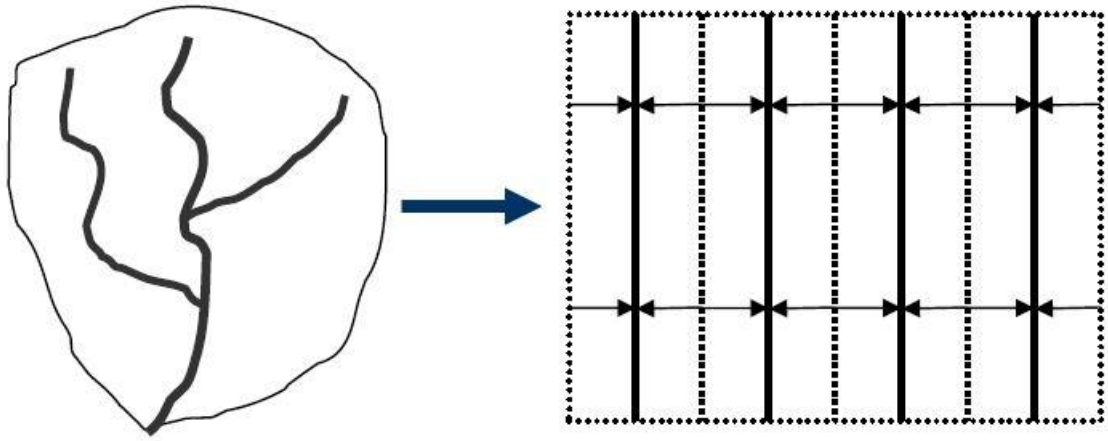

Figure 5.3. Conceptual representation of drainage in the basin where the channels are of unit length and drainage density of 4/ square root (Area) (Solid lines are channels, dashes lines are drainage divides and the arrows show drainage directions). (Hughes, 2004)

The number of channel lines is calculated from:

$$L = \rho D * A \qquad \text{Equation 5.3}$$

Where: *L= Channel length [km]; ρD= Drainage density [km km^{-2}]; A=Area [km^2]*

The ratio of basin width/length is assumed to be related to drainage density as follows:

$$W = L * 2.0 * \rho D \qquad \text{Equation 5.4}$$

Where: *W=Width [km], L=Length [km], ρD=Drainage density [km km^{-2}]*

Therefore:

$$L = \sqrt{\left(\frac{A}{2 \times \rho D}\right)} \qquad \text{Equation 5.5}$$

Where: *L= Length [km], A= Area [km^2], ρD= Drainage density [km km^{-2}]*

By definition (and from Figure 5.4):

$$\text{No. of DSLP} = 2.0 \times \frac{\rho D \times A}{L} \quad \text{Equation 5.6}$$

Where: *DSLP=Drainage slope [Dimensionless], ρD= Drainage density [km km^{-2}], A= Area [km^2], L= Length [km]*

The number of drainage slopes is equal to 2 * number of channels, however Equation 5.9 has to be corrected to generate an even integer number of drainage slopes, each of which has a width given by:

$$DW = \frac{W}{No.\ of\ DSLP} \quad \text{Equation 5.7}$$

Where: *DW= Drainage width [km], W=Channel Width [km], DSLP= Drainage slope [Dimensionless]*

Figure 5.4 illustrates the concept behind a single drainage slope and the volume of the groundwater 'wedge' stored under that drainage slope (assuming that the lower boundary is the channel at the bottom of the slope) can be calculated as:

$$V_{wd} = DW^2 \times \frac{dh}{dL} \times \frac{DL}{2} \quad \text{Equation 5.8}$$

Where: *V_{wd}= 'wedge' volume [m^3], DW= Drainage width [km], dh/dL= hydraulic gradient of the groundwater flowing toward the river channel or away from the channel when the groundwater is below the channel [Dimensionless], DL=Drainage length [km]*

$$V_w = V_{wd} * S \quad \text{Equation 5.9}$$

Where: *V_w= Volume of water in 'wedge [m^3], V_{wd}= 'wedge' volume [m^3], S= Storativity [Dimensionless]*

Outflows from this wedge to the river channel, within a single slope element can be calculated by:

$$Q = T * \frac{dh}{dL} * dt * L \qquad \text{Equation 5.10}$$

Where Q= Discharge (runoff) [m^3 s^{-1}], T= Transmissivity [m^2 day^{-1}], dh/dL= gradient [Dimensionless], dt= Time step [s], L= channel length [km]

The total width of each groundwater slope or gradient is divided into two parts – a 'near channel' or lower slope (40% of the total width) and a 'remote from channel' or upper slope (60% of the total width) that are modelled separately. The main principle for including the two compartments within each slope element is related to the manner in which groundwater abstractions are expected to impact on discharge to the channel (Kapangaziwiri, 2008).

Increments to, and losses from the aquifer are used in the volumetric calculations based on:

i. The slope element widths and lengths;

ii. Simulated lateral groundwater gradients (i.e. across the slope elements); and

iii. The storativity parameter.

As the volume of water changes within the conceptual aquifer, the two gradients also change. The gradient variables relate the movements of water within the aquifer (from the 'remote from channel' to the 'near channel' compartment), as well as discharge from the aquifer to the channel. In the 'near channel' compartment the aquifer is assumed to be always in contact with the river channel and therefore when the water table is below the river, the groundwater slope is simulated a negative gradient. Simple geometry is used to calculate the volume of water in an aquifer compartment as follows:

$$V = [(DW)2 * DL * \frac{dh}{dL} * S]/2$$ Equation 5.11

Where: *V= Volume [m^3], DW= Drainage width** [km], DL= Drainage length** [km], dh/dL = gradient [Dimensionless], S= Storativity [Dimensionless]*

** Drainage width and gradient variables refer to the values in either the 'near channel' or 'remote from channel' compartments.*

Increments to the aquifer occur as:

i. Recharge from the surface component of the model,
ii. Groundwater drainage from an upstream catchment, and
iii. Flow from the channel on condition that the 'near channel' compartment gradient is negative.

The first two of these are added to the two compartments in proportion to their widths (40: 60).

Losses from groundwater occur as:

i. drainage to downstream catchment,
ii. evaporative losses in the riparian strip ('near channel' only),
iii. discharge to the channel ('near channel' only), and
iv. discharge to the 'near channel' compartment from the 'remote from channel' compartments and abstractions.

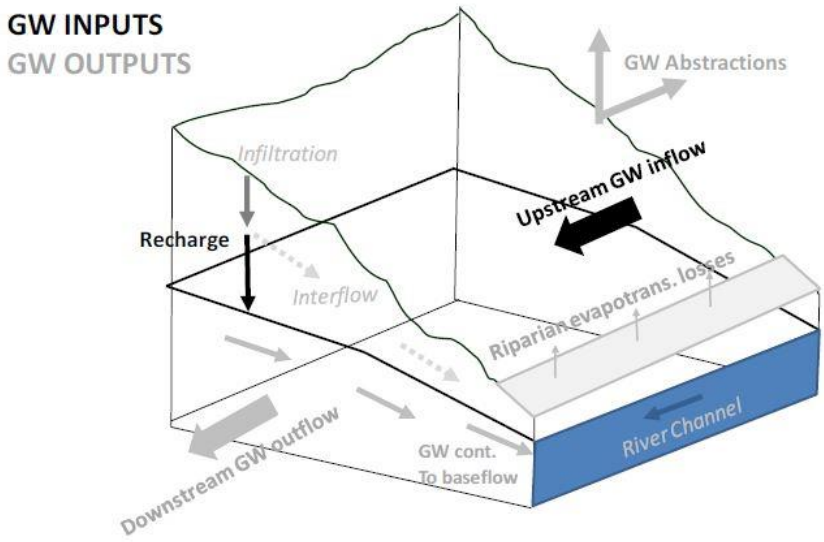

Figure 5.4. The main interaction components of the modified Pitman Model are illustrated in a scenario where groundwater is contributing to surface water. The 'wedge' represents the segment of the groundwater body that is above the conceptual river channel and can contribute to discharge (Tanner, 2013).

Quantifying the groundwater discharge to stream flow requires an estimation of the following parameters: DD, T, S, RSF and RWL. *DD* refers to the subsurface *drainage density* of the basin and is expressed as a ratio of the total channel length expected to receive groundwater discharge to the basin area given in km km^2 (Kapangaziwiri, 2008). In the model the drainage density for headwater basins is usually estimated to 0.4 however for downstream basins a value of 0.2 to 0.3 is usually more appropriate (Tanner, 2013). The parameters *T* and *S* respectively define the *transmissivity*, a product of the permeability and saturated aquifer thickness measured in m^2d^{-1}, and the *storativity*, a measure of the capacity of the aquifer to store water. The values used to express these parameters are based on the knowledge of the rock type (aquifer type) and its hydraulic properties.

Any groundwater discharge to the channel is reduced by evapotranspiration losses (Tanner, 2013). The *riparian strip factor* (*RSF*) parameter accounts for the effect of riparian vegetation on groundwater. It represents the percentage of the total slope element width over which evapotranspiration losses, linked to transpiration by riparian vegetation and evaporation from channel beds and banks are assumed to occur

(Kapangaziwiri, 2008). In reality, the riparian strip factor parameter should reflect the areal extent and type of riparian vegetation which is likely to use near surface groundwater directly or intercept groundwater contributions to stream flow (Tanner, 2013). The *rest water level* (*RWL*) parameter defines the maximum depth below the channel that an aquifer is assumed to reach and expresses the depth of the connecting point between the upper and lower slope elements at which the groundwater is considered to be inaccessible to abstractions and evapotranspiration (Tanner, 2013). The conceptual definition of the parameter is related to the groundwater geometry calculations in the model expressed as:

$$GW_d = \left[\frac{dh_{RWL}}{dL_{RWL}} - \frac{dh}{dL}\right] \Big/ \frac{dh_{RWL}}{dL_{RWL}} \qquad \text{Equation 5.12}$$

Where: *GW_d= Groundwater depletion factor [Dimensionless], dh_{RWL}/dL_{RWL}=Gradient at rest water level [Dimensionless], dh/dL= Current gradient [Dimensionless]*

Evapotranspiration losses are also reduced by this depletion factor accordingly:

$$E_{loss} = \mathrm{DW} * E_{net} * \mathrm{RSF} * x_d \qquad \text{Equation 5.13}$$

Where: *E_{loss}= Evaporative losses [mm], DW= Drainage width [km], E_{net}= Net evaporation [mm], RSF = Riparian Strip Factor [Dimensionless], x_d= Depletion factor [Dimensionless]*

The net evaporation refers to the difference between potential evaporation demand and rainfall. If the net evaporation is negative (i.e. where rainfall exceeds potential evaporation), the value is corrected to zero (to avoid duplicating the recharge function over the riparian strip).

5.1.3.5 Channel transmission losses: effects of the groundwater slope

The development of the Pitman Model has included the addition of an explicit channel transmission loss function. The function is however discussed in section 5.2, alongside

the wetland and reservoir functions, as an approach to simulating and quantifying channel losses. In this section, the effect of the gradient of the groundwater slope on channel losses is considered. Four scenarios are described by Kapangaziwiri (2008) detailing the occurrence of channel transmission losses based on the gradients of the 'near' and 'remote from' channel slopes (Figure 5.5):

A. *Positive gradients within both compartments:*

The 'remote from channel' compartment drains to the 'near channel', the 'near channel' compartment drains to the channel (and is subject to riparian evaporative losses) and both compartments drain to downstream catchments and no channel losses would occur but groundwater will contribute to flow in the channel.

B. *Positive 'near channel' gradient, negative 'remote from channel' gradient:*

This scenario can only occur if abstractions from the 'remote from channel' compartment have drawn the water level down or a combination of recharge and channel losses have increased the volume and therefore gradient of the 'near channel' compartment. Downstream drainage would occur from both compartment and groundwater would contribute to flow in the channel (no channel losses).

C. *Negative 'near channel' gradient, positive 'remote from channel' gradient:*

Drainage from the 'remote from channel' to the 'near channel' will occur as well as riparian evaporative losses from the 'near channel' compartment. Channel losses to the 'near channel' will also occur.

D. *Negative gradients within both compartments:*

This situation could exist if groundwater abstractions occurred in the 'remote from channel' compartment at a rate that exceeded the groundwater recharge. A cone of depression would surround the abstracting borehole and no contribution of groundwater to channel would however channel losses may occur.

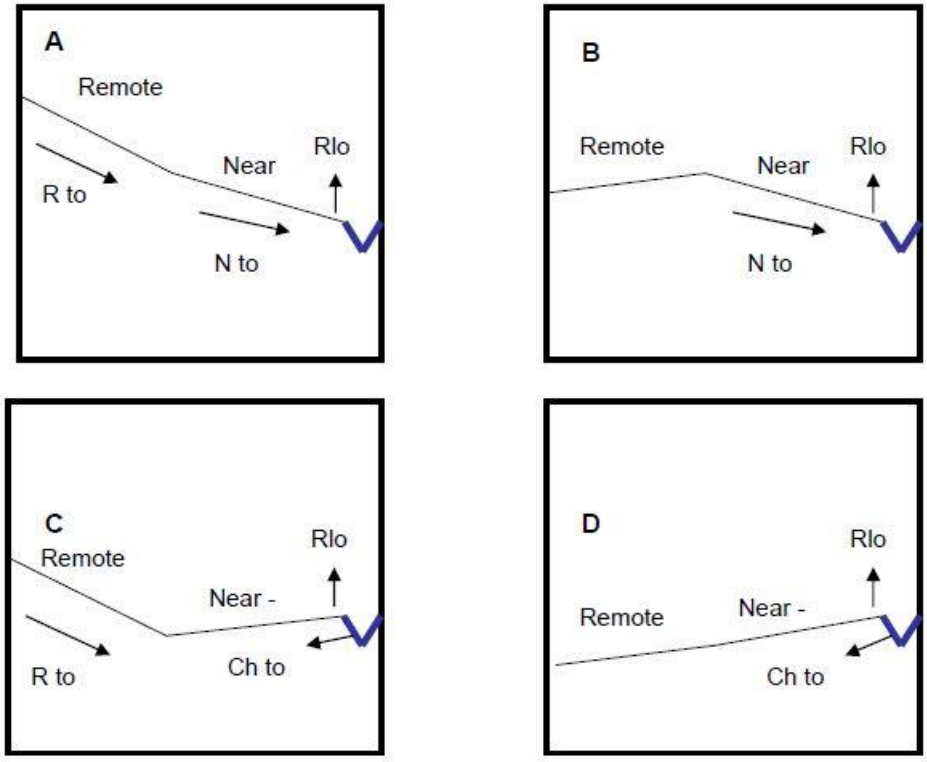

Figure 5.5. Illustration of the channel width compartments and the different conditions that can exist within the geometry of the conceptual aquifer (R is remote from channel compartment, N is near channel compartment, Ch denotes the channel and Rlo refers to evaporation loss from riparian vegetation. The arrows indicate the direction of movement of water) (Kapangaziwiri, 2008).

Other factors that need to be taken into consideration when simulating groundwater recharge and discharge include the discharge to downstream basins as well as local groundwater abstractions. With regards to discharge to downstream basins, a regional groundwater gradient parameter (GWSlope) is included that refers to the gradient appropriate for estimating outflows from one catchment to the next downstream one. The equation used to model groundwater flow towards downstream catchments is as follows:

$$Q_x = Transmissivity \times \frac{dh}{dl} \times dt \times s \qquad \text{Equation 5.14}$$

Where: *Q_x= Downstream outflow [mm], T = Transmissivity [m^2 day^{-1}], dh/dl= Regional gradient [Dimensionless], dt= time step [s], sw= Slope width*

The total outflow equates to Equation 5.16 multiplied by the number of slope elements which alludes to the significant impact of drainage density on the volume of downstream outflow. The outflow is also reduced by the groundwater depletion factor (Equation 5.14) when the lower slope element gradient is negative. In terms of groundwater abstractions, the response of the regional groundwater slope differs depending on the proximity to the channel (as noted in Figure 5.5). Groundwater abstraction parameters (annual volume and seasonal distributions) can therefore be applied to the 'near channel' and 'remote from channel' compartments independently and these are represented by water use parameters GW Abstractions (

Table 5.1). The seasonal distribution of groundwater is included as part of the monthly distribution data requirement. Hughes (2004) has acknowledged that the geometric representation of groundwater flow in the Pitman model is largely simplistic and disregards several of the realities of groundwater movements; however it is conceptually useful in quantifying groundwater recharge and discharge and not complicated as most of the calculations are simple geometric equations.

5.2 APPROACHES TO SIMULATING TRANSMISSION LOSSES

The Pitman model (Hughes *et al.*, 2006) can be used to simulate channel transmission losses in different ways. These include using an explicit transmission loss function, the use of wetland function to represent channel-floodplain storage exchanges or the use of a 'dummy' reservoir to represent floodplain storage and evapotranspiration losses.

5.2.1 Using the transmission loss function

The transmission loss function is a relatively recent development to the Pitman Model. Prior to its development, channel transmission losses were simulated through use of the wetland and 'dummy' reservoir functions. Its addition followed the incorporation of groundwater recharge and discharge functions to the model (Hughes, 2004). The

addition of the groundwater recharge and discharge functions was pivotal in the simulation of surface water-groundwater interactions as it allowed streamflow to contribute to groundwater when the phreatic surface was simulated as below channel level, which allowed channel transmission losses to have a notable impact on the overall water balance (Hughes *et al.*, 2007). The transmission loss function relies on a simple geometry to conceptualise the water balance within the groundwater store. While a detailed description of the geometry is provided by Hughes (2004), Hughes *et al.* (2007), Kapangaziwiri (2008) and Tanner (2013), it is summarised in Section 5.1.4.

The process of simulating transmission losses in the model assumes that the rate of loss will be due to characteristics of the channel, the head difference between the channel and the groundwater and the transmissivity of the material under the channel (Hughes *et al.*, 2007).

In downstream catchments receiving inflows from an upstream catchment, there are two components of channel loss calculated by the model:

i. The first component is channel losses from the incremental runoff generated within a catchment; and
ii. The second component is channel losses from flow in the main channel.

Although these components are treated separately in the model, the same algorithm which is based on two factors relating to the near channel ground water storage level and the relative flow rate in the channel respectively, is used (Hughes *et al.*, 2007; Tanner, 2013). The two components are discussed:

5.2.1.1 Channel losses from the incremental runoff generated within a catchment

Three variables (MAXQ, TLQ and TLG) are required. MAXQ is the maximum runoff (in mm) for the catchment being modelled and is estimated during the first run of the model (it is set to a default value of 20 mm at the start of the first run) and a further

variable TLQ estimated from the current months runoff (Q) and its value calculated using the following equations (see Figure 5.6):

$$TLQ = \begin{cases} 0.5 \cdot \left(tanh \left(2.5 \left(\frac{Q}{MAXQ} - 0.25 \right) \right) + 1.0 \right), & if \ \frac{Q}{MAXQ} < 0.25 \\ 0.5 \cdot \left(tanh \left(6 \left(\frac{Q}{MAXQ} - 0.625 \right) \right) + 1.0 \right), & if \ \frac{Q}{MAXQ} \geq 0.25 \end{cases}$$

Equation 5.15

Where: *TLQ= Dimensionless Channel loss from incremental runoff factor [Dimensionless], Q=Discharge (runoff) [mm], MAXQ= Maximum discharge (runoff) [mm]*

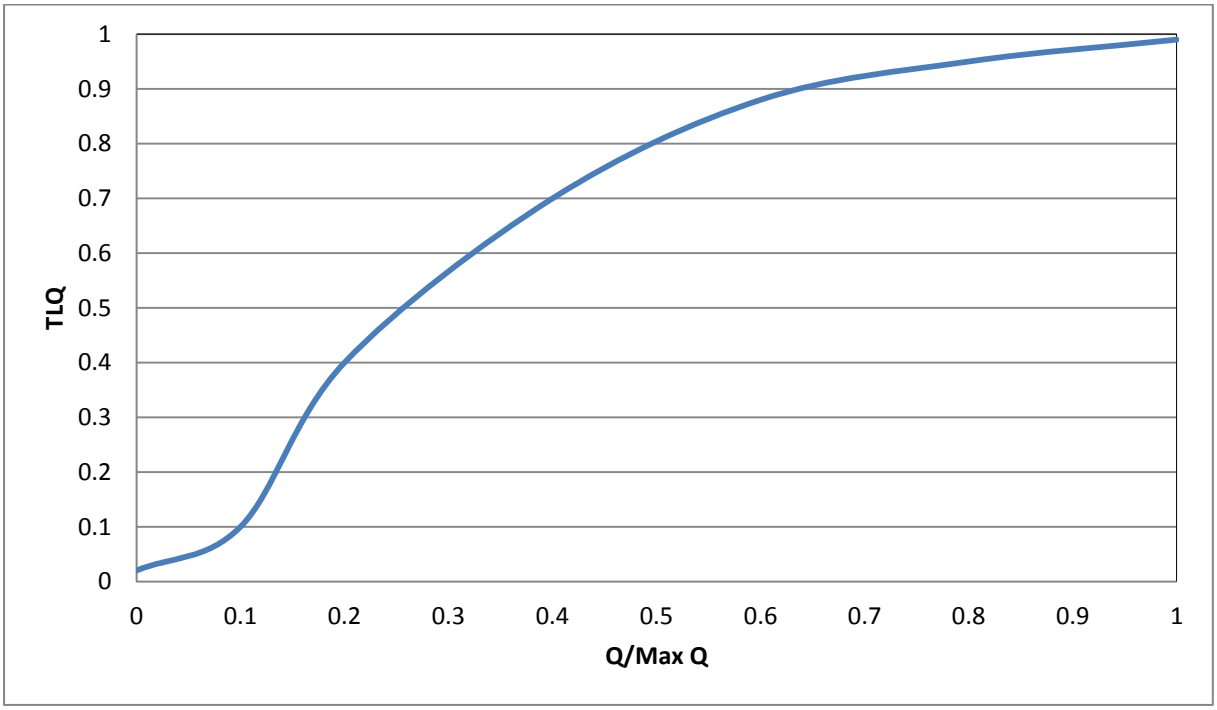

Figure 5.6. Shape of the power relationship between current month discharge (mm), relative to a maximum value (20mm in this case) and a model variable, TLQ (Hughes *et al.*, 2007).

A further variable TLG (Figure 5.7) is estimated from the current gradient relative to a maximum gradient defined by 0.7 of the gradient at the '*Rest Water Level*'. The variable is therefore a measure of the head difference between the channel and the groundwater (i.e. groundwater gradient of the near channel slope element) and they are related to each other by a power function (Tanner, 2013).

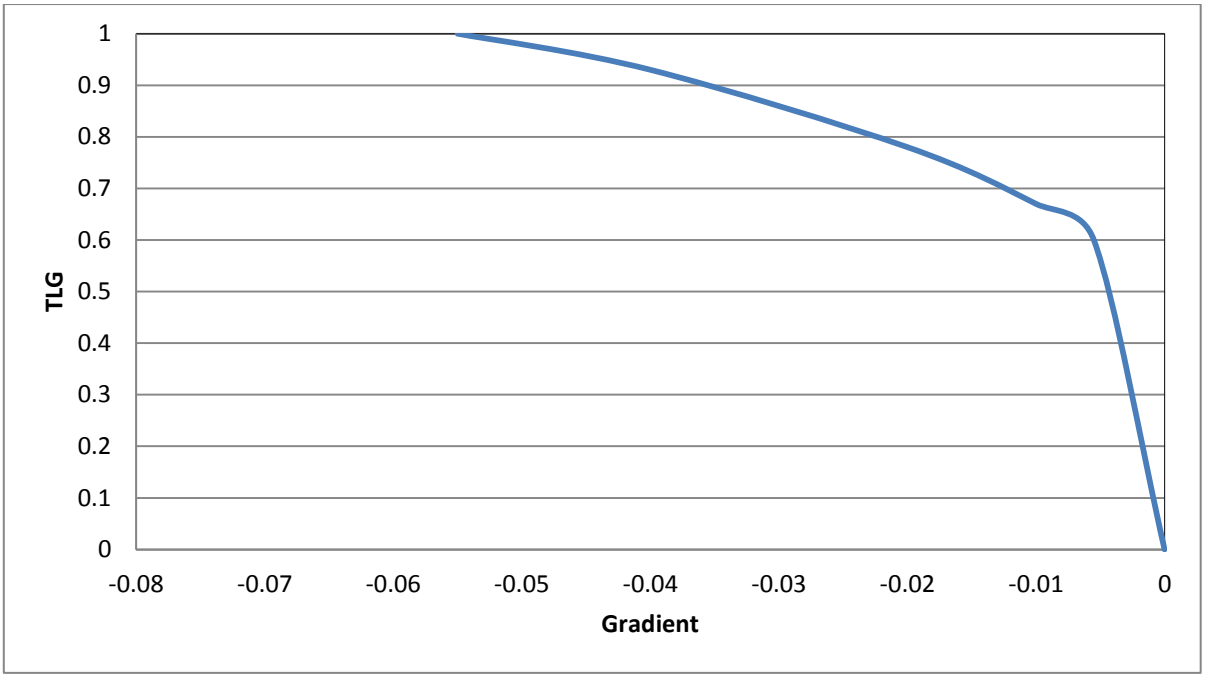

Figure 5.7. Shape of the power relationship between current downslope gradient and a model variable, TLG. The maximum value of TLG is defined by a model parameter (Hughes *et al.*, 2007).

$$\mathrm{TLG} = \begin{cases} 1, & \text{if } \dfrac{dh}{dL} < 0.7 * \mathrm{RWLGrad} \\ \dfrac{\dfrac{dh}{dL}}{(0.7 \cdot \mathrm{RWLGrad}) \cdot 0.25}, & \text{if } \dfrac{dh}{dL} \geq 0.7 * \mathrm{RWLGrad} \end{cases}$$ Equation 5.16

Where: *TLG= groundwater gradient of the near channel slope element [Dimensionless], dh/dL= Channel gradient [Dimensionless], RWLGrad = gradient of the rest water level [Dimensionless]*

Channel loss (mm) is then the product TLQ * TLG * TLGMax, which is removed from any available runoff and added to the lower slope component. The two exponents (0.4 and 0.25) have been fixed in the current version of the model to avoid introducing additional parameters that will be very difficult to quantify (Hughes *et al.*, 2007; Tanner, 2013). TLGMax is therefore the only additional parameter and it represents the maximum channel loss which is expressed as runoff from the whole catchment in mm month^{-1}. This maximum loss will occur when the lower slope gradient is lower than

70% of the gradient at the rest water level and when the catchment runoff is at its maximum value (Hughes *et al.*, 2007).

5.2.1.2 Channel losses from flow in the main channel

As indicated, the first channel loss routine only applies to incremental runoff generated within the catchment of the distribution system and not to upstream runoff that passes through that catchment. The simulation of cumulative channel losses uses the same functions as described above for catchment channel losses, however these are applied to the upstream inflow to the catchment. The groundwater gradient component of the function remains the same (Equations 5.18 and 5.19), except that *TLGMax* now represents a maximum channel loss from upstream inflow (in Mm^3). *TLGmax*_Inflow is calculated from the *TLGmax* parameter for incremental flow using the following scheme:

$$TLGmax_{Inflow} = TLGMax \cdot \left(\frac{MaxQ\_Inflow}{MaxQ}\right) \qquad \text{Equation 5.17}$$

Where: $TLGmax_{Inflow}$*= Maximum channel loss from upstream inflow [*$Mm^3\ month^{-1}$*], TLGMax = Maximum runoff loss from the whole sub-basin [mm* $month^{-1}$*], MaxQ_Inflow = Maximum upstream inflow [mm], MaxQ= Maximum catchment runoff [mm]*

Where MAXQ is defined previously as the maximum sub-area runoff (mm) and MAXQ_Inflow is the maximum upstream inflow. Both of these are set to initial values in the first run of the model (MAXQ = 20 mm, MAXQ_Inflow = 20 mm * cumulative upstream basin area) and are then re-calculated for the second run from the data simulated during the first run (Hughes *et al.*, 2007).

Equations 5.17 and 5.18 are also used to estimate the TLQ component, but with MAXQ replaced by MAXQ_Inflow and Q defined as the upstream inflow in any one month.

The cumulative inflow channel losses are estimated at the start of a single month's simulation and reduce the upstream inflow (there is no iteration of this calculation). The additional volume is then added to the near channel (or lower element) groundwater storage in equal amounts over the four model iteration steps.

Table 5.3. The parameters typically used in the channel transmission loss simulation

Parameter	Units	Description
GW	mm month^{-1}	Maximum recharge depth at maximum moisture capacity (ST)
GPOW	-	Power of the moisture storage recharge equation
ST	mm month^{-1}	Maximum moisture storage capacity
TLGMax	mm month^{-1}	Maximum channel loss (both incremental runoff (within one catchment) and runoff from upstream catchments are considered)
DD	km km^{-2}	Effective drainage density for groundwater inputs to streamflow
T	m^2 day^{-1}	Groundwater transmissivity
S	-	Groundwater storativity
Initial Groundwater drainage slope	-	Regional groundwater drainage slope
RWL	m	Rest water level roughly taken as aquifer depth/thickness. The lowest pont below which ground water processes cease.
RSF	%	Riparian Strip Factor. Controls riparian evaporation losses from groundwater storage

Hughes *et al.* (2007) have noted several shortcomings in relation to the simplified groundwater store geometry (Figure 5.4) and the estimation of the TLGMax parameter. In terms of the groundwater store geometry, the division of the basin into slope elements is indicative of all the channels while upstream inflow losses should only apply to the main channel. In reality, however, catchments that experience main stem channel losses would probably not have internal basin tributaries that could possibly generate groundwater flow. It is assumed that the effective channel network and drainage density for the purposes of groundwater-surface water interactions would be made up only of the main channel, therefore the drainage density would be low and the ratio between basin width and length also relatively low which should be a reasonable reflection of reality. Subsequent evaluations of the model have also noted

that Equations 5.17 and 5.18 resulted in unrealistic outcomes – extremely minimal channel losses were generated for various groundwater conditions. Additionally, TLGMax is considered to be a parameter that will always be difficult to quantify, largely due to the highly non-linear nature of channel loss processes (Hughes *et al.*, 2007; Tanner, 2013). In this study the maximum losses were determined by calculating the maximum volume of water that could be stored by the alluvial aquifer based on the average thicknesses reported as well as the effective porosity of the soil material. The actual transmission losses however would depend on other factors including the level of flow, the size of the aquifer in contact with the riverbed, regional slope for water loss into the adjacent areas, antecedent moisture content of the aquifer and riparian evapotranspiration (Moyce *et al.*, 2006). The use of TLGMax for both loss functions might be considered problematic; however, where there are major losses from upstream runoff, there is likely to be very little incremental flow within the catchment. The value of TLGMax will therefore be dominated by the range of values of upstream inflow, rather than local runoff. If the TLGMax parameter is set too high relative to simulated runoff depths it is possible that a large part of the runoff generated from other model components could be lost to groundwater. The relevance and inclusion of this parameter is a necessity for dry environments where the groundwater lower slope element gradient will be nearly always negative.

5.2.2 Using the wetland function

The wetland function in SPATSIM is based on a simple water balance approach with water draining into and out of the wetland (Hughes *et al.*, 2013). The function was added to the model to account for the downstream impact of wetlands and natural lake systems on streamflow (Hughes *et al.*, 2013). Processes associated with wetlands and lakes can exert a considerable influence on downstream flow regimes through attenuation, storage and slow release processes that occur as a consequence of the water bodies. These processes are critical to understanding the general patterns of runoff generation at the basin scale (Tanner, 2013). Prior to the addition of the explicit

function, wetlands were represented by a dummy reservoir (Mwelwa, 2004). However, simulation results did not adequately represent the processes prevalent in wetlands; hence the addition of the more specific wetland module. Since its addition, the function has been successfully applied by Tshimanga (2012) in Bangweulu wetland in Zambia, the Kamalondo depression wetland in Congo River basin and Lake Tanganyika. Hughes *et al.* (2013) used the function in the Kafue River basin, Congo River and the Okavango basin where it was applied to three sites – the steep valley and flat floodplains of the Kafue River, the natural lakes of the Congo River and the linear valley bottom type of wetlands of the Okavango River. Table 5.4 indicates the wetland parameters that are used for this sub-model, most of which are physically-based.

The wetland module has also been designed to work over four time steps within a month to avoid excessively large changes in any single component of the wetland water balance before other components are updated. Hughes *et al.* (2013) provides a detailed description of the setup of the wetland model. The description is summarised as follows:

- The maximum area of the wetland (including area inundated periodically or permanently) is given by MaxWA. The surface areas of the wetlands (WA) are estimated using the area-volume relationship:

$$\mathrm{WA} = \mathrm{AVC} * \mathrm{WV}^{AVP} \qquad \text{Equation 5.18}$$

Where: WA =Surface area of the wetland [km^2], WV = Wetland storage volume [Mm^3], AVC and AVP = constant and power in the area-volume relationship [Dimensionless].

Table 5.4. The parameters and algorithms used for the wetlands function in the SPATSIM Pitman Model. Dimensionless parameters are denoted with (-) (Hughes *et al.*, 2013)

Parameter	Units	Description and use
Code for Wetland function (-99)	-	Activates wetland function
MaxWA	km^2	Maximum wetland area, permanently or temporarily flooded, accounts for local runoff entering directly in to the wetland.
RWV	$m^3 * 10^6$	Residual wetland storage volume below which there are no return flows to the river channel.
IWV	$m^3 * 10^6$	Initial wetland storage volume at the start of the simulation.
AVC	m^{-1}	Constant in the $WA=AVC*WV^{AVP}$ relationship, where WA (m^2) and WV (m^3) are the current wetland area (limited to MaxWA) and volume, respectively; also represented as A in Area (m^2) = A * Volume (m^3) ^{B}
AVP	-	Power in the $WA=AVC * WV^{AVP}$ relationship; also represented as A in Area (m^2) = A * Volume (m^3) ^{B}
QCap	$m^3 * 10^6$	Channel capacity for spillage; capacity below which there is no spill from the channel to the wetland.
QSF	-	Channel spill factor in SPILL= QSF * (Q–QCAP), where Q is the upstream flow, and SPILL is the volume added to wetland storage. That is the proportion of flow above the channel that is assumed to spill to the wetland.
RFC	-	Return flow constant in $RFF = RFC * (WV / RWV)^{RFP}$ [also represented as AA in Return Flow = AA* $(Vol/RWS)^{BB}$] where RFF is a Return Flow Factor that determines the amount of water that returns from the wetland to the river channel and contributes to downstream. A maximum fraction is assumed to be 0.95
RFP	-	Return flow power in the $RFF = RFC * (WV / RWV)^{RFP}$ (wetland storage-return flow relationship) [also represented as BB in Return Flow = AA * $(Vol/RWS)^{BB}$] designed to account for non-linear relationships.
EVAP	mm	Annual evaporation from the wetland (distributed into monthly values using a table of calendar month percentages).
ABS	$m^3 * 10^6$	Annual water abstractions from the wetland (distributed into monthly values using a table of calendar month percentages).
AA Scaling factor	-	Dimensionless scaling factor
Max. Return Flow Fraction	-	Dimensionless maximum return flow fraction

Local runoff is added to the part of maximum wetland area (MaxWA) that is not inundated. The volume of rainfall is assumed to be added on the basis of the rainfall depth falling on the inundated area of the wetland (WA). The maximum area of the

wetland (MaxWA) can be estimated using topographic data. The residual volume of the wetlands and the empirical parameters of the non-linear relationship (AVP and AVC) can be estimated from measurable properties of the wetlands.

- Water is added to the wetland through:
  - Direct precipitation falling onto the wetland;
  - Surface runoff from the contributing basin area; and
- Surface water inflow from stream, calculated as a proportion of the total upstream channel. The inflow from the channel is calculated as a fixed proportion (QSF) of the total upstream flow.
- Water in the wetlands is lost through:
  - Potential evapotranspiration. Evapotranspiration losses from wetlands are calculated using an annual potential evaporation (PEVAP) distributed in 12 months values and the current submerged wetland area (WA).
  - Return flow from the wetlands to the stream- determines the amount of water that returns from the wetland to the river channel and contributes to downstream.The size of the flow is determined by a power function between a return flow fraction (RFF, with maximum value of 0.95) and the ratio of the current storage of the wetland (WV) to the residual (RWV), where RWV is the volume below which water is unable to flow back to the channel.
  - Abstractions from the wetland used for irrigation, domestic use and other uses. Artificial abstractions from the wetlands are calculated from an annual value, (ABS), which is distributed into twelve month values based on knowledge of abstraction patterns.

With regards to the estimation of transmission losses, it is important to note that this simplified water balance approach employed by the wetland function ignores any interactions between the wetland and the groundwater component of the natural hydrology of the basin. Incorporating the wetland function affects low flows by reducing stream flows which can change the base flow response (Tanner, 2013).

5.2.3 Using the dummy dam approach

Prior to the addition of an explicit transmission loss function (Hughes, 2004), such losses were simulated through the use of 'dummy' dams representing loss storage and evaporating area (Görgens and Boroto, 2003; Hughes *et al.*, 2003). Morgan (1996) detailed the use of an earlier version of the Pitman Model, WRSM90 Version 2.1 (Pitman and Kakebeeke, 1991), in estimating transmission losses and was critical of the model as it accounted for transmission losses to evaporation and infiltration artificially - the losses were estimated and included in the model as a series of 'dummy' dams to model the floodplain. The sizes of the 'dummy' dams were then adjusted by trial and error until the required inflow-outflow relationship from the floodplain was generated. This is however only possible in gauged basins. A study (Hughes *et al.*, 2006) focussing on the impact of climate change and development scenarios on flow patterns in the Okavango River represented channel transmission losses as 'dummy' reservoirs based on a quantification of channel lengths and widths of floodplains and swamps - riparian areas that were hypothesised to be fed by seepage from the river, and from which water was assumed to evaporate, were modelled as open water surfaces ("dummy" reservoirs). The study noted that the presence of the 'dummy' reservoir reduced streamflow from the Omatako catchment to zero flow at the outlet, which was the right behavioural effect. However this was deemed not quite a good representation as the parameter values that were used were based on inadequate information.

The basis of the reservoir function, as a water use component of the Pitman Model, is to simulate the impact of large dams on the basin's streamflow. Inflows to the reservoir include flow originating within the catchment and from all upstream catchments (Hughes *et al.*, 2006). The requirements for the reservoir function are monthly distributions of normal drafts or fraction of annual abstraction requirement (ABS in Table 5.5) and compensation flow requirements, as determined by the parameter COMP (

Table 5.5), as well as monthly distributions of drafts and compensation flow for up to five reserve supply levels as defined by parameters RES1–RES5 (
Table 5.5).

Table 5.5. Reservoir function parameters.

Parameter	Units	Description and use
CAP	m^3*10^6	Reservoir storage capacity
DEAD	%	Dead storage of the reservoir
INIT	%	Initial Storage (reservoir magnitude at the beginning of the simulation period)
A	-	Parameters in non-linear dam area-volume relationship; A in Area(m^2) = A* Volume(m^3)^B
B	-	B in Area(m^2) = A * Volume(m^3)^B
RES1-5	%	5 levels of operating rules used to reduce abstraction of reduced storage.
ABS	m^3*10^6	Annual Abstraction Volume (demand from the reservoir)
COMP	m^3*10^6	Annual Compensation Flow (downstream compensation flow released into the river)
AR	-	Reserve constant in Reserve (%) = AR * Volume (% Capacity)^{BR}
BR	-	Reserve power in Reserve (%) = AR * Volume (% Capacity)^{BR}

Dimensionless parameters are denoted by (-).

Although the 'dummy' reservoir approach to simulating transmission losses has been successfully applied in a number of studies, Hughes (2008) was concerned that the approach relates to the simulation for perennial rivers flowing through arid areas and that the 'dummy' reservoir was always full with the losses dependent only on the evaporation rate and the surface area.

5.3 UNCERTAINTY ANALYSIS IN SPATSIM

While the concept of uncertainty in hydrological modelling and water resources planning dates back as far as the 1970s (Stephenson and Freeze, 1974), its inclusion in hydrological predictions is a relatively recent development (Hromadka and McCuen, 1988; Melching *et al.,* 1990; Beven and Binley, 1992). In general terms, 'uncertainty' is

a lack in confidence. When applied to decision-making, the Business Dictionary (2016) described it as a 'situation where the current state of knowledge is such that the consequences, extent, or magnitude of circumstances, conditions, or events is unpredictable'. In hydrological modelling, 'predictive uncertainty' refers to the 'probability of occurrence of a future value of a predictand (such as water level, discharge or water volume) conditional upon prior observations and knowledge as well as on all the information we can obtain on that specific future value from model forecasts' (Coccia and Todini, 2011). This definition of uncertainty relates to the need for thoughtful consideration of variations in data used for predictive hydrological models applied in water resource management and planning. The consideration of uncertainty in hydrological modelling is thus premised on the notion that a better understanding of uncertainty is likely to result in improved interpretations of the resulting model predictions, regardless of the condition of data in the basin (Mwenge Kahinda *et al.*, 2016). Hydrological modelling studies have consequently focussed on investigating the possible sources of uncertainty, quantifying the uncertainty, assessing its impact in hydrologic predictions and trying to reduce it where possible. Along with data input, uncertainties in the hydrological modelling process are introduced through four main sources, namely (Renard *et al.*, 2010; Kapangaziwiri, 2011; Hughes *et al.*, 2015):

i. input data, which considers the quality (errors and relevance, e.g. rating curve errors affecting runoff estimates) and quantity of data used to drive (or guide) model simulations;
ii. output data, which relates to the quality and accuracy of the results obtained from the modelling process; as well as the modeller's knowledge in adequately interpreting the results;
iii. model structure, relates to the capability of the model to adequately represent complex hydrological reality using simplifications in hydrologic models; and

iv. parameter estimation, relates to the inability to specify exact values of model parameters due to errors in the calibration and input data, imperfect process understanding or model approximations.

The effect, whether combined or not, of these uncertainties on modelling results ultimately impacts the qualitative and quantitative assessment of available resources. Estimation of uncertainties is thus essential for determining the level of confidence that could be expressed in the model-generated data which inform the decision and policy-making process, leading to better risk assessment (Reichert and Borsuk, 2005; Kapangaziwiri *et al.*, 2012).

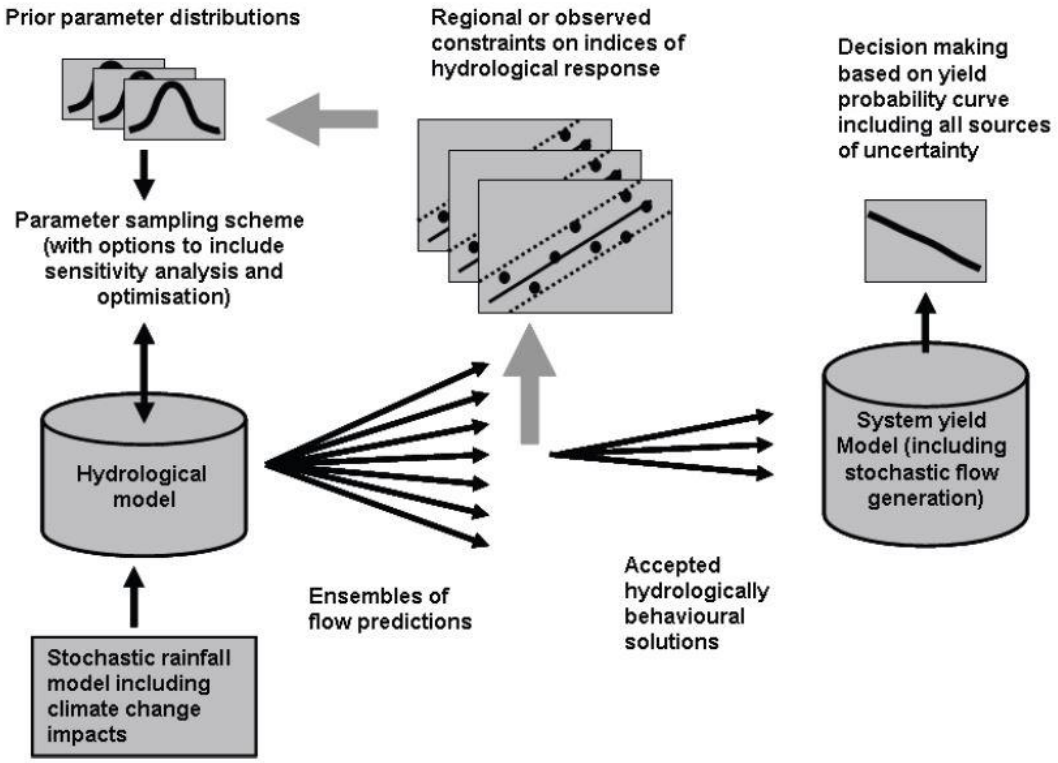

Figure 5.8. The Pitman Model uncertainty framework in SPATSIM (Tshimanga, 2012; Hughes *et al.*, 2015).

Performing uncertainty analyses on large basins with numerous catchments is exceedingly complex; therefore a revised approach to including uncertainty was developed for the Pitman model (Hughes *et al.*, 2015). The revised method utilises a two-step approach which involves firstly, the use of manually calibrated regional or

local constraints (based on natural runoff characteristics such as mean monthly flow and flow duration curve indices) to identify behavioural parameter sets in the simulation of natural incremental flows for each-basin based on inputs of uniform parameter distributions defined by minimum and maximum values for each catchment and Monte Carlo random sampling to generate a specified number of ensembles (e.g. 10 000) of simulated streamflow (Tumbo, 2014; Tanner and Hughes, 2015; Hughes *et al.*, 2015). The distributions of lower and upper bounds are assumed to represent variations of calibrated parameters (Sawunyama, 2008). Behavioural parameter sets are those that are considered to best simulate the 'real-life' active processes occurring in a hydrological basin against a likelihood measure (Beven, 2001; Kapangaziwiri, 2008). The parameter sets determined and saved from the incremental uncertainty run (Step 1) can then be used with uncertain non-natural water use parameters in the second run of the model when the cumulative flows at the outlet of all catchments are simulated (Hughes *et al.*, 2015). In the context with this study, channel transmission loss parameters are included in the second run with the water use parameters such as the anthropogenic reservoir functions. The second run of the model (the cumulative uncertainty run) generates ensembles that are saved in the SPATSIM database and can be viewed and analysed using any spreadsheet software (such as Excel). Figure 5.8 is a schematic of the uncertainty framework used in SPATSIM. As illustrated in the diagram, the uncertainty approaches used in the Pitman model have been developed to be compatible with both the traditional approach of using stochastic streamflow flow sequences in the yield model and the approach of using stochastic rainfall sequences within the hydrological model.

5.4 HYDROLOGICAL MODELLING

The Pitman Model was setup with data that was described in Chapter 4. Models parameters representing interflow runoff (FT and POW), surface runoff (ZMIN, ZAVE, ZMAX), unsaturated soil moisture storage (ST) and groundwater recharge processes (GW) were calibrated against observed (naturalised) flow data. The groundwater

parameters (DD, GWSlope, RWL, S, T, RSP) were not calibrated but estimated from alluvial aquifer conditions detailed in Chapter 3. Insufficient aquifer data was supplemented with information from the GRAII database (DWAF, 2005). At this point in the model run, channel transmission losses were not included. The calibration of the model parameters was initiated in the headwater catchments and progressed downstream. It involved trial runs of the 'single run' version to establish mean parameter values considered likely to represent hydrological responses for each catchment. The model performance was evaluated against the observed flow data, where available, with the intention being to simulate flow that is similar to the observed.

Once the appropriate model performance was established, the mean monthly runoff (MMQ: MCM), mean monthly groundwater recharge and three percentiles (10%, 50%, 90%) of the flow duration curve (FDC) as well as the percentage zero flows were used to establish constraints for the model, which are required for running the uncertainty version of the model.

The uncertainty version of the model was firstly run to simulate the incremental flows for individual catchments and to identify behavioural parameter sets from 10 000 ensembles using Monte Carlo sampling. Uncertainty analysis is described in Section 5.3. The mean parameters established from the single run were used to establish the parameter sampling space, which was defined from setting maximum and minimum model parameter values. Once suitable behavioural parameter sets were established for each catchment, the cumulative uncertainty run was initiated to simulate cumulative flows for the whole sub-basin.

Subsequent to the two uncertainty runs being performed, channel transmission losses were added to the model input data through the: (i) explicit transmission loss function (TLGMax parameter); (ii) wetland function and (iii) reservoir function. This modelling step involved running each function independently, using the single run version. Other

model parameters were kept constant for the simulation. For each sub-basin, the parameters of the three functions were setup as follows:

i. Transmission loss function (Table 5.1): The TLGMax parameter was adjusted until a suitable channel loss was simulated.
ii. Wetland function (Table 5.4): MaxWA represents the area of the delineated alluvial aquifer; RWV represents the estimated capacity of the alluvial aquifer; values for the wetland area-volume equation were estimated from the dimensions of large dams in each respective sub-basin

Reservoir function (

iii. Table 5.5): CAP represents the capacity of the delineated alluvial aquifer; values for the dam area-volume equation were estimated from the dimensions of large dams in each respective sub-basin.

An assessment of the model performance was carried out, after the inclusion of channel transmission losses based on an evaluation of the correlation between observed and simulated flow. Three objective functions were used for the evaluation criteria, each calculated on the basis of both untransformed and natural log-transformed data, as suggested by Hughes *et al.* (2006). The objective functions include the coefficient of determination (R^2), coefficient of efficiency (CE) (Nash and Sutcliffe, 1970) and the mean monthly percentage difference error of the simulated flows (relative to observed) (PBIAS). The coefficient of determination (R^2), which ranges from 0 to 1, describes the goodness of fit of the model simulation i.e. it determines whether there is good correlation between the observed and simulated data (Moriasi *et al.,* 2007). The coefficient of efficiency or the Nash-Sutcliffe efficiency (NSE) indicates how well the plot of observed data versus simulated data fits the 1:1 line (Nash and Sutcliffe, 1970; Moriasi *et al.*, 2007). It quantifies the ability of the model simulation in predicting the outcome variable. The percentage difference error (percentage bias, PBIAS) determines whether the simulation is consistently under- or overestimated

compared to the observed data. The recommended statistics for model performance (Moriasi *et al.*, 2007) are indicated in Table 5.6.

Table 5.6. General performance ratings for recommended statistics for a monthly time step hydrological model. (After Moriasi *et al.*, 2007).

Performance rating	**Metric (CE or R^2)**	**PBIAS (% Mean Difference)**
Very good	0.75 <Metric<1	PBIAS <+/-10
Good	0.65 <Metric<0.75	+/-10 ≤PBIAS <+/-15
Satisfactory	0.50 <Metric<0.65	+/-15 ≤PBIAS <+/-25
Unsatisfactory	Metric<0.5	PBIAS ≥+/-25

CE denotes coefficient of efficiency; PBIAS denotes mean percentage difference between observed and simulated flow

5.5 CLOSING REMARKS

The Pitman model is the preferred hydrological model for this study. Apart from it being an integrated model that can support regional water resource assessments, it can be relatively easily parameterised in data scarce areas (using relatively easily accessible data in the southern Africa region) and it allows the incorporation of estimates of uncertainty, which is critical for water assessment processes in semi-arid regions like the Limpopo River Basin. The model has been used extensively across a variety of semi-arid southern Africa environments and it also has channel transmission loss estimation capabilities – a significant surface stream channel process with an impact on available water resources in the basin and is also the focus of this study. The setup of the Pitman Model for each sub-basin has also been described. Parameters used for each function are indicated in the Chapter 6.

CHAPTER 6
Results and discussion

6.1 INTRODUCTION

This chapter presents the results of the study, accompanied with a discussion of the observations made. The delineation of alluvial aquifers across the Limpopo River Basin is considered, with focus being placed on the physical properties and estimation of saturated capacity of the alluvial aquifers in the selected study areas. An illustration of the conceptual understanding of channel loss processes in each of the study areas is also presented. The outcomes of hydrological modelling for each selected catchment are also presented, along with an account of the impact of channel transmission losses on water resource estimation.

6.2 RESULTS

6.2.1 Delineation of alluvial aquifers in the Limpopo River Basin

The study focused on delineating alluvial aquifers along the major tributaries of the Limpopo River Basin. While the aquifer dimensions for each sub-basin in the Limpopo River Basin are detailed in Kapangaziwiri *et al.* (2016), only the results of the three selected study areas are discussed in this dissertation.

6.2.1.1 Mokolo sub-basin

In the Mokolo sub-basin, alluvial aquifers occur as upper and lower catchment aquifers and comprise both channel and floodplain deposits (Figure 6.1).

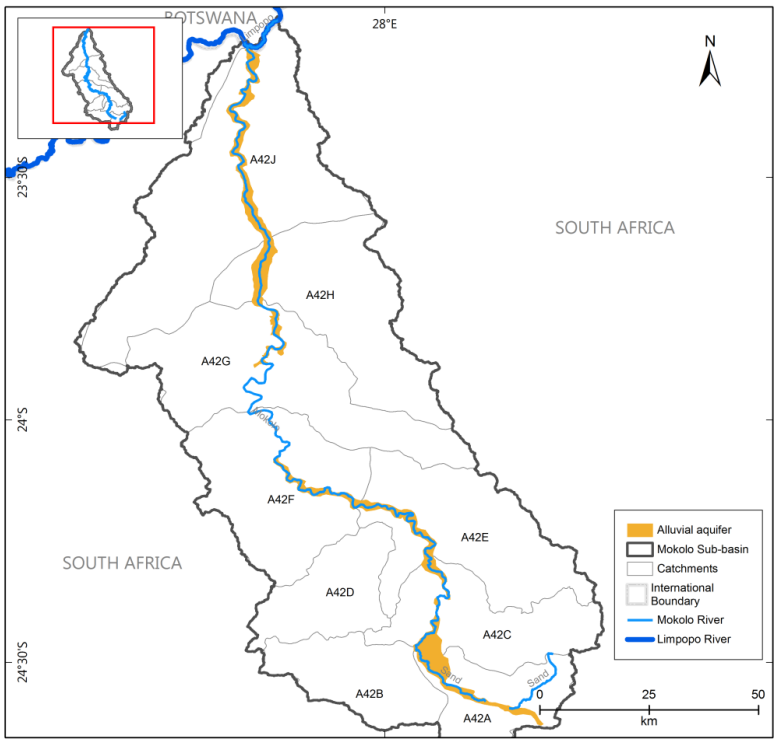

Figure 6.1. Delineation of alluvial aquifers in the Mokolo sub-basin

The upper catchment aquifer is separated from the lower aquifer by a steep gorge that occurs along the middle reach of the Mokolo River. The channel alluvial aquifer occurs as 0.2 km (average) wide deposits covering an approximate areal extent of 20 km^2 while the floodplain deposits average to a width of 0.5 km, covering an approximate areal extent of 304 km^2 (Table 6.1); the total alluvial aquifer extent is therefore an estimated 324 km^2. The length of the aquifer zone measures 242 km. According to Prucha *et al.* (2016), the alluvial deposits along the Mokolo River reach up to 2 km in width and range from 4 m thickness upstream of the Mokolo Dam, to more than 9 m toward the confluence with the Limpopo River.

Table 6.1. Characterisitcs of the Mokolo River alluvial aquifer

Mokolo River Alluvial Aquifer	
Estimated length of alluvial aquifer	242 km
Approximate area of alluvial aquifer	324 km^2
Alluvial sediments characteristics	Acrisol, Leptosol, Arenosol, Luvisol, Lixisol, Cambisol
Regional slope (average)	%
Channel alluvial aquifer	
Channel type	Meandering
Channel width (average)	0.2 km
Approximate areal extent of channel deposits	20 km^2
Natural/ Artificial barriers	Cultivated areas along channel, gorge
Alluvial plains	
Plains width (average)	0.5 km
Approximate areal extent of alluvial plains (range)	304 km^2

6.2.1.2 Motloutse sub-basin

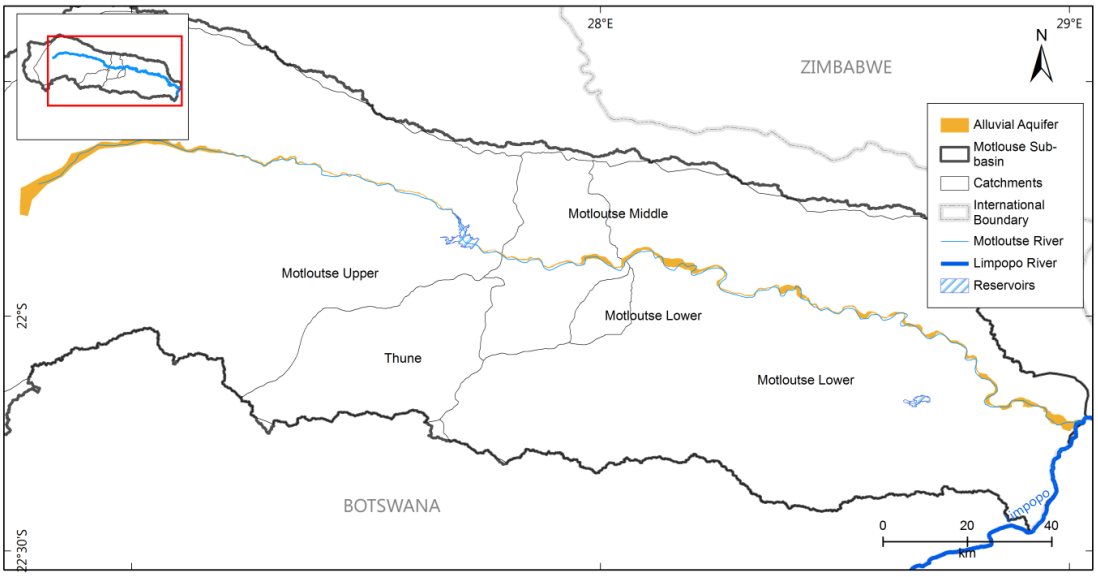

Figure 6.2. Delineation of alluvial aquifers in the Motloutse sub-basin

As a result of the relatively flat terrain of the Motloutse sub-basin, alluvial aquifers occur as both upper and lower catchment aquifers and comprise both channel and plains deposits (Figure 6.2). The channel alluvial aquifer occurs as 0.3 km (average) wide deposits covering an approximate areal extent of 131 km^2 while the floodplain deposits average to a width of 1 km, covering an approximate areal extent of 62 km^2 (Table 6.2). The total alluvial aquifer extent is therefore an estimated 193 km^2. The length of the aquifer zone measures 319 km. The upstream reach of the Motloutse is associated with significant alluvial deposits that were mined for diamonds in the late 1950s (Moore, 1988). According to De Wit and Cavaliere-Parzaneze (1990), the younger alluvial deposits along the Motloutse River are 0.5 km wide while older deposits are broader. Ranges of soil depth are given as 4 - 9 m over the length of the river from about 20 km upstream of Mmadinare to the Limpopo confluence (Botswana DWA, 1989).

Table 6.2. Characteristics of the Motloutse River alluvial aquifer

Motloutse River Alluvial Aquifer	
Estimated length of alluvial aquifer	319 km
Approximate area of alluvial aquifer	193 km^2
Alluvial sediments characteristics	Cambisol, Luvisol, Leptosol, Arenosol, Regosol
Regional slope (average)	0.2 %
Channel alluvial aquifer	
Channel type	Relatively straight upstream, meandering downstream
Channel width (average)	0.3 km
Approximate areal extent of channel deposits	131 km^2
Natural/ Artificial barriers	Dryland cultivation
Alluvial plains	
Plains width (average)	1 km
Approximate areal extent of alluvial plains (range)	62 km^2

6.2.1.3 Mzingwane sub-basin

Channel and floodplain alluvial deposits were delineated in the upper and lower catchments of the Mzingwane sub-basin (Figure 6.3). The channel alluvium occurs as 0.25 km (average) wide deposits covering an approximate areal extent of 40 km^2 while the floodplain deposits average to a width of 0.35 km, covering an approximate areal extent of 57 km^2 (Table 6.3).

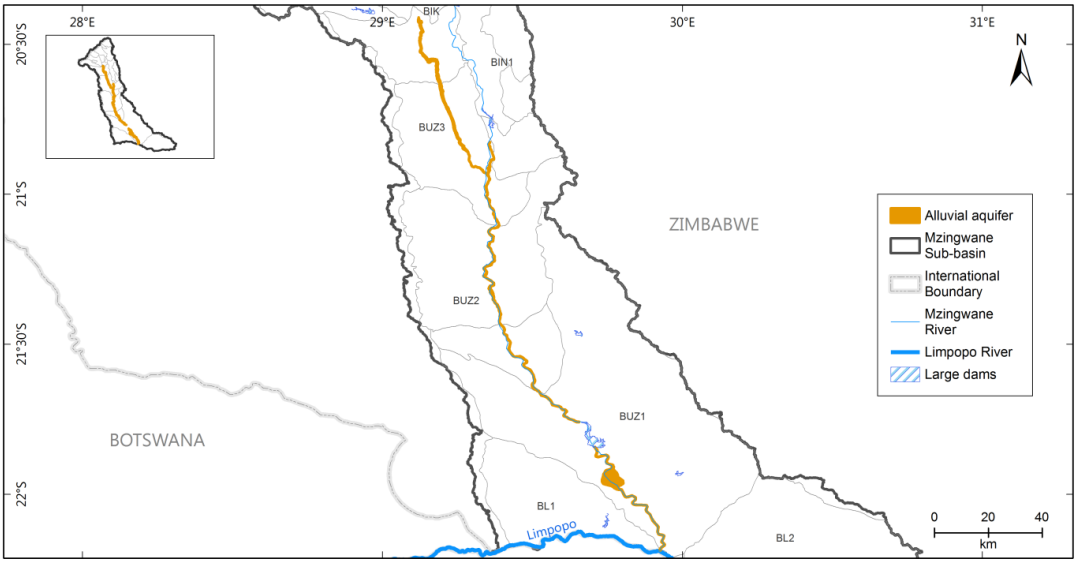

Figure 6.3. Alluvial aquifer delineated in the Mzingwane sub-basin.

The total alluvial aquifer extent is therefore an estimated 97 km^2. The length of the aquifer zone measures 262 km. In characterising the alluvial aquifers in the Mzingwane sub-basin, Love *et al.* (2007) stated that the deposits are generally less than 1 km in width and areal extents ranging from 1 km^2 to 2.55 km^2 in the channels and 0.85 km^2 to 4.3 km^2 on the flood plains. Moyce *et al.* (2006) indicated that alluvial aquifers occur almost everywhere along the length of the Mzingwane River. However, individual alluvial aquifers were measured with areal extents ranging from 0.45 km^2 to 7.23 km^2 in the channels and 0.75 km^2 to 21.96 km^2 on the floodplains. Moyce *et al.* (2006) measured saturated alluvial thicknesses ranging from 1 m to 5 m, while Masvopo (2008) measured an average saturated thickness of 12.65 m for the Malala alluvial aquifer, which is found in the lower reach of the Mzingwane River past the confluence

with the Mtetwenge River. This significant range of thicknesses is accounted for in the estimation for alluvial aquifer capacity.

Table 6.3. Characteristics of the Mzingwane alluvial aquifer

Mzingwane River Alluvial Aquifer	
Estimated length of alluvial aquifer	262 km
Approximate area of alluvial aquifer	97 km^2
Alluvial sediments characteristics	Luvisols, Leptosols
Regional slope (average)	2.4%
Channel alluvial aquifer	
Channel type	Relatively straight river course, meanders along downstream catchments
Channel width (average)	0.25 km
Approximate areal extent of channel deposits	40 km^2
Natural/ Artificial barriers	Upstream cultivated lands, downstream river valley
Alluvial plains	
Plains width (average)	0.35 km
Approximate areal extent of alluvial plains (range)	57 km^2

6.2.2 Conceptual framework of transmission losses in the Limpopo River Basin

The occurrence of transmission losses along a river channel depends on a number of physical and climatic factors that characterise a basin and its water resources (Hameed *et al.*, 1996; Smakhtin and Watkins, 1997; Boroto and Görgens, 2003). Several of these factors can be quantified (e.g. evaporation, groundwater recharge); however others such as aquifer depth are not easily incorporated into precise calculations as a result of a lack of data, particularly in under-resourced semi-arid basins such as the Limpopo (Hameed *et al.*, 1996; Hughes, 2008a). As a result of climatic variability and other uncertainties, prediction of channel transmission losses in water resource management cannot be done confidently. Be that as it may, the use of conceptual models is

beneficial in gaining at least a theoretical understanding of the apparent dynamics that influence transmission losses. In deriving a conceptual hydrological framework for the Limpopo River Basin, Kapangaziwiri *et al.* (2016) (Figure 6.4) adopted the general model applied by Tshimanga (2012). The conceptual framework (Figure 6.4) shows the propagation of water through the hydrological cycle and the various hydrological stores.

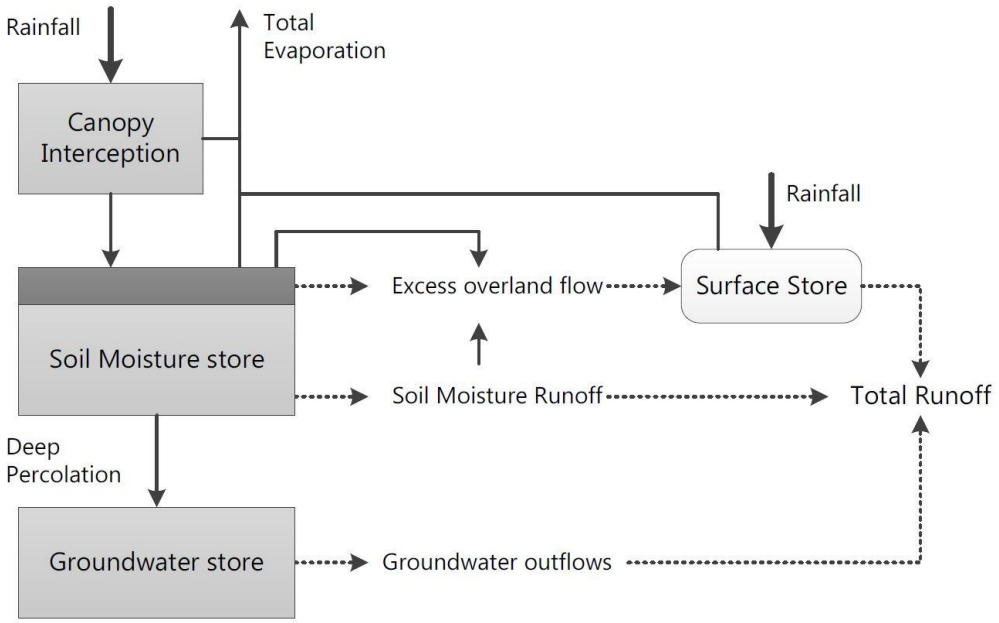

Figure 6.4. Conceptual hydrological framework for the Limpopo River Basin (Kapangaziwiri *et al.*, 2016)

The conceptual hydrological framework for this study is thus based on this framework by Kapangaziwiri *et al.* (2016), given the assumption that the hydrological processes would not be entirely different. The schematic (Figure 6.5) illustrates an adapted generalised conceptual water budget, which considers the dominant natural processes and anthropogenic activities that impact on the availability of streamflow in the study areas. The framework indicates the propagation of water through the basin, from when it 'enters' the hydrological regime as mean annual precipitation (MAP) to when it 'exits' at the outlet catchment as mean annual runoff (MAR). In between the 'entryway' of the framework (which represents the headwaters of the basin) and the outlet, streamflow

in the channel is impacted by various water users. Natural water 'users' include environmental water requirements (fauna and flora) that need to be met to sustain a functional ecosystem and natural hydrological processes (evaporation, evapotranspiration, groundwater recharge) that reduce streamflow in the channel and can therefore be summed up as channel transmission loss processes. Anthropogenic water uses are broadly described as surface water use and groundwater abstractions. Surface water use includes storage of stream flow in large municipality dams for urban, domestic and industrial use and smaller farm dams that supply irrigation for commercial agricultural lands and livestock etc.; and large commercial plantations. Groundwater abstractions, for domestic use and irrigation, are also indicated in the category of anthropogenic water uses.

The conceptualisation of channel transmission loss processes is based on the study area descriptions provided earlier in Chapter 3 as well as the literature reviewed in Chapter 2, which detail the dynamics of channel transmission losses and alluvial aquifers.

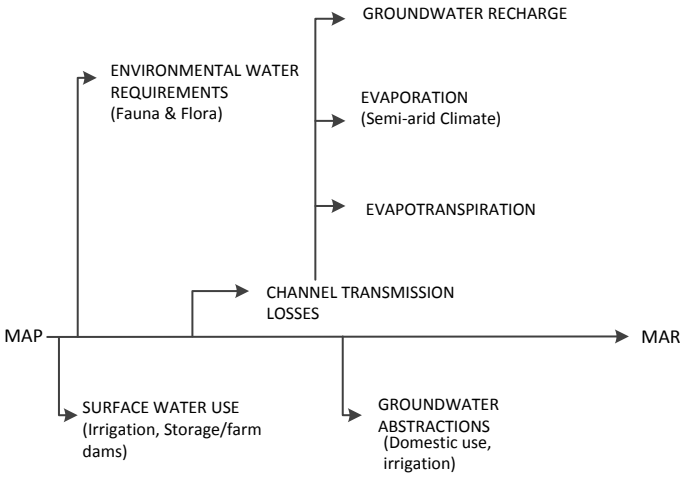

Figure 6.5 Conceptual hydrological framework for the Mokolo, Motloutse and Mzingwane catchments

The climate of the Mokolo sub-basin ranges from arid to semi-arid with evaporation becoming increasingly higher than precipitation towards the north. Figure 6.5 illustrates this conceptually. It is therefore expected that evaporation, from the free water surface and from recharged banks and the riverbed, will contribute significantly to the loss processes in the catchment. The catchment has a predominantly flat topography which presumably has enabled the deposition of alluvium along much of the Mokolo River, with deeper soils occurring near the mouth of the river. The abundance of alluvium along the river means that the riverbed and banks will need to be recharged before flow can occur in the river. However sand mining of the alluvium, which is a major activity in the catchment, may reduce the capacity of the alluvial aquifer and as a result of the soil disturbance, recharge processes may be limited. The pits left by sand mining can however increase recharge by storing water when it rains or floods. In upstream areas, floodplains are used as agricultural lands therefore evapotranspiration from cultivated areas poses as a major contributor to loss processes. Streamflow in the Mokolo River is highly regulated by the Mokolo Dam therefore loss processes also depend on the regularity of flow in the river.

The Motloutse sub-basin is characterised by a semi-arid climate with rainfall being highly seasonal, therefore loss processes are expected to be dominated by evaporation and seasonal recharge of available stores. Extensive and deep alluvial deposits line the channel bed and would need to be recharged before any flow can occur in the Motloutse River. Land use in the Motloutse sub-basin is predominantly subsistence farming, with water for irrigation being accessed from boreholes dug into the alluvial aquifers. The abstraction of groundwater from alluvial aquifers means that the water table in the vicinity is consistently lowered by the withdrawal of water, thus the connectivity between surface water and groundwater is affected.

The Mzingwane sub-basin is also largely semi-arid therefore evaporation from the free water surface and recharged riverbed and banks is expected to be one of the dominant transmission loss processes in the region – it is generally accepted that indirect

recharge by transmission losses increases with aridity (De Vries and Simmers, 2002). As an ephemeral river, the Mzingwane River experiences flow during the rainy season presumably after the bed and banks of the river have been recharged. The sandy deposits which make up the alluvial aquifer environment of the Mzingwane system are also major groundwater sources therefore streamflow is reduced due to groundwater abstractions.

6.2.3 Estimation of transmission losses based on physical basin characteristics

Table 6.4 toTable 6.6 give the estimated volume of water that can be stored in the delineated alluvial aquifers. This is the product of the derived areal extents of the alluvium, the average saturated aquifer thickness and the estimated effective porosity of the soil material making up the alluvial deposit. The estimated saturated aquifer thickness and effective porosity are based on previous hydrogeological work conducted in the Limpopo River Basin and literature for similar alluvial aquifer environments. The method applied (Equation 4.1) is discussed by Masike (2007) who further indicates that estimation of aquifer capacity comes with great uncertainty due to the high variability of aquifer properties. Several assumptions were made in estimating the volumetric capacity of each alluvial aquifer, namely:

v. The estimated average thickness of the alluvial aquifer was assumed to be fully saturated;
vi. With regard to hydraulic properties, the alluvial material was assumed to behave in a homogenous manner along the length of the delineated aquifer;
vii. The alluvial aquifer was assumed to occur as a closed system in that exchanges with underlying lithology were not considered.
viii. Flow in the river channel is naturalised, therefore the impact of groundwater abstractions and surface water withdrawals is not considered.

6.2.3.1 Alluvial aquifers of the Mokolo sub-basin

The channel and floodplain alluvial deposits of the Mokolo sub-basin were estimated to have a capacity of 62 Mm^3 and 607 Mm^3, respectively, which results in 669 Mm^3 in total (Table 6.4). The alluvial aquifer can store approximately 2.8 Mm3 per km length of the river. The upstream floodplains in catchments A42A to A42F are mainly large cultivated agricultural fields which utilise the fertile alluvium. The capacity increases towards the confluence of the Mokolo River with the Limpopo River main stem due to a gentler gradient which facilitates the extensive deposition of broader and thicker alluvium.

Table 6.4. Estimation of the capacity of the Mokolo River alluvial aquifer

	Channel alluvial aquifer				**Floodplain alluvial aquifer**			
Catch	**A (km^2)**	**b (m)**	**ñ (%)**	**V_w (Mm^3)**	**A (km^2)**	**b (m)**	**ñ (%)**	**V_w (Mm^3)**
A42A	-	-	-	-	60.03	3	0.37	66.63
A42C	-	-	-	-	41.83	4	0.37	61.91
A42E	-	-	-	-	40.24	4	0.37	59.56
A42F	-	-	-	-	29.77	5	0.37	55.07
A42G	5.44	7	0.37	14.09	19.19	6	0.37	42.60
A42H	2.95	8	0.37	8.73	37.48	7	0.37	97.07
A42J	11.89	9	0.37	39.59	75.58	8	0.37	223.72
Total	20.28			62.42	304.12			606.56

'Catch' denotes the catchment. A denotes alluvial aquifer areal extent, b denotes the estimated aquifer thickness, ñ denotes the average effective porosity, Vw denotes the aquifer capacity and (-) denotes that channel alluvial aquifer is not specified in that catchment.

6.2.3.2 Alluvial aquifers of the Motloutse sub-basin

The capacity of the Motloutse alluvial aquifer (

Table 6.5) was estimated to be 329 Mm^3, comprising 217 Mm^3 from channel alluvium and 112 Mm^3 from floodplain deposits. The alluvial aquifer can store an approximate 1.0 Mm^3 water per km length of the river channel.

Table 6.5. Estimation of the capacity of the Motloutse River alluvial aquifer

Catch	Channel alluvial aquifer				Floodplain alluvial aquifer			
	A (km^2)	**b (m)**	**ñ (%)**	**V_w (Mm^3)**	**A (km^2)**	**b (m)**	**ñ (%)**	**V_w (Mm^3)**
Upper Motloutse	95.38	5	0.37	141.16	1.55	4	0.37	2.29
Middle Motloutse	6.12	5	0.37	11.32	5.96	4	0.37	8.82
Lower Motloutse 2	29.22	6	0.37	64.86	54.51	5	0.37	100.84
Total	130.74			217.35	62.02			111.96

'Catch' denotes the catchment. A denotes alluvial aquifer areal extent, b denotes the estimated aquifer thickness, ñ denotes the average effective porosity and Vw denotes the aquifer capacity.

6.2.3.3 Alluvial aquifers of the Mzingwane sub-basin

The channel and floodplain alluvial deposits of the Mzingwane sub-basin were estimated to respectively have a capacity of 59 Mm^3 and 126 Mm^3 which results in 185 Mm^3 for the Mzingwane (Table 6.6). According to Moyce *et al.* (2006), the estimated water volumes of the aquifers along the Mzingwane River range between 0.175 Mm^3 and 5.43 Mm^3 for channel alluvium, and 0.08 Mm^3 and 6.9 Mm^3 for floodplain alluvium. Moyce *et al.* (2006) however indicated that the volumes calculated are an underestimate, on the basis that minimum saturated aquifer thickness was used in the calculation. Based on the aquifer capacity calculated in the current study, the alluvial aquifer can store approximately 0.7 Mm^3 water per km length of the river channel.

Table 6.6. Estimation of the capacity of the Mzingwane River alluvial aquifer

Catch	Channel alluvial aquifer				Floodplain alluvial aquifer			
	A (km^2)	**b (m)**	**ñ (%)**	**V_w (Mm^3)**	**A (km^2)**	**b (m)**	**ñ (%)**	**V_w (Mm^3)**
B20	1.63	1	0.35	0.57	12.81	1	0.35	4.48
B22	6.91	1	0.35	2.42	10.73	1	0.35	3.76
B62	10.67	2	0.35	7.47	-	-	-	0
B91	9.90	4	0.35	13.99	-	-	-	0
$BUZ1_{MZ}$	10.84	9	0.35	34.15	33.61	10	0.35	117.64
Total	39.95			58.59	57.15			125.87

'Catch' denotes the catchment. A denotes alluvial aquifer areal extent, b denotes the estimated aquifer thickness, ñ denotes the average effective porosity, Vw denotes the aquifer capacity and (-) indicates that alluvial deposits were not delineated in the area.

The estimation of the volumetric capacity of the alluvial aquifer is highly dependent on the aquifer dimensions provided, therefore if there is under- or over-estimation of the dimensions, the capacity of the alluvial aquifers will also be affected. In addition, the saturated thickness of the alluvium is also dependent on the flow regime of each river system which is affected by seasonal variations in precipitation and evaporation as well as water use and development along the respective river system. The saturated zone therefore may change across seasons, however maximum total volumes would not be affected. The assumptions that were made regarding the flow exchange dynamics between the alluvial aquifers and underlying lithology also impact the amount of water that can be considered stored by the alluvial aquifer e.g. if any of the alluvial aquifers are underlain by a fractured rock aquifer, the alluvial aquifer could possibly 'lose' stored water to the fractured rock. Therefore if any of the assumptions are changed, the estimated aquifer capacity could be comprised.

6.2.4 Channel transmission losses as a percentage of natural mean annual runoff

To estimate the impact of channel transmission losses on water resources in each sub-basin, calculated channel transmission losses were compared to the natural mean annual runoff as reported by the Limpopo River Basin Monograph Study (Howard *et al.*, 2013). The values (Table 6.4) that have been used to calculate channel transmission losses as a percentage of the natural mean annual runoff are derived from Tables Table 6.1 toTable 6.3 which relay the characteristics of the delineated alluvial aquifers. Notably, given a range of saturated aquifer thicknesses this study used the upper limit of the range resulting in greater aquifer dimensions. To assess the impact of transmission losses at a more standardised saturated aquifer thickness, a 1 m aquifer thickness is also considered.

Table 6.7. Channel transmission losses as a percentage of natural mean annual runoff (LIMCOM, 2013)

Sub-basin	Calculated Transmission losses (Mm^3)	Transmission losses based on 1 m thickness (Mm^3)	MAR (Mm^3)	Calculated Transmission losses as %MAR	Transmission loss (1 m) as %MAR
Mokolo	669	120	210	318	57
Motloutse	319	71	125	263	57
Mzingwane	185	34	438	42	8

'A' denotes approximate aquifer areal extent (km^2), 'L' denotes approximate length (km), 'ñ' denotes the effective porosity (dimensionless), 'MAR' denotes the natural mean annual runoff ((Mm^3) and 'b' denotes the calculated soil depth (m).

When comparing the results (Table 6.7) of using a maximum saturated aquifer thickness versus a standardised 1 m saturated aquifer thickness it is clear that transmission losses are greatly exaggerated when expressed as a percentage of the mean annual runoff. This is expected because one of the assumptions made by the study was that the aquifer thickness would be fully saturated, which is not entirely the case in reality. The LRBMS (Howard *et al.*, 2013) have reported that transmission losses contribute about 30% to the basin's water balance along the Limpopo River main stem, which is more comparable to the results of the transmission losses calculated at a standardised saturated aquifer thickness of 1 m. The results would however be better compared if an uncertainty range was provided for transmission loss contribution reported by the LRBMS.

6.2.5 Hydrological modelling

The setup of the Pitman Model for hydrological modelling is explained in Chapter 5. In this section, the model parameter setup for each sub-basin is indicated and the results of the channel transmission losses simulation, presented.

6.2.5.1 Simulations of transmission losses in the Mokolo sub-basin

Model setup for Mokolo sub-basin

Nine catchments were setup for the Mokolo sub-basin, however in Table 6.8 only the catchments that are traversed by the delineated alluvial aquifer are shown. Catchment A42F was selected as the reporting catchment as there are several flow gauges near its outlet, however only A4H010 had sufficient data.

Table 6.8. Model parameter setup for the Mokolo sub-basin before the inclusion of channel transmission losses

Parameter	A42A	A42C	A42E	A42F	A42G	A42H	A42J
PEVAP (mm)	1701	1700	1700	1800	1900	1900	1950
ZMIN (mm month^{-1})	998	100	998	998	25	25	25
ZMAX (mm month^{-1})	1000	720	1000	1000	750	750	1000
ST (mm month^{-1})	180	250	100	100	100	100	200
POW (-)	3	3	3	3	3	3	3
FT (mm month^{-1})	15	15	6	6	0	0	0
GW (mm month^{-1})	7.2	9.5	5	6	6.5	4	2.7
Channel loss TLGMAX (mm)	0	0	0	0	0	0	0
DD (km km^{-2})	0.4	0.4	0.4	0.4	0.4	0.4	0.4
T (m^2 day^{-1})	12	15	18.8	15.7	8.4	8.8	8
S (-)	0.004	0.004	0.004	0.004	0.004	0.004	0.01
Regional GW slope (-)	0.01	0.01	0.01	0.01	0.01	0.01	0.01
RWL (m below surface)	15	25	20	20	10	10	25
RSP (% slope width)	0.2	0.2	0.2	0.2	0.2	0.2	0.2

A description of the Parameters is provided in Chapter 5. Dimensionless parameters are denoted by (-).

Channel loss function for Mokolo sub-basin

The channel loss parameter (TLGMax) was increased from 0 to a mean value of 10 mm and it simulated a monthly mean channel loss of 2.2 Mm^3 month^{-1} which is an annual loss of 26.4 Mm^3; values greater than 10 mm simulated lower channel losses

Wetland function for Mokolo sub-basin

The wetland parameters applied in the Mokolo sub-basin are indicated in Table 6.9. The wetland function simulated a mean reservoir volume of 54.95 Mm^3 for catchment A42F.

Table 6.9. Wetland parameters for Mokolo sub-basin.

Parameter	A42A	A42C	A42E	A42F	A42G	A42H	A42J
Code for Wetland function (-99)	-99	-99	-99	-99	-99	-99	-99
Local catchment area (km^2)	60	42	40	30	25	40	87
Residual Wetland storage (Mm^3)	67	62	60	55	57	105	263
Initial Storage (Mm^3)	87	82	80	35	77	125	283
A in Area(m^2) = A * Volume(m^3)^B	4	3	3	2	2	2	3
B in Area(m^2) = A * Volume(m^3)^B	0.62	0.62	0.62	0.62	0.62	0.62	0.62
Channel capacity for spillage (Mm^3)	0	0	0	0	0	0	0
Channel Spill Factor (Fraction)	1	1	1	0.1	1	1	1
AA in (Ret.Flow = AA*(Vol/RWS)^BB)	0.8	0.8	0.8	0.8	0.8	0.8	0.8
BB in (Ret.Flow = AA*(Vol/RWS)^BB)	0.8	0.8	0.8	0.8	0.8	0.8	0.8
Annual Evaporation (mm)	1701	1700	1700	1800	1900	1900	1950
Annual Abstraction (Mm^3)	0	0	0	0	0	0	0
AA scaling factor	0	0	0	0	0	0	0
Max. Return Flow Fraction	1	1	1	1	1	1	1

A description of the Parameters is provided in Chapter 5.

Reservoir function for the Mokolo sub-basin

The parameters used for the reservoir function for the Mokolo sub-basin are indicated in Table 6.10. The reservoir function simulated a mean reservoir volume of 54.78 Mm^3 for catchment A42F.

Table 6.10. Reservoir parameters for the Mokolo sub-basin

Parameter	A42A	A42C	A42E	A42F	A42G	A42H	A42J
Reservoir Capacity (Mm^3)	66	62	60	55	57	106	263
Dead Storage (% Capacity)	10	10	10	10	10	10	10
Initial Storage (% Capacity)	10	10	10	10	10	10	10
A in Area(m^2) = A * Volume(m^3)^B	6.17	4.49	4.36	3.45	2.81	3.06	3.79
B in Area(m^2) = A * Volume(m^3)^B	0.62	0.62	0.62	0.62	0.62	0.62	0.62
Reserve level 1-5 (% Capacity)	0	0	0	0	0	0	0
Annual Abstraction (Mm^3)	0	0	0	0	0	0	0
Annual Compensation Flow (Mm^3)	0	0	0	0	0	0	0
AR in Reserve (%) = AR*Volume (% Cap.)	0	0	0	0	0	0	0
BR in Reserve (%) = AR*Volume (% Cap.)	0	0	0	0	0	0	0

A description of the Parameters is provided in Chapter 5.

Model performance for catchment A42F of the Mokolo sub-basin

According to the guidelines by Moriasi *et al.* (2007) (Table 5.6), the model performance (Table 6.11) for the Mokolo sub-basin is satisfactory (CE >0.50, PBIAS <25) even before the inclusion of channel transmission losses. Notably, the simulated mean monthly flow is significantly greater than the observed flow, which was derived from WR2012 data. The likely cause of this major difference is inadequate representation of water use data, particularly dam storage data and groundwater abstractions. If the flow simulated without transmission losses is used as the proxy for the observed flow, it is evident that channel transmission loss function and the reservoir function reduced the mean monthly flow from 11.708 Mm^3 to 11.466 Mm^3 and 11.599 Mm^3, respectively. The wetland function however increased the mean monthly flow from 11.708 Mm^3 to 11.718 Mm^3.

Table 6.11. Model performance for the Mokolo sub-basin set up

Objective Function	**Simulated flow (no TL)**	**Channel loss function**	**Wetland function**	**Reservoir function**
Coefficient of determination (R^2)	0.512	0.535	0.514	0.512
R^2(ln)	0.410	0.407	0.410	0.409
Coefficient of efficiency (CE)	0.507	0.530	0.509	0.507
CE (ln)	0.417	0.483	0.417	0.491
Percentage monthly error	22.054	19.534	22.162	20.194
Mean monthly flow (Obs. 9.592 Mm^3)	11.708	11.466	11.718	11.599

Obs. denotes observed monthly flow; TL denotes channel transmission losses.

Channel transmission loss simulations for catchment A42F of the Mokolo sub-basin

The modelling results for the Mokolo sub-basin are presented on a semi-logarithmic graph in Figure 6.6. From the graph it is evident that although the flow is over-simulated, the shapes of the simulated flows do correlate with the observed flow.

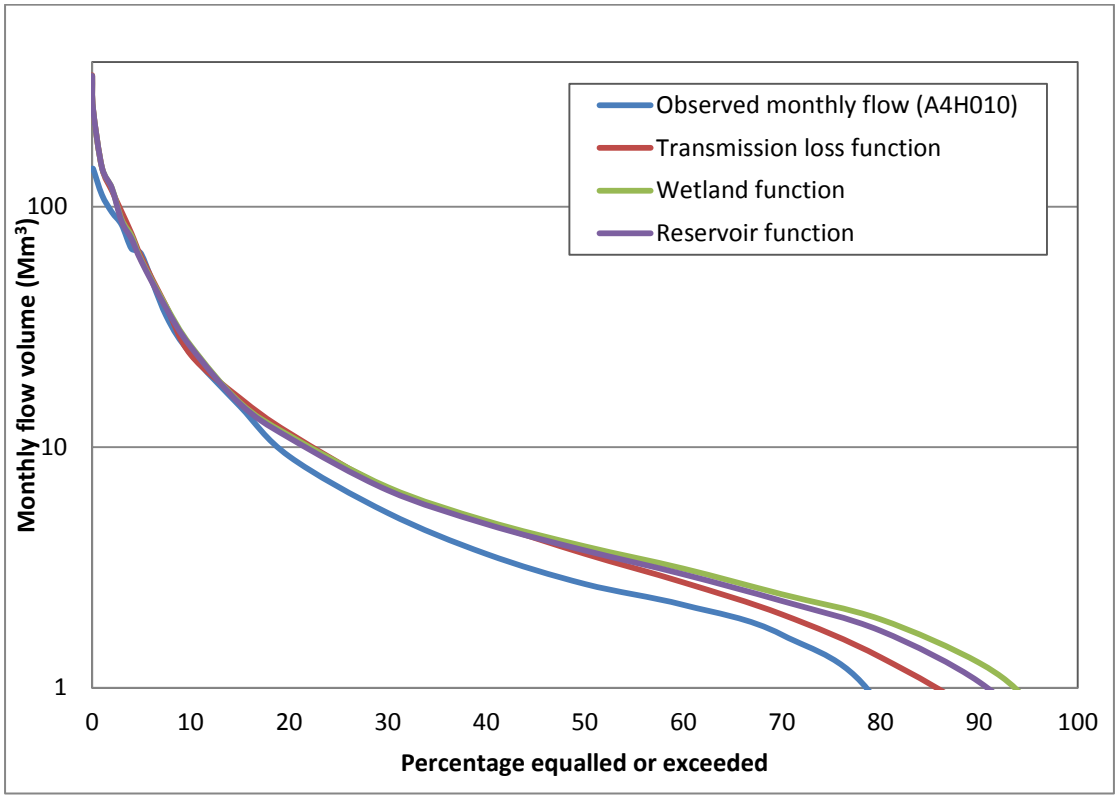

Figure 6.6 Comparison of observed and simulated flow volumes at selected flow duration curve percentage points for catchment A42F of the Mokolo sub-basin.

While there is minimal over-simulation between the high flows of the observed and simulated flow, greater variation is noted between the low flows which may indicate the inclusion of channel transmission losses.

6.2.5.2 Simulations of transmission losses in the Motloutse sub-basin

Model setup for the Motloutse sub-basin

Five catchments were set up for the Motloutse sub-basin, however only the three that are traversed by the delineated alluvial aquifer are indicated in Table 6.12. The Upper Motloutse catchment, UM, marks the headwaters of the sub-basin while the Lower Motloutse 2 (LM2) is closer to the outlet. Catchment MM was selected for reporting as

it has Flow gauge 4121 near its outlet; Flow gauge 4121 is the only one provided by the Limpopo River Basin Monograph Study (Howard *et al.*, 2013).

Table 6.12. Model parameters used for the Motloutse sub-basin

Parameter	UM	MM	LM2
PEVAP (mm)	2400	2000	2000
ZMIN (mm month^{-1})	100	100	100
ZMAX (mm month^{-1})	1200	1200	1200
ST (mm month^{-1})	550	550	550
POW (-)	3.2	3.2	3.2
FT (mm month^{-1})	10	10	10
GW (mm month^{-1})	0.5	0.5	0.5
Channel loss TLGMAX (mm)	0	0	0
DD (km km^{-2})	0.4	0.3	0.3
T (m^2 day^{-1})	20	20	15
S (-)	0.004	0.004	0.003
Regional GW slope (-)	0.01	0.01	0.01
RWL (m below surface)	30	30	30
RSP (% slope width)	0.2	0.2	0.2

A description of the Parameters is provided in Chapter 5.

Channel transmission loss function for the Motloutse sub-basin

The channel loss parameter was increased from 0 to a mean value of 20 mm and it simulated a monthly mean channel loss of 1.62 Mm^3 month^{-1}, therefore 19.44 Mm^3 annually.

Wetland function for the Motloutse sub-basin

The wetland parameters applied in the Motloutse sub-basin are indicated in Table 6.13. The wetland function simulated a mean reservoir volume of 19.77 Mm^3 for MM.

Table 6.13. Wetland parameters for the Motloutse sub-basin

Parameter	UM	MM	LM2
Code for Wetland function (-99)	-99	-99	-99
Local catchment area (km^2)	97	12	84
Residual Wetland storage (Mm^3)	143	20	166
Initial Storage (Mm^3)	123	10	146
A in Area(m^2) = A * Volume(m^3)^B	4.3	1.9	3.4
B in Area(m^2) = A * Volume(m^3)^B	0.65	0.65	0.65
Channel capacity for spillage (Mm^3)	0	0	0
Channel Spill Factor (Fraction)	1	1	1
AA in (Ret.Flow = AA*(Vol/RWS)^BB)	0.8	0.8	0.8
BB in (Ret.Flow = AA*(Vol/RWS)^BB)	0.8	0.8	0.8
Annual Evaporation (mm)	2400	2000	2000
Annual Abstraction (Mm^3)	0	0	0
AA scaling factor	0	0	0
Max. Return Flow Fraction	1	1	1

A description of the Parameters is provided in Chapter 5. 'UM', 'MM','LM2' respectively denote upper Motloutse, middle Motloutse and lower Motloutse 2.

Reservoir function

The parameters used for the reservoir function for the Motloutse sub-basin are indicated in Table 6.14. The reservoir function simulated a mean reservoir volume of 18.33 Mm^3 for catchment MM, which translates to the estimated alluvial aquifer capacity and hence amount of water that could be lost through transmission losses.

Table 6.14. Reservoir parameters for the Motloutse sub-basin

Parameter	UM	MM	LM2
Reservoir Capacity (Mm^3)	143	20	166
Dead Storage (% Capacity)	10	10	10
Initial Storage (% Capacity)	10	10	10
A in Area(m^2) = A * Volume(m^3)^B	4.3	1.9	3.4
B in Area(m^2) = A * Volume(m^3)^B	0.65	0.65	0.65
Reserve level 1-5 (% Capacity)	0	0	0
Annual Abstraction (Mm^3)	0	0	0
Annual Compensation Flow (Mm^3)	0	0	0
AR in Reserve (%) = AR*Volume (% Cap.)	0	0	0
BR in Reserve (%) = AR*Volume (% Cap.)	0	0	0

A description of the Parameters is provided in Chapter 5. 'UM', 'MM','LM2' respectively denote upper Motloutse, middle Motloutse and lower Motloutse 2.

Model performance for the Motloutse sub-basin

The model performance for the Motloutse sub-basin is unsatisfactory even before the inclusion of channel transmission losses (CE < 0.5, PBIAS>35). As indicated, the simulated monthly flow is significantly greater than the observed. In some cases the addition of transmission losses does reduce the flow but not as low as the observed flow which points out that not all the water uses have been accounted for.

Table 6.15. Model performance for the Motloutse sub-basin at catchment MM

Objective Function	Simulated flow (no TL)	Channel loss function	Wetland function	Reservoir function
Coefficient of determination (R^2)	0.366	0.357	0.362	0.366
R^2(ln)	0.328	0.359	0.323	0.393
Coefficient of efficiency (CE)	0.440	0.428	0.468	0.470
CE (ln)	0.343	0.306	0.417	0.301
Percentage monthly error	54.488	49.284	54.885	52.502
Mean (Obs. 7.813)	12.070	11.663	12.101	11.914

A description of the each Object Function is provided in Chapter 5.TL denotes transmission losses; Obs. denotes observed mean monthly flow.

Channel transmission loss simulations

Figure 6. illustrates the modelling results for the Motloutse sub-basin which are presented on a semi-logarithmic graph. The duration of flow for the Motloutse is particularly less than that of the other three sub-basins; approximately 70% zero flows are simulated on the observed monthly flow duration curve. The steepness of the flow duration curve for the observed flow and all three functions alludes to fairly rapid recharge of the stream. High flows are over-simulated by all three functions while middle and low flows are under-simulated, with exception of the simulation of the wetland function.

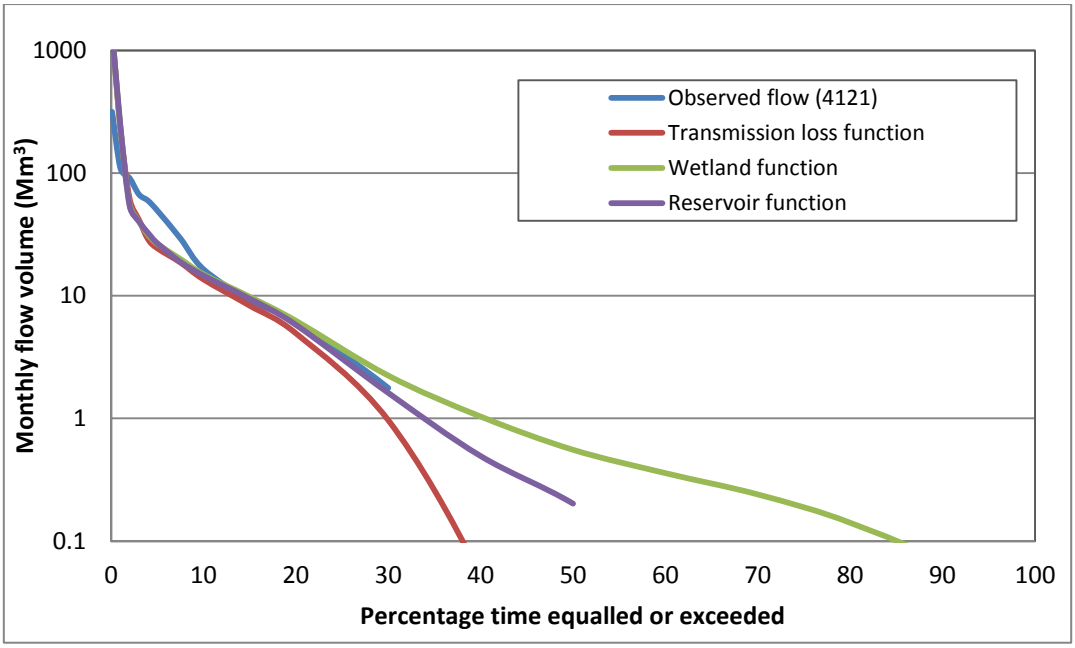

Figure 6.7. Comparison of flow volumes (Mm^3) for the Motloutse sub-basin at selected flow duration curve percentage points.

6.2.5.3 Simulations of transmission losses in the Mzingwane sub-basin

Model set up for the Mzingwane sub-basin

Nodes, depicting flow gauge stations, were used for the model set up of the Mzingwane. Unlike the other sub-basins, the Mzingwane sub-basin has adequate patched flow gauge data from several stations situated along the course of the river that could be used as observed data for the modelling exercise. Eight stations were chosen (Table 6.16) however B20, which is the most upstream station, is used for reporting. Similar to the catchments in the other sub-basins, each node was modelled as an individual but connected entity.

Table 6.16. Model parameter setup for the Mzingwane sub-basin before the inclusion of channel losses.

Parameter	B20	B60	B75	B22	B62	B91	B90	BUZ_{MZ}
PEVAP (mm)	1878	1865	1865	1874	1874	1927	1927	1977
ZMIN (mm $month^{-1}$)	70	100	100	80	80	100	100	50
ZMAX (mm $month^{-1}$)	1030	1200	1200	920	920	1000	1000	1550
ST (mm $month^{-1}$)	250	200	200	100	200	200	120	100
POW (-)	2.7	3.7	3.7	3.0	3.0	3.5	3.5	3.5
FT (mm $month^{-1}$)	2.0	2.5	2.5	3.0	2.0	2.0	1.0	1.0
GW (mm $month^{-1}$)	18	17.5	17.5	20	20	25	23	26
Channel loss TLGMAX (mm)	0	0	0	0	0	0	0	0
DD (km km^{-2})	0.4	0.4	0.4	0.4	0.4	0.4	0.4	0.4
T (m^2 day^{-1})	25	35	35	16	16	20	20	12
S (-)	0.002	0.001	0.001	0.003	0.003	0.003	0.003	0.004
Regional GW slope (-)	0.02	0.01	0.01	0.01	0.01	0.01	0.01	0.005
RWL (m below surface)	15	25	25	25	25	30	30	40
RSP (% slope width)	0.2	0.2	0.2	0.2	0.2	0.2	0.2	0.2

A description of the Parameters is provided in Chapter 5.

Channel transmission loss function for the Mzingwane sub-basin

The channel loss parameter was increased from 0 to a mean value of 20 mm $month^{-1}$ in an effort to match simulated losses to estimated losses. A monthly mean channel loss of 0.39 Mm^3 $month^{-1}$ was simulated, which converts to 4.68 Mm^3 a^{-1}.

Wetland function

The parameters used for the wetland function are shown in Table 6.17. The reservoir function simulated an average reservoir volume of 4.93 Mm^3 for catchment B20.

Table 6.17. Wetland function for the Mzingwane sub-basin

Parameter	B20	B22	B62	B91	$BUZ1_{MZ}$
Code for Wetland function (-99)	-99	-99	-99	-99	-99
Local catchment area (km^2)	14	18	11	10	44
Residual Wetland storage (Mm^3)	5	6	7	14	152
Initial Storage (Mm^3)	3	4	5	12	120
A in Area(m^2) = A * Volume(m^3)^B	6	6	3	2	2
B in Area(m^2) = A * Volume(m^3)^B	0.65	0.65	0.65	0.65	0.65
Channel capacity for spillage (Mm^3)	0	0	0	0	0
Channel Spill Factor (Fraction)	1	1	1	1	1
AA in (Ret.Flow = AA*(Vol/RWS)^BB)	0.8	0.8	0.8	0.8	0.8
BB in (Ret.Flow = AA*(Vol/RWS)^BB)	0.8	0.8	0.8	0.8	0.8
Annual Evaporation (mm)	1878	1874	1874	1927	1977
Annual Abstraction (Mm^3)	0	0	0	0	0
AA scaling factor	0	0	0	0	0
Max. Return Flow Fraction	1	1	1	1	1

A description of the Parameters is provided in Chapter 5.

Reservoir function

The parameters used for the reservoir function are shown in Table 6.18. The reservoir function simulated a mean reservoir volume of 4.97 Mm^3 for catchment B20.

Table 6.18. Reservoir parameter for the Mzingwane sub-basin

Parameter	B20	B22	B62	91	BUZ
Reservoir Capacity (Mm^3)	5	6	7	14	152
Dead Storage (% Capacity)	10	10	10	10	10
Initial Storage (% Capacity)	10	10	10	10	10
A in Area(m^2) = A * Volume(m^3)^B	6	6	3	2	2
B in Area(m^2) = A * Volume(m^3)^B	0.65	0.65	0.65	0.65	0.65
Reserve level 1-5 (% Capacity)	0	0	0	0	0
Annual Abstraction (Mm^3)	0	0	0	0	0
Annual Compensation Flow (Mm^3)	0	0	0	0	0
AR in Reserve (%) = AR*Volume (% Cap.)	0	0	0	0	0
BR in Reserve (%) = AR*Volume (% Cap.)	0	0	0	0	0

A description of the Parameters is provided in Chapter 5.

Model performance for the Mzingwane sub-basin

The model performance for the Mzingwane sub-basin (Table 6.19), before the inclusion of the transmission loss simulations is satisfactory (CE >0.50, PBIAS <25). The similarity between the monthly distribution graphs (Figure 6.8) further illustrates the agreement

between the observed monthly flow and simulated flow, however peak flow are underestimated which can be attributed to lack of water use data.

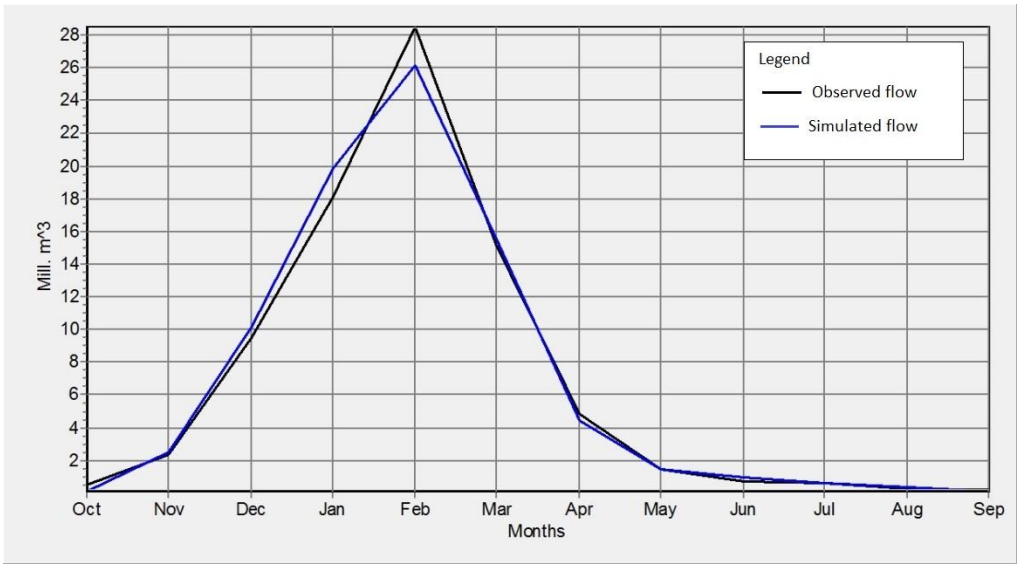

Figure 6.8. Monthly distribution for B20, before the inclusion of channel transmission losses.

Table 6.19: Model performance statistics for the Mzingwane sub-basin at node B20

Objective Function	Simulated flow (no TL)	Channel loss function	Wetland function	Reservoir function
Coefficient of determination (R^2)	0.349	0.348	0.348	0.349
R^2(ln)	0.576	0.540	0.552	0.550
Coefficient of efficiency (CE)	0.565	0.599	0.534	0.565
CE (ln)	0.562	0.549	0.534	0.519
Percentage monthly error	5.011	5.781	10.793	5.999
Mean (Obs. 6.884)	6.539	6.486	6.141	6.471

A description of the Objective Function is provided in Chapter 5. TL denotes transmission losses; Obs. denotes observed mean monthly flow.

Channel transmission loss simulations for the Mzingwane sub-basin

The modelling results for the Mzingwane sub-basin are presented on a semi-logarithmic graph in Figure 6.9. On the graph it is evident that the simulated high flows compare relatively well to the observed high flows however both medium and low flows are over-simulated. Additionally, the observed flow ceases at 60% on the flow

duration curve (40% zero flows), with the simulated flow showing an exceedance of 5-35% to the observed. The over-simulation of flow may be associated with inadequate representation of water use impacts. This over-simulation is further evidenced by the relative steepness of the flow duration curve which indicates that high flows are being simulated at a greater frequency than expected. The inclusion of channel transmission losses is illustrated by the variation in the low flows. All three functions relay this interaction, however with the transmission loss function, over-simulated low flows are less frequent.

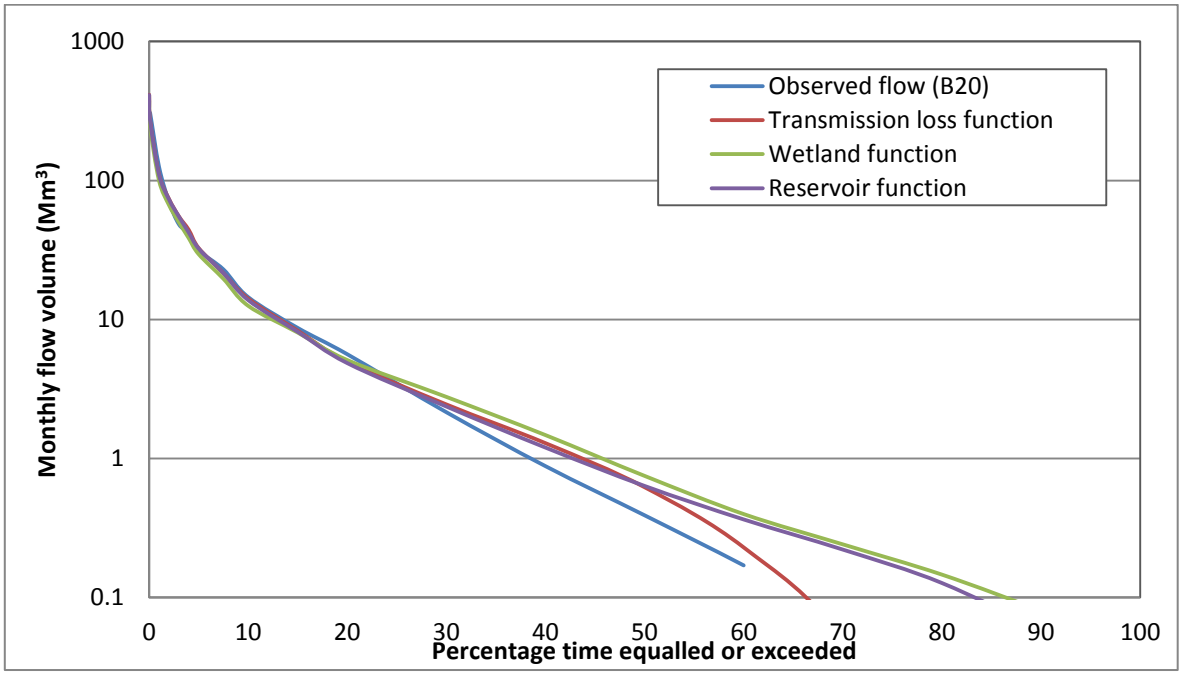

Figure 6.9. Comparison of flow volumes (Mm^3) at selected flow duration curve percentage points for catchment B20 of the Mzingwane sub-basin.

Uncertainty analysis

An uncertainty analysis was conducted for node B20 of the Mzingwane catchment, incorporating the explicit channel transmission loss function. To estimate the uncertainties associated with the calculation of transmission losses, all parameters were kept constant except for parameters ST (maximum storage capacity) and GW (maximum recharge rate). Using the output of the explicit channel loss function, the simulated monthly flow was estimated as 6.486 Mm^3 (Table 6.19).

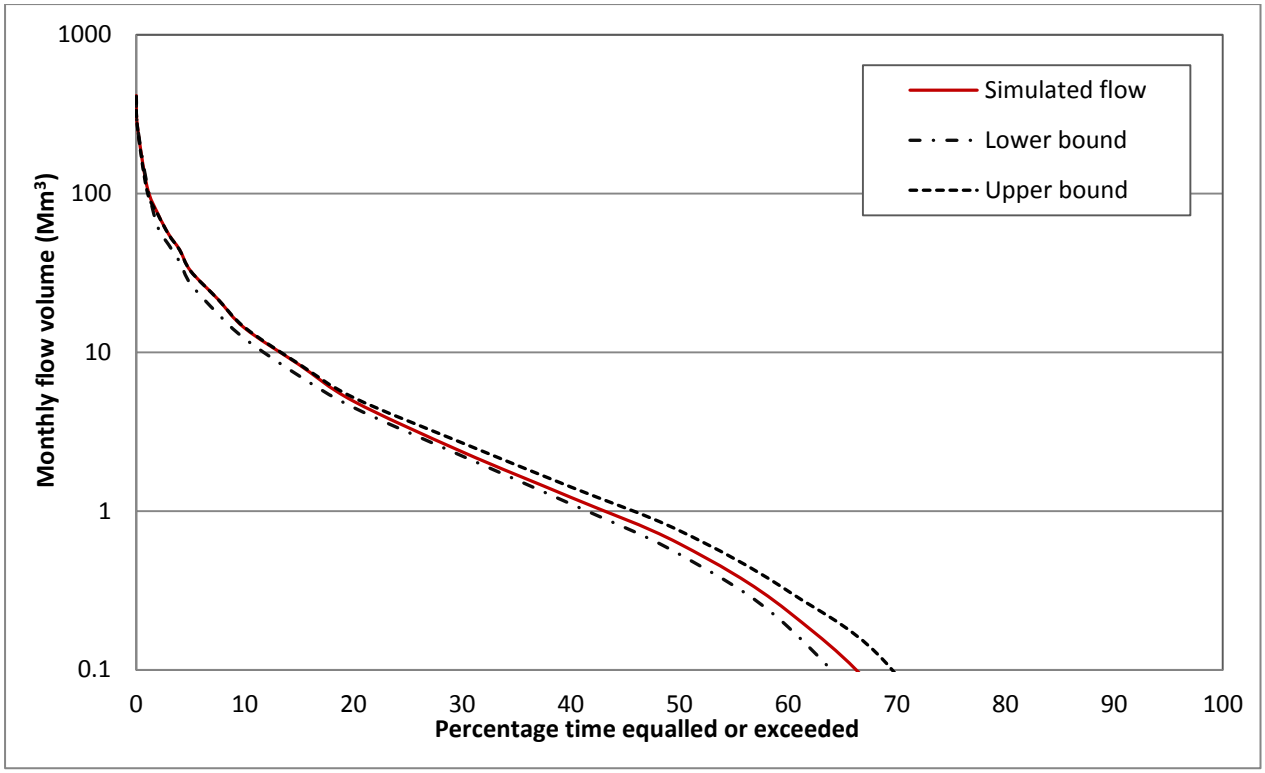

Figure 6.10 Uncertainty analysis incorporating the channel transmission loss function. Lower bound is the minimum of the ensemble of 10 000 simulations, and upper is the maximum.

The upper bound of the uncertainty estimation reports a maximum mean monthly flow of 6.9 Mm^3, whereas the lower bound reports a minimum mean monthly flow of 6.0 Mm^3. ST and GW values associated with the upper bound were 457.871 mm $month^{-1}$ and 5.137 mm $month^{-1}$, respectively, while slightly lower values of 457.249 mm $month^{-1}$ and 4.291 mm $month^{-1}$ were observed for the lower bound. The results (Figure 6.10) show that the upper bound stays almost the same except for the middle and low flows where it increases gradually towards the low flows. In contrast, the lower bound shows consistently lower values across the high, middle and low flows, with slightly greater variation along the low flows. The characteristics of the alluvial aquifer that are associated with the parameter ST are aquifer thickness (soil depth), porosity and area (Kapangaziwiri and Hughes, 2008) therefore it is evident that changes in these physical properties has a direct impact on the quantification of channel transmission losses. Similarly the GW parameter is associated with the regional groundwater gradient

which is central to the approach applied by the Pitman model in estimating channel transmission losses, therefore changes in GW also affect the quantification of channel transmission losses.

6.3 DISCUSSION

6.3.1 Delineation of alluvial aquifers

To facilitate the understanding and quantification of channel transmission losses in the Limpopo River Basin, the study located and delineated alluvial aquifers in three sub-basins, namely the Mokolo (South Africa), Motloutse (Botswana) and Mzingwane (Zimbabwe), using LandSat 8 imagery and remote sensing techniques. The use of satellite imagery provided a broad and quick overview of the Limpopo River Basin and was therefore beneficial for the identification of river channels associated with alluvial aquifers and the determination of the areal extents of the alluvial aquifers. Several techniques of delineating alluvial aquifers were reviewed and from these techniques, land cover classification was selected as the most appropriate for the study due to the accessibility of resources (i.e. freely downloadable satellite data, availability of remote sensing and GIS software and spatial datasets for validation) as well as the modeller's knowledge and experience in the technique. Much of the delineation and characterisation of the alluvial aquifers also relied on past hydrogeological studies that had identified and classified aquifers across the Limpopo River Basin. These studies, both literature and spatial data sets, provided valuable information/data on important characteristics of the alluvial aquifers that could not be determined through land cover classification e.g. thicknesses of the alluvium, soil type and effective porosities of the soil material. Alternatively, this information could have been sourced through field exploration however that type of data collection was beyond the scope of the research project.

Alluvial aquifers across the three sub-basins were delineated along the main rivers i.e. the Mokolo, Motloutse and Mzingwane rivers and were characterised by upper and lower catchment channel and floodplain alluvial deposits. When comparing the results of the alluvial aquifer delineation to descriptions collected from available literature, the locations of the alluvial aquifers generally coincide, thus validating the accuracy of the delineation. Some disparities regarding the dimensions of the alluvial aquifers do, however, exist. The areal extent and average saturated aquifer thickness are greater than some values quoted in literature. This is expected because the majority of the studies (e.g. Moyce *et al.*, 2006; Masvopo, 2008) provide aquifer dimensions (width, length) based on individual, isolated alluvial deposits and therefore do not account for deposits outside of their study area, whereas this study is more extensive and estimates dimensions across the length of each respective river channel. With regards to the Mzingwane alluvial aquifer, both Moyce *et al.* (2006) and Masvopo (2008) mention that minimum saturated aquifer thicknesses were used in their studies, therefore the estimated aquifer dimensions and associated groundwater potential were expected to be less than what is probably available along the river channel. This study averaged the higher end (maximum) of the range of aquifer thicknesses quoted in literature. Therefore, the implication of the difference in measurements is that there is an 'over-estimation' of the aquifer dimensions which impacts the estimated aquifer capacity, and thus potential transmission losses are greater, when compared to existing knowledge. The results of the aquifer delineation and associated estimation of aquifer capacity are thus expected to provide potential maximum channel transmission losses, which are also dependent on seasonal flow.

6.3.2 Quantification of channel transmission losses

The volume of water that can be stored in the delineated alluvial aquifers (and can theoretically be 'lost' through channel transmission losses) was estimated from the derived areal extents of the alluvium, the saturated aquifer thickness and the effective porosity of the soil material of the alluvial deposit. As discussed, information relating

to the aquifer thickness and hydraulic properties of the soil material was collected from past hydrogeological studies conducted in the Limpopo River Basin and in cases where data was lacking, the information was estimated and inferred from neighbouring sub-basins. While this approach enabled a generalised quantification of possible channel transmission losses in the selected sub-basins, it also confirmed the much-discussed (Hameed *et al.*, 1996; Hughes, 2008) topic of data-related uncertainties surrounding the estimation of loss processes in semi-arid regions. Additionally, several assumptions needed to be made to simplify the estimation of the capacity of each alluvial aquifer. These included the assumption that the average thickness of the alluvial aquifer would be fully saturated and that the alluvial material behaved in a homogenous manner along the length of the delineated aquifer. It should be taken into account that river sections are heterogeneous in nature (Masvopo, 2008), however lack of knowledge and data regarding these variations calls for a generalised approach to loss calculations. Furthermore, the saturated depth of alluvial deposits depends on multiple factors including seasonal variations of streamflow, groundwater level and the hydraulic properties (e.g. transmissivity, permeability, hydraulic conductivity) of the alluvium. The alluvial aquifer was also assumed to occur in a closed system meaning that exchanges with underlying lithology were not considered and flow in the river channel was assumed to be naturalised, therefore the impact of groundwater abstractions and surface water withdrawals was not considered. These assumptions allude to the complexities associated with quantifying loss processes.

6.3.3 Conceptual understanding of channel transmission losses in the Limpopo River Basin

Gaining a conceptual understanding of the likely processes and dynamics of channel transmission losses was one of the main objectives of the study. An analysis of the main climatic and physical basin properties and water uses provided a holistic, catchment-scale comprehension of the various factors which facilitate the occurrence

of streamflow losses in the basin. A general hydrological framework was adopted as the best approach to conceptualising loss processes as it illustrates the propagation of water through the sub-basin and indicates the various manners in which streamflow is reduced during its cycle through each sub-basin. Although the conceptualisation of the sub-basins' water budget was not a quantitative assessment, it did point out the prevailing dynamics involved in channel transmission loss processes in the Limpopo River basin. These are now understood to be influenced by:

- The semi-arid climate that dominates the region causing low rainfall and significant evaporation to prevail, leading to direct evaporation from the free water surface and evaporation and evapotranspiration from the recharged beds and banks;
- Channel beds and banks that are characterised by shallow to deep sandy and loamy alluvium which need to be recharged before any flow can occur in the channel, therefore recharge of channel bed storage and infiltration of bank storage plays a dominant role in loss processes;
- Majority of the river banks are naturally vegetated, while others are used for agricultural purposes therefore evapotranspiration from the riparian vegetation is a significant contributor to streamflow losses;
- The occurrence of major water uses in each sub-basin e.g. storage dams, agriculture, commercial forestry, mining, urban and rural domestic water use all contribute to reducing streamflow and therefore affect the magnitude of channel transmission losses to alluvial aquifers.

The factors that have been described as being characteristic of channel transmission loss processes in the Limpopo River Basin are not entirely unique when compared to the factors which operate in other semi-arid environments. For example, studies by Knighton and Nanson (1994) in the USA, Brown (2005) in South Africa and Jarihani *et al.* (2015) in Australia also reported evaporation and evapotranspiration as the

dominant influences on the streamflow losses in their respective study areas. The magnitude of the impact of these factors is expected to be unique considering that it is a comparison between different geographical regions, however only quantitative assessments can confirm that. With regards to other operating factors such as infiltration or seepage into aquifers, a comparison of the hydrogeology and its associated hydraulic characteristics as well as the nature of the streamflow in each respective study area would have to be considered. Additionally, water uses which affect the streamflow would also have to be accounted for. Ultimately, the magnitude of channel transmission losses in each respective study area depends on the total effect of the operating factors and the nature of the river being studied as well as the scale at which it is studied.

6.3.4 Hydrological modelling

The aim of simulating channel transmission losses with three different functions of the Pitman Model was to assess the capability of existing loss modelling routines and determine which of the three functions best represents the dynamics of channel transmission losses processes. To compare the three transmission loss simulation approaches, each function was ran independently and then the simulation outputs were used to assess the degree of change between the observed flow (no transmission losses included) and a model run with channel transmission losses. Additionally, the outputs simulated by the transmission loss function, wetland function and 'dummy' dam function were also compared to determine which function performed better in simulating the estimated channel transmission losses for each sub-basin. The alluvial aquifer storage in each sub-basin and hence the potential quantity of channel transmission losses was calculated by using the dimensions of alluvial aquifers delineated in each sub-basin. An assessment of the model performance was carried out, after the inclusion of channel transmission losses based on an evaluation of the correlation between observed and simulated flow, based on the recommended statistics for model performance by Moriasi *et al.*, 2007. The model performances for

both the Mokolo and Mzingwane sub-basins were satisfactory (CE >0.50, PBIAS <25) even before the inclusion of channel transmission losses, however the simulated mean monthly flows were significantly greater than the observed flow. The model performance for the Motloutse sub-basin was unsatisfactory even before the inclusion of channel transmission losses (CE < 0.5, PBIAS>35), however results indicate that all three functions were able to simulate losses, although with differing magnitudes.

Channel transmission losses measuring 55 Mm^3 were estimated for catchment A42F of the Mokolo sub-basin, based on results acquired from delineation and characterisation of alluvial aquifers in the Mokolo sub-basin. The transmission loss, wetland and reservoir functions respectively simulated channel losses measuring 2.2 Mm^3 $month^{-1}$ (26.4 Mm^3 a^{-1}), 56.95 Mm^3 and 54.78 Mm^3. Following the inclusion of transmission losses, simulated mean annual runoff (MAR) measuring 11.71 Mm^3 was respectively reduced to 11.47 Mm^3 and 11.60 Mm^3 by the transmission loss and reservoir functions; MAR increased to 11.72 Mm^3 when losses were added through the wetland function. In the Motloutse sub-basin, losses were estimated to amount to 20 Mm^3 for the Middle Motloutse catchment. Losses of 22.8 Mm^3 a^{-1}, 19.77 Mm^3 and 18.33 Mm^3 were simulated by the transmission loss, wetland and reservoir functions, respectively. The simulated MAR of 12.070 Mm^3, was respectively reduced to 11.663 Mm^3 and 11.914 Mm^3 by the channel loss and reservoir functions and increased to 12.101 Mm^3 by the wetland function. For the Mzingwane sub-basin, channel transmission losses measuring 5 Mm^3 were estimated for node B20. The transmission loss, wetland and reservoir functions respectively simulated channel losses measuring 0.39 Mm^3 $month^{-1}$ (4.68 Mm^3 a^{-1}), 4.93 Mm^3 and 4.97 Mm^3. Following the inclusion of transmission losses, simulated MAR measuring 6.539 Mm^3 was respectively reduced to 6.486 Mm^3, 6.141 Mm^3 and 6.471 Mm^3 by the transmission loss, wetland and reservoir functions. Table 6.20 compares the magnitude of the transmission losses that were estimated from the delineated alluvial aquifers with the magnitude of losses simulated by the three modelling functions. It is clear that most of the time, transmission losses

were adequately simulated by all three functions, however some discrepancies exists that are indicative of parameter and model structural uncertainties.

Table 6.20. Comparison of simulated transmission losses versus estimated losses from alluvial aquifer delineation.

Sub-basin	Estimated transmission losses for catchment (Mm^3)	Annual Losses estimated by explicit transmission loss function (Mm^3)	Losses estimated by wetland function (Mm^3)	Losses estimated by 'dummy' reservoir (Mm^3)
Mokolo	55	26.4	54.95	54.78
Motloutse	20	22.8	19.77	18.33
Mzingwane	5	4.68	4.93	4.97

The effect of loss processes on the regional observed streamflow was not adequately presented. Typically, the simulated mean monthly flow would be less than the observed monthly flow (as flow in the channel is reduced due to recharge of the alluvial aquifer), however in these case studies unaccounted water uses made exact quantification and representation of the loss processes difficult to attain. Simulated monthly flow on the FDC graph was almost always over-simulated. When flow that was simulated without transmission losses was used as a proxy for observed flow, comparisons with flow that incorporated transmission losses showed reductions in flow. Overall, the results from the three modelling simulations demonstrate the potential of each approach in reproducing the dynamics of channel transmission losses between channel and alluvial aquifer within an existing sub-basin scale hydrological model. It is believed that better quantification of losses and more efficient qualitative determination of the function which best represents transmission losses, can be attained with more reliable observed data. Knowledge of the structure of the transmission loss function dictates that it is better at representing the dynamics of channel transmission losses, as it takes into account the contribution of losses to groundwater recharge whereas the other two functions do not.

Although not a major objective of the study, an uncertainty analysis was conducted for node B20 of the Mzingwane sub-basin, with focus being placed on the explicit

transmission loss function. One of significant attributes of the Pitman Model is its ability to calculate uncertainties and considering the various sources of uncertainties that have been noted in this study, it was considered beneficial to assess the range of uncertainty that could exist in such a study. Uncertainty was placed around the parameters ST (maximum storage capacity) and GW (maximum recharge rate) which respectively are associated with the data relating to aquifer thickness (soil depth), porosity and area, and regional groundwater gradient. With a simulated monthly flow of 6.486 Mm^3 for B20 (using the transmission loss function), the upper and lower bounds of uncertainty were calculated as 6.9 Mm^3 and 6.0 Mm^3. This gives an uncertainty range of approximately 6-7.5 percent. It is therefore evident that variations in the physical properties of alluvial aquifers have a direct impact on the quantification of water resources.

6.3.5 Impact of transmission losses on water resources estimation

Channel transmission losses are understood to contribute significantly to the water balance of the Limpopo River Basin. Both Görgens and Boroto (2003) and the LRBMS (LIMCOM, 2013) have indicated that contributions amount to approximately 30% of the main stem water balance. The LRBMS (LIMCOM, 2013) noted that losses vary depending on the total volume of water being transferred by the channel. Based on the results of the case studies presented, it is clear that channel transmission losses do affect the magnitude of the flow available in the channel. It was observed that using a maximum saturated aquifer thickness results in exaggerated transmission losses when losses are expressed as a percentage of the mean annual runoff. Using a standardised 1 m saturated aquifer thickness, channel transmission losses, when expressed as a percentage of the mean annual runoff, ranged from 8-56% which is more comparable to the 30% reported by the LRBMS (Howard *et al.*, 2013). It is anticipated that, coupled with abstractions and other water uses this value would decrease. Incorporating an estimate of the magnitude of loss transfers between channel and aquifer is vital to

groundwater estimation, as it is evident that low flows are highly affected by the inclusion of transmission losses.

While is it clear that including channel transmission losses to water resources estimation initiatives may be beneficial, it is imperative to account for uncertainties surrounding the quantification of loss processes. Quantification of losses is dependent on the knowledge of the hydrological processes that influence the occurrence of streamflow losses, data availability and efficient modelling strategies, therefore uncertainties that arise in channel transmission loss estimation are linked to the factors.

6.4 CLOSING REMARKS

Chapter 6 has presented a detailed account of the results of the study and provided a thorough and critical discussion on the observed outcomes. The results of alluvial aquifer delineation and estimation of channel transmission losses were compared to findings from similar existing studies in the Limpopo River Basin to observe differences and similarities and determine the implication thereof. The discussion highlights the contribution of the study to the general understanding of channel transmission loss processes in the Limpopo River Basin.

CHAPTER 7
Conclusions and recommendations

Chapter 7 summarises the main research outcomes achieved and relates the findings to the objectives of the study. Additionally, limitations that were encountered while conducting the study are discussed and contextualised in an effort to provide recommendations for future studies.

7.1 SUMMARY OF THE RESEARCH OUTCOMES

The main aim of this study was to understand and quantify channel transmission losses in the Limpopo River Basin. The ability to understand and quantify the impact of key hydrological processes on the availability of water resources is viewed as an integral component of equitable and sustainable resource management. In the semi-arid Limpopo River Basin of southern Africa, the dynamic between channel transmission losses and alluvial aquifers has been noted to impact significantly on the basin's water balance - channel transmission losses reportedly contribute about 30% to the basin's water balance (Boroto and Görgens, 2003; Howard *et al.*, 2013), however findings are primarily based on the Limpopo River main stem. To advance the knowledge surrounding channel transmission losses in the basin, the study focused on conceptualising and quantifying channel transmission loss processes in the sub-basins of the Limpopo River Basin, beyond the main stem. The specific study objectives that were identified and the resulting research outcomes are indicated as follows:

1. *Identifying reaches within the Limpopo River Basin system where channel transmission losses are expected to be prevalent.*

A review of literature indicated that the occurrence of significant channel transmission losses in the Limpopo River Basin is linked to the presence of notable alluvial aquifers

along some of the channel reaches. Identifying these reaches, determining the extent of the alluvial aquifers and the aquifer characteristics which facilitate the occurrence of channel transmission losses was therefore deemed essential for conceptualising and quantifying channel transmission loss processes. Multiple data sources, including literature and hydrogeological datasets were consulted when identifying the channel reaches. The actual delineation of alluvial aquifers was conducted through use of remote sensing and GIS mapping techniques. Remote sensing comprised land cover classification of Landsat-8 OLI imagery using false colour composite images (FCC 456) and DEM data was employed. Alluvial deposits where delineated across the whole Limpopo River Basin, however for this study the delineation of the alluvial aquifers along the Mokolo, Motloutse and Mzingwane rivers is presented as these are the selected study areas. Results of the delineation show that alluvial aquifers occur mostly along the reaches of the rivers that have low gradients, deep alluvium and experience relatively high aridity. The alluvial aquifers could also be easily identified with agricultural plots that line some reaches of the river channels. To validate the delineation results, comparisons were made with hydrogeological studies that were previously conducted in the basin.

The estimation of the hydraulic properties of the alluvial aquifer was based on available spatial datasets as well as literature pertaining to similar alluvial aquifer environments in neighbouring sub-basins.

2. *Developing a conceptual understanding of the likely processes and dynamics of transmission losses in the basin.*

   The dynamic of channel transmission losses processes in the Limpopo River Basin was considered from a catchment-scale point of view. A conceptual schematic was developed which illustrates a generalised water budget for all the study areas, and considers the dominant natural processes and anthropogenic activities that impact

on the availability of streamflow in each study areas. Through knowledge attained from a review of literature and consideration of the meteorological and physical properties of each sub-basin, it is understood that:

- The semi-arid climate that dominates the region causes low rainfall and significant evaporation to prevail, leading to direct evaporation from the free water surface and evaporation and evapotranspiration from the recharged beds and banks;
- Similar to other tributaries of the Limpopo River, the Mokolo, Motloutse and Mzingwane rivers have channel beds and banks that are characterised by shallow to deep sandy and loamy alluvium which need to be recharged before any flow can occur in the channel, therefore recharge of channel bed storage and infiltration of bank storage plays a dominant role in loss processes;
- Majority of the river banks are naturally vegetated, while others are used for agricultural purposes therefore evapotranspiration from the riparian vegetation is a significant contributor to streamflow losses;
- The occurrence of major water uses in each sub-basin e.g. storage dams, agriculture, commercial forestry, mining, urban and rural domestic water use all contribute to reducing streamflow and therefore affect the magnitude of channel transmission losses to alluvial aquifers.

Channel transmission losses in the Limpopo River Basin are therefore characterised and influenced by the factors indicated above, however the total effect of each of these factors on the magnitude of the channel transmission losses ultimately depends on the nature of the river being studied.

3. Assess the suitability of existing channel transmission loss modelling approaches.

The revised version of the Pitman Model was selected as the preferred modelling platform for assessing the suitability of existing channel transmission loss modelling

approaches. It is widely-used across southern Africa and is equipped with three modelling functions that are applicable to the simulation of channel transmission losses. These functions include the explicit channel loss, wetland and reservoir functions of the Pitman monthly rainfall-runoff model. The three functions were used independently to determine their effectiveness in simulating the impact of channel transmission losses on catchment water resources. Results indicate that all three functions are capable of simulating channel transmission losses. The structure of the explicit transmission loss function however is the preferred function as it 'gives the right answers for the right reasons'. The function simulates accounts for losses to a groundwater system (groundwater recharge parameter increases as losses are simulated), therefore indicating proper representation of loss processes. The wetland and reservoir function may simulate streamflow losses, but they do not account for interactions with a groundwater system. They simply store water and release it back to the channel.

7.2 LIMITATIONS AND RECOMMENDATIONS

While the study was able to improve understanding of channel transmission losses in the Mokolo, Motloutse and Mzingwane sub-basins of the Limpopo River basin and quantify streamflow losses in each sub-basin, albeit with some uncertainty, a few limitations to the methods applied were noted:

- Aquifer delineation:

The dimensions of the delineated alluvial aquifers were not consistent with aquifer dimensions provided by other studies along the same rivers. This uncertainty can be linked to differences in the data employed, differences in delineation methods and human error.

- Quantification of channel transmission loss processes:

Lack of site-specific alluvial aquifer hydraulic data e.g. effective porosity, meant that average regional values had to be used in calculating the capacity of the delineated alluvial aquifers.

- Simulation of channel transmission losses:

The study noted that output monthly flows were often over-simulated, meaning that exact quantification of channel transmission losses could not be attained. This over-simulation has been linked to inadequate representation of water use data, particularly dam storage and groundwater abstractions data which were unavailable to the study.

To improve the outcomes of this study and guide future studies of this nature, particularly with regards to water resource quantification and management, the following developments are recommended:

- Aquifer delineation:
    - Improve accuracy of delineation by using remote sensing data with higher spatial resolution e.g. Sentinel-2 imagery has spatial resolution of 10 m (Landsat-8 has spatial resolution of 30 m)
    - If site-specific groundwater level data, geological data, hydrogeological data, soil/ aquifer depth, evaporation data, regional slope data etc., are available, employ GIS spatial analysis methods to delineate alluvial aquifers.
- Quantification and simulation of channel transmission losses:
    - Collection of alluvial aquifer field data is recommended, particularly relating to aquifer depth as this affects the estimation of aquifer capacity. Methods such as borehole siting can be used to determine the depth of the alluvium.
    - Determine the soil profile: available soil data in the Limpopo River Basin is highly generalised, leading to overly generalised estimation of alluvial aquifer properties.

- Determine the relationship between alluvial aquifer and underlying aquifer (if any) because alluvial aquifers can discharge to underlying fractured sedimentary or hard-rock aquifers through fractures, thus affecting the flux mechanism (channel transmission losses) between the channel and its adjacent alluvial aquifer.
- Maintenance to flow gauges: improved records of flow data are beneficial to channel transmission loss estimation particularly because observed flow data can be used to validate simulation of streamflow losses during hydrological modelling and flow measurements between two gauges on the same channel can be used to determine magnitude of 'loss',

References

Abdulrazzak, M.J., 1994. Losses of floodwater from alluvial channels. *Arid Soil Research and Rehabilitation* **9**, 15-24.

Abdulrazzak, M. J. and Sorman, A.U., 1994. Transmission losses from ephemeral stream in arid region. *Journal of Irrigation and Drainage Engineering* **20** (3), 669-675.

Afify, A. A., Arafat, S.S., Aboel har, M. and Khader, M.H., 2010. Physiographic soil map delineation for the Nile alluvium and desert outskirts in middle Egypt using remote sensing data of EgyptSat-1. *The Egyptian Journal of Remote Sensing and Space Sciences* **13**, 129-135.

Alemaw, B.F., Scott, K. and Merrey, D., 2008. *Limpopo River Basin Focal Project: Literature on Work Package 2- Water Availability and Access*. FANRPAN Draft Report, 4.

Ashton, P.J., Love, D., Mahachi, H. and Dirks, P.H.G.M., 2001. *An Overview of the Impact of Mining and Mineral Processing Operations on Water Resources and Water Quality in the Zambezi, Limpopo and Olifants Catchments in Southern Africa*. Contract Report to the Mining, Minerals and Sustainable Development (Southern African) Project by CSIR, Pretoria, South Africa and Geology Department, University of Zimbabwe, Harare, Zimbabwe. Report No. ENV-P-C 2001-042.

Bailey, A., 2008. *Water Resources Simulation Model (WRSM2000) for Windows, Theory Document*. PWMA 04/000/00/6107. (DWAF, WRC, SSI).

Barsi, J.A., Lee, K., Kvaran, G., Markham, B.L., Pedelty, J.A., 2014. The Spectral Response of the Landsat-8 Operational Land Imager. *Remote Sensing* **6**, 10232-10251.

Batjies, N.H., 2004. *SOTER-based soil parameter estimates for Southern Africa*. Report 2004/04, ISRIC - World Soil Information, Wageningen. Accessed from http://www.isric.org/isric/webdocs/docs/ISRIC_Report_2004_04.pdf

Bhattacharya, P., Chatterjee, D. and Jacks, G., 1997. Occurrence of arsenic-contaminated groundwater in alluvial aquifers from Delta Plains, Eastern India: Options for safe drinking water supply. *International Journal of Water Resources Development* **13** (1), 79-92.

Berg, R. R., Beuster, H. and Görgens, A. H. M., 1991. Innovative modelling strategies for flow generation in developed winter rainfall catchments. *Proceedings of the Fifth South African National Hydrological Symposium*. Stellenbosch, 2-3-1-2-3-8.

Beven, K.J., 2001. Rainfall-Runoff Modelling – the Primer. *Wiley*, Chichester, UK. 356pp.

Beven, K.J. and Binley, A.M., 1992. The future of distributed models: model calibration and uncertainty prediction. *Hydrological Processes* **6**, 279-298.

Birkhead, A.L., 2000. Interaction between channel flow and bank storage in rivers. *Unpublished PhD Dissertation*. University of the Witwatersrand.

Brenot, A., Petelet-Giraud, E. and Gourcy, L., 2015. Insight from surface water-groundwater interactions in an alluvial aquifer: contributions of $\delta^{2}H$ and $\delta^{18}O$ of water, $\delta^{34}S_{SO4}$ and $\delta^{18}O_{SO4}$ of sulfates, $^{87}Sr/^{86}Sr$ ratio. *Procedia Earth and Planetary Science* **13**, 84-87.

Boroto, R.A.J. and Görgens, A.H.M., 1999. *Hydrological Modelling of the Limpopo River Main Stem*. Report by Department of Civil Engineering, University of Stellenbosch and Ninham Shand Consulting Engineers, to Department of Water Affairs & Forestry. DWAF Report No. PA000/00/0399.

Boroto, R.J. and Görgens, A.H.M., 2003. Estimating transmission losses along the Limpopo River: an overview of alternative methods. *International Association of Hydrological Sciences, Publication* **278**, 138-43.

Boroto, R.A.J., 2001. Limpopo River: steps towards sustainable and integrated water resource management. Regional Management of Water Resources. *International Association of Hydrological Sciences Publication* **268**, 33-38.

Botswana DWA (Department of Water Affairs), 1989. *Motloutse Dam Feasibility/ Preliminary Design Study: Hydrology Draft*. Sir M MacDonald and Partners, Cambridge, England. Accessed from http://resources.bgs.ac.uk/sadcreports/botswana1989macdonaldmotloutsedamhydrologyannexa.pdf on 24 March 2016.

Burkham, D.E., 1970. *Depletion of Streamflow by Infiltration in the Main Channels of the Tucson Basin, SE Arizona*. USGS. Water-supply Paper 1939-B.

Busari, O., 2008. Groundwater in the Limpopo Basin: occurrences, use and impact. *Environment, Development and Sustainability* **10**(6), 943-957.

BD (Business Dictionary). 2016. 'Uncertainty' Accessed from http://www.businessdictionary.com/definition/uncertainty.html on 12 September 2016.

Campbell, J.B. and Wynne, R.H., 2011. *Introduction to Remote Sensing*. The Guilford Press, New York. pp 3-7, 13-18.

CAR (Centre for Applied Research), 2005. *Draft Botswana Country Water Report*. Prepared for UN ECA as part of the prepapration of the African Water Development Report.

Cataldo, J., Behr, C., Montalto, F. and Pierce, R.J., 2005. *An Analysis of Transmission Losses in Ephemeral Streams: A Case Study in Walnut Gulch Experimental Watershed, Tombstone, Arizona.* Report to the National Centre for Housing and the Environment, USA.

Cataldo, J.C., Behr, C., Montalto, F.A. and Pierce, R.J., 2010. Prediction of Transmission Losses in Ephemeral Stream, Western U.S.A. *The Open Hydrology Journal* **4**, 19-34.

Chinoda, G., Moyce, W., Matura, N. and Owen, R., 2009. G*eology of the Limpopo River Basin: a contribution to the Challenge Program on Water and Food Project 17.* WaterNet Working Paper 7.

Coccia, G. and Todini, E., 2011. Recent developments in predictive uncertainty assessment based on the Model Conditional processor approach. *Hydrology and Earth System Sciences* **15**, 3253-3274.

Costa, A.C., Bronstert, A. and De Araújo, J.C., 2012. A channel transmission losses model for different dryland rivers. *Hydrology and Earth System Sciences* **16**(4), 1111-1135.

Costa, A.C., Foerster, S., de Araujo, J.C. and Bronstert, A., 2013. Analysis of channel transmission losses in a dryland river reach in north-eastern Brazil using streamflow series, groundwater level series and multi-temporal satellite data. *Hydrological Processes* **27**, 1046-1-60.

Costelloe, J.F., Grayson, R.B., McMahon, T.A. and Argent, R.M., 2003. Modelling the flow regime of an arid zone, fllodplain river, Diamantina River, Australia. *Environmental Modelling and Software* **18**, 693-703.

Council for Scientific and Industrial Research (CSIR)-Environmentek., 2003. *Protection and strategic uses of groundwater resources in drought prone areas of the SADC Region: Groundwater situation analysis of the Limpopo River Basin - Final Report*. Environmentek Report No. ENV-P-C 2003-026, Pretoria.

Cowie, R., 2014. Surface water and Groundwater interactions in Natural and Mining Impacted Mountain Catchments. *Unpublished PhD Dissertation*. University of Colorado, USA.

Dafalla, D.S., 2016. Artificial recharge to Alluvial Aquifer, Northeastern Nuba Mountains, Sudan. *International Journal of Research in Engineering and Science* **3**(1), 62-66.

Dahan, O., Tatarsky, B., Enzel, Y., Kulls, C., Seely, M., and Benito, G., 2008. Dynamics of flood water infiltration and ground water recharge in hyperarid desert *Ground Water* **46**, 450–46.

De Klerk, A.R. and De Klerk, L.P., 2011. *A Baseline Study of the Mokolo and Lephalala Rivers in the Waterberg Area*. Accessed from

https://researchspace.csir.co.za/dspace/bitstream/handle/10204/5417/De%20Klerk_2011.pdf?sequence=1

Dlamini, E.M., 2014. An Overview of the Limpopo River Basin Monograph Study. *Proceedings of the 17th South African Committee for the International Association of Hydrological Sciences*. 1st -3rd September 2014, Cape Town, South Africa.

DEA (Department of Environmental Affairs) National Landcover (TIFF) 2014 [Raster]. Accessed from https://egis.environment.gov.za/gis-data

De Hamer, W., Love, D., Owen, R., Booij, M.J. and Hoekstra, A.Y., 2008. Potential water supply of a small reservoir and alluvial aquifers system in southern Zimbabwe. *Physics and Chemistry of the Earth* **33**, 633-639.

De Wit, P.V., Cavaliere-Parzaneze, A., 1990. *Soils and land suitability of the Motloutse area between Mmadinare and Bobonong*. FAO/UNDP/Government of Botswana. Soil Mapping and Advisory Services Project AG: BOT/85/011, Field Document 6.

Dobos, E., Seres, A., Vadnai, P., Michéli, E., Fuchs, M., Láng, V., Bertóti, R.D. and Kovács, K., 2013. Soil parent material delineation using MODIS and SRTM data. *Hungarian Geographical Bulletin* **62** (2), 133–156.

Duan, Q., Gupta, V.K. and Sorooshian, S., 1992. Effective and efficient global optimization fro conceptual rainfall-runoff models. *Water Resources Research* **76**(3), 501-521.

Dunkerley D. and Brown K., 1999. Flow behaviour, suspended sediment transport and transmission losses in a small (sub-bank-full) flow event in an Australian desert stream. *Hydrological Processes* **13**, 1577-1588.

DWA (Department of Water Affairs), 2012. *Classification of Significant Water Resources in the Mokolo Catchment: Limpopo Water Management Area (Wma) and Crocodile (West) and Marico WMA WP 10506: Information Analysis Report: Mokolo and Matlabas catchments: Limpopo WMA*. Report No: RDM/WMA1,3/00/CON/CLA/0112B. Pretoria, South Africa.

DWAF (Department of Water and Forestry), 2010. *Hydrogeological assessment and Aquifer recharge Potential within the Lephalale (Ellisras) Local Municipality Area.* Report No. PWMA 01/A42/00/02209_0.

DWS (Department of Water Affairs, South Africa)., 2010. *Hydrogeological Assessment and Aquifer Recharge Potential within the Lephalale (Ellisras) Local Municipality Area*. Prepared by VSALEBOA Consulting. Report No. PWMA 01/A42/00/02209_01.

DWS (Department of Water and Sanitation, South Africa)., 2011. *Online Groundwater Dictionary: Second Edition*. Accessed 14 May 2015 on https://www.dwaf.gov.za/Groundwater/GroundwaterDictionary.aspx.

DWS (Department of Water and Sanitation)., 2016. *New Water Management Areas of South Africa*. Government Gazette No. 40279, 16 September 2016, 169-172. Accessed from http://www.gov.za/sites/www.gov.za/files/40279_gon1056.pdf on 17 January 2017.

DWS (Department of Water and Sanitation), 2017. *Limpopo province State of Dams on 2017-05-01*. Accessed from http://www.dwa.gov.za/Hydrology/Weekly/ProvinceWeek.aspx?region=LP on 03 May 2017.

Džubáková, K., 2010. Rainfall-Runoff Modelling: Its development, classification and possible applications. *Acta Geographica Universitatis Comeniaae* **54**(2), 173-181.

Elbeih, S.F., 2015. An overview of integrated remote sensing and GIS for groundwater mapping in Egypt. *Ain Shams Engineering Journal* **6(**1), 1-15.

Esterhuyse, S., 2012. *Geology of the Mokolo River. Specialist report for Centre for Environmental Management*. University of the Free State. WRC Project K5/1798. WRC Report No. TT579/13. Water Research Commission, Pretoria.

FAO (Food and Agriculture Organization of the United Nations), 2004. *Drought impact mitigation and prevention in the Limpopo River Basin: A situational analysis*. Land and water Discussion Paper 4. Rome, Italy.

Ferro, B.P., and Bouman, D., 1987. Hydrogeological map of Mozambique. Ministry of Construction and Water/UNICEF.

Freeze, R.A. and Cherry, J.A., 1979. *Groundwater*. Prentice-Hall, Englewood Cliffs, New Jersey, 604pp.

Gannon, J.M., and Vogelgesang, J.A., 2014. *Aquifer Characterization and Drought Assessment, Ocheyedan River Alluvial Aquifer*. Iowa Geological Survey – IIHR Hydroscience and Engineering. Water Resources Investigation Report No. 10.

GCBP-SRK (Groundwater Consultants Bee Pee (Pty) Ltd and SRK Consulting (Pty) Ltd., 2002. *Compilation of the Hydrogeological Map and Atlas for the SADC Region: Zimbabwe*.

Gonthier, G.J., 1998. *Quality of ground water in Pleistocene and Holocene Subunits of the Mississippi River Valley Alluival Aquifer*. Water resources Investigations Report 03-4202, National Water Quality Assessment Program, USGS.

Google Earth Pro 7.1.5.1557. March 27, 2016. Accessed via Google Earth Pro computer application © Google Inc. 2015.

Görgens, A.H.M., Beuster, H. and Hallifax, P., 1991. The Upper Limpopo: Flow generation in a very large semi-arid river basin. *Proceedings of the 5th South African Committee for the International Association of Hydrological Sciences*. 1st-4th November 1991, Stellenbosch, South Africa.

Görgens, A.H.M. and Boroto, R.A.J., 1997. Flow balance anomalies, surprises and implications for Integrated Water Resource Management. *Proceedings of the 8th SA Hydrological Symposium, SANCIAHS, Pretoria, South Africa*.

Görgens, A.H.M., Howard, G., Walker, N., Kleynhans, M. and Denys, F., 2014. Long-term surface water balance for the Limpopo Basin. *Proceedings of the 17th South African Committee for the International Association of Hydrological Sciences*. 1st -3rd September 2014, Cape Town, South Africa.

Gosain, A.K., Mani, A. and Dwivedi, C., 2009. *Hydrological Modelling-Literature Review*. Climawater, Report NO.1.

Goulden, M., Conway, D. and Persechino, A., 2009. Adaptation to climate change in international river basins in Africa: a review. *Hydrological Sciences Journal* **54**(5), 805-828.

GWP (Global Water Partnership), 2009. *A Handbook for Integrated Water Resources Management in Basins*. Global Water Partnership (GWP) and the International Network of Basin Organizations (INBO), 1-104.

GWP (Global Water Partnerships), 2014. *GWP Strategy Towards 2020: A Water Secure World*. GWP Secretariat, Sweden.

Hadjimitsis, D.G., Papadavid, G., Agapiou, A., Themistocleous, K., Retalis, A., Michaelides, S., Chrysoulakis, N., Toulios, L., and Clayton, C.R.I., 2010. Atmospheric correction for satellite remotely sensed data intended for hydrological cycle applications: impact on vegetation indices. *Natural Hazards and Earth System Sciences* **10**, 89–95.

Hameed, T., Marion, M.A. and Cheema, M.N., 1996. Time series modelling of channel transmission losses. *Agricultural Water Management* **29**(3), 283-298.

Hancock, P.J., 2002. Human impacts on the stream-groundwater exchange zone. *Environmental Management* **29**(6), 763-781.

Horning, N., 2004. *Selecting the appropriate band combination for an RGB image using Landsat imagery Version 1.0*. American Museum of Natural History, Center for Biodiversity and Conservation. Accessed from http://biodiversityinformatics.amnh.org. on 12 May 2016.

Howard, G., Denys, F., Walker, N. and Görgens, A., 2013. Volume C1- Surface Water Hydrology: Limpopo River BasinMS-81137945. Supplementary Report to Final Limpopo River Basin Monograph. Prepared for LIMCOM

Hughes, D.A., 1997. *Southern African "FRIEND"—The application of rainfall–runoff models in the SADC region*. WRC Report no. 235/1/97, Water Research Commission, Pretoria, South Africa.

Hughes, D.A., 2004. Incorporating ground water recharge and discharge functions into an existing monthly rainfall-runoff model. *Hydrological Science Journal* **49**(2), 297-311.

Hughes, D.A., 2004. Three decades of hydrological modelling research in South Africa. *South African Journal of Science* **100** (11-12), 638-642.

Hughes, D.A. (Ed)., 2005. *SPATSIM, an integrating framework for ecological reserve determination and implementation*. WRC Report No. TT 245/04. Water Research Commission, Pretoria, South Africa.

Hughes, D.A., 2005. Hydrological issues associated with the determination of environmental water requirements of ephemeral rivers. *River Research and Applications* **21**(8), 899-908.

Hughes, D.A., 2008a. *Modelling semi-arid and arid hydrology and water resources- The Southern African Experience*. Accessed from gwadi.org/sites/gadi.org/files/hughes_L5.pdf on 26 May 2015.

Hughes, D.A., 2008b. *Hydrological information requirements and methods to support the determination of environmental water requirements in ephemeral river systems*. Water Research Commission Report No. KV 205/08. Pretoria, South Africa.

Hughes, D.A., 2012. *Implementing uncertainty analysis in water resources assessment and planning*. Water Research Commission Project No. J5/2056, Deliverable No. 3. Water Research Commission, Pretoria, South Africa.

Hughes, D.A., 2013. A review of 40 years of hydrological science and practice in southern Africa using the Pitman rainfall-runoff model. *Journal of Hydrology* **501**, 111–124.

Hughes, D.A. and Sami, K. 1992. Transmission losses to alluvium and associated moisture dynamics in a semiarid ephemeral channel system in southern Africa. *Hydrological Processes* **6**, 45-53.

Hughes, D.A. and Metzler, W., 1998. Assessment of three monthly rainfall-runoff models for estimating the water resource yield of semiarid catchments in Namibia. *Hydrological Sciences Journal* **43**(2), 283-297.

Hughes, D. A., Hannart, P. and Watkins, D., 2003. Continuous baseflow separation from time series of daily and monthly streamflow data. *Water SA* **29**(1), 43–48.

Hughes, D.A. and Parsons, R.P., 2005. Improved explicit ground water recharge and discharge simulation methods for the Pitman model - explanation and example applications. *Proceedings of the 12th South African National Hydrology Symposium*, September 2005, Midrand, South Africa.

Hughes, D.A. and Forsyth, D.A., 2006. A generic database and spatial interface for the application of hydrological and water resource models. *Computers & Geosciences* **32** (9), 1389-1402.

Hughes, D., Andersson, L., Wilk, J. and Savenije, H.H.G., 2006. Regional calibration of the Pitman model for the Okavango River. *Journal of Hydrology* **331**(1-2), 30–42.

Hughes, D., Parsons, R. and Conrad, J., 2007. *Quantification of the Groundwater Contribution to Baseflow*. WRC Report No. 1498/1/07 ISBN 978-1-77005-583-4.

Hughes, D.A. and Mantel, S.K., 2010. Estimating uncertainties in simulations of natural and modified stream flow regimes in South Africa. In: E. Servat, *et al.*, eds. Global change—facing risks and threats to water resources, proceedings of the sixth friend world conference. Wallingford, UK: International Association of Hydrological Sciences, *IAHS Publication*. 340, 358–364.

Hughes, D.A., Kapangaziwiri, E. and Baker, K., 2010. Initial evaluation of a simple coupled surface and groundwater hydrological model to assess sustainable groundwater abstractions at the regional scale. *Hydrology Research* **41**(1), 1-12.

Hughes, D.A., Kapangaziwiri, E. and Sawunyama, T., 2010. Hydrological model uncertainty assessment in southern Africa. *Journal of Hydrology* 387(**3**), 221–232.

Hughes, D.A., Tshimanga, R.M., Tirivarombo, S. and Tanner, J., 2013. Simulating wetland impacts on stream flow in southern Africa using a monthly hydrological model. *Hydrological Processes* **28**(4), 1775–1786.

Hromdaka, T.V. and McCuen, R,H., 1988. Uncertainty estimated for surface runoff models. *Advances in Water Resources* **11**(1), 2-14.

IHP (International Hydrology Programme)., 1997. Rainfall–runoff modelling. Ch. 5 in, *Southern African FRIEND*, 94–129. International Hydrological Programme, IHP-V, Tech. Documents in Hydrology No. 15, UNESCO, Paris, France.

Ivkovic, K.M., 2009. A top–down approach to characterise aquifer–river interaction processes. *Journal of Hydrology* **365**(3), 145–155.

Jajarmizadeh, M., Harun, S. and Salarpour, M., 2012. A Review on Theoretical Consideration and Types of Models in Hydrology. *Journal of Environmental Science and Technology*, 1-13.

Jarihani, A.A., Larsen, J.R., Callow, J.N., McVicar, T.R. and Johansen, K., 2015. Where does all the water go? Partitioning water transmission losses in a data-sparse, multi-channel and low-gradient dryland river system using modelling and remote sensing. *Journal of Hydrology* **529**, 1511-1529.

Jarvis A, Reuter H.I., Nelson A. and Guevara E., 2008. Hole-filled SRTM for the globe. Version 4, available from the CGIAR-CSI SRTM 90 m Database. http://srtm.csi.cgiar.org.

Javed, A. and Wani, M.H., 2009. Delineation of groundwater potential zones in Kakund Watershed, Eastern Rajasthan, using Remote Sensing and GIS Techniques. *Journal Geological Society of India* **73**, 229-236.

Jordan P. R., 1977. Streamflow transmission losses in Western Kansas. Proceedings of the American Society of Civil Engineers. *Journal of the Hydraulics Division* **103** (HY8), 905-919.

JULBS (Joint Upper Limpopo Basin Study) Government of South Africa – Department of Water Affairs and Forestry (GOSA–DWAF)., 1991. *Joint Upper Limpopo Basin Study*. Pretoria, Ninham Shand/MacDonald and Partners.

Kapangaziwiri, E., 2008. Revised parameter estimation methods for the Pitman monthly rainfall-runoff model. *MSc Dissertation*, Rhodes University, Grahamstown, South Africa.

Kapangaziwiri, E. and Hughes, D.A., 2008. Towards revised physically-based parameter estimation methods for the Pitman monthly rainfall-runoff model. *Water SA* **32** (2), 183-191.

Kapangaziwiri, E., 2011. Regional application of the Pitman Monthly Rainfall-Runoff Model in southern Africa incorporating Uncertainty. *PhD Dissertation*, Rhodes University, Grahamstown, South Africa.

Kapangaziwiri, E., Hughes, D.A., Tanner, J.L. and Slaughter, A., 2011. Resolving uncertainties in the source of low flows in South African rivers using conceptual and modelling studies. Conceptual and modelling studies of integrated groundwater, surface water and ecological systems, *Proceedings of Symposium H01 held during IUGG 2011*, Melbourne, Australia, July 2011. *IAHS Publication* **345**, 127-132.

Kapangaziwiri, E., Hughes, D.A., and Wagener, T., 2012. Constraining uncertainty in hydrological predictions for ungauged basins in southern Africa. *Hydrological Sciences Journal* 57(**5**), 1000-1019.

Kapangaziwiri, E., Mwenge Kahinda, J., Mvandaba, V., Oosthuizen, N., Hobbs, P.J. and Hughes, D.A., 2017. Water Resources Assessment of the Limpopo River Basin Including Estimates of Uncertainty. Interim Report 4 of the WRC Project K5/2439/1: Upstream-downstream hydrological linkages in the Limpopo River Basin. Water Research Commission, Pretoria, South Africa.

Keshava, N., 2004. Distance metrics and band selection in hyperspectral processingwith applications to material identification and spectral libraries. *IEEE Transactions on Geoscience and Remote Sensing* **42** (7), 1552–1565.

Khan, M.A. and Moharana, P.C., 2002. Use of remote sensing and geographical system in the delineation and characterization of ground water prospect zones. *Journal of the Indian Society of Remote Sensing* **30**(3), 131-141.

Knighton A. D. and Nanson G. C., 1994. Flow transmission along an arid zone anastomosing river, Cooper Creek, Australia. *Hydrological Processes* **8**, 137-154.

Kulawardhana, R.W., Thenkabail, P.S., Vithanage, J., Biradar, C., Islam Md. A., Gunasinghe, S. and Alankara, R., 2007. Evaluation of the Wetland Mapping Methods using Landsat ETM+ and SRTM Data. *Journal of Spatial Hydrology* **7**(2), 62-96.

Kundu, P.M. Mathivha, F.I. and Nkuna, T.R., 2015. *The use of GIS and remote sensing techniques to evaluate the impact of land use and land cover changes on the hydrology of the Luvuvhu River Catchment in Limpopo Province*, WRC Report No. 2246/1/15 ISBN 978-1-4312-0705-3

Lane, L.J., Ferreira V. J. and Shirley E.D., 1980. Estimating transmission losses in ephemeral stream channels: Hydrology and Water Resources in Arizona and the South West. In: *Proceedings 1980 Meeting Arizona Section, A.W.R.A. and Hydrology Section Arizona Nevada Academy of Science*, 193-202.

Lange, J., 2005. Dynamics of transmission losses in a large arid stream channel. *Journal of Hydrology* **306**(1-4), 112-126.

Le Maitre, D.C., Scott, D.F. and Colvin, C., 1999. A review of information on interactions between vegetation and groundwater. *Water SA* **25** (2), 137-152.

LBPTC (Limpopo Basin Permanent Technical Committee)., 2010. Joint Limpopo River Basin Study Scoping Phase. Final Report. BIGCON Consortium.

Leonhard, L., Burton, K. and Milligan, N., 2013. Gascoyne River, Western Australia; Alluvial Aquifer, Groundwater Management and Tools. *Groundwater in the Coastal Zones of Asia-Pacific* **7**, 359-378.

Leopold, L.B. and Wolman, M.G., 1957. *River Channel Patterns: Braided, Meandering and Straight*. Physiographic and Hydraulic Studies of River, Geological Survey Professional Paper 282-B, United States Government Printing Office, Washington.

Lerner, D.N., 2002. Identifying and Quantifying Urban Recharge: A Review. *Hydrogeology Journal* **10**, 143-152.

Letcher, R.A., Croke, B.F.W. and Jakeman, A.J., 2007. Integrated assessment modelling for water resource allocation and management: A generalised conceptual framework. *Environmental Modelling & Software* **22**(5), 733-742.

Levick, S.R. and Rogers, K.H., 2011. Context-dependent vegetation dynamics in an African savanna, *Landscape Ecology* **26**, 515–528.

LIMCOM (Limpopo River Basin Commission), 2013. *Limpopo River Basin Monograph Study: Review of Potential Climate Change Impacts on the Limpopo River Basin: Supplementary Report to the Final Monograph*, LIMCOM.

Love, D., 2006. Alluvial aquifers in the Mzingwane Catchment: A preliminary report. Unpublished Report. Delft, The Netherlands, UNESCO-IHE.

Lorentz, S.A., Thornton-Dibb, S., Pretorius, J. and Goba, P., 2004. *Hydrological Systems Modelling Research Programme: Hydrological Processes, Phase II: Quantification of Hillslope, Riparian and Wetland Processes*. WRC Report No. K5/1061 and K5/1086. Water Research Commission, Pretoria.

Lorentz, S.A., Bursey, K., Idowu, O., Pretorius, J. and Ngeleka, K., 2007. *Definition and Upscaling of Key Hydrological Processes for Application in Models*. WRC Report No. K5/1320. Water Research Commission, Pretoria.

Love, D., Owen, R., Uhlenbrook, S., van der Zaag, P. and Moyce, W., 2007. *The lower Mzingwane alluvial aquifer: managed releases, groundwater- surface water interactions and the challenge of salinity*. Interim Paper for WaterNet.

Love, D., Uhlenbrook, S., Twomlow, S. and van der Zaag, P., 2010. Changing hydroclimatic and discharge patterns in the northern Limpopo Basin, Zimbabwe. *Water SA* **36**(3), 335-350.

Mabiza, C.C., Van der Zaag, P., Manzungu, E. and Ahlers, R., 2007. The making of a catchment plan: experiences of the Mzingwane Catchment, Zimbabwe. Accessed from www.waternetonline.ihe.nl/downloads/uploads/symposium/zambia-2007/ on 1 April 2017.

Magesh, N.S., Chandrasekar, N. and Soundranayagam, J.P., 2012. Delineation of groundwater potential zones in Theni district, Tamil Nadu, using remote sensing, GIS and MIF techniques. *Geoscience Frontiers* **3**(2), 189-196.

Maliva, R. and Missimer, T., 2012. *Arid Lands, Water Evaluation and Management*. Environmental Science and Engineering, Springer-Verlag Berlin, 153.

Mansell, M.G. and Hussey, S.W., 2005. An investigation of flows and losses within the alluvial sands of ephemeral rivers in Zimbabwe. *Journal of Hydrology* **314**, 192-203.

Maser, C., 2015. Interactions of Land, Ocean and Humans: A Global Perspective. *CRC Press*, 23pp.

Masike, S., 2007. The Impacts of Climate Change on Cattle Water Demand and Supply in Khurutshe, Botswana. *Unpublished PhD Dissertation*, International Global Change Institute, University of Waikato. New Zealand.

Masvopo, T.H., 2008. Evaluation of the Groundwater Potential of the Malala Alluvial Aquifer, Lower Mzingwane River, Zimbabwe. *Unpublished MSc dissertation,* University of Zimbabwe, Zimbabwe.

Masvopo, T., Love, D. and Makurira, H., 2008. *Evaluation of the groundwater-potential of the Malala Alluvial Aquifer, Lower Mzingwane River, Zimbabwe*. Paper presented at the 9th WaterNet/WARFSA/GWP-SA Annual Symposium, Johannesburg, South Africa, 29-31 October 2008. Amsterdam, Netherlands: WaterNet. Accessed from http://www.waternetonline.ihe.nl/challengeprogram /P57%20Masvopo%20Malala%20aquifer.pdf on 02 September 2015.

Maxwell, J. A., 2005. Qualitative research design: An interactive approach (2nd Ed.). *SAGE Publications*, California, USA.

Mazvimavi, D., Meijerink, A.M.I. and Stein, A., 2004. Prediction of base flows from basin characteristics, a case study from Zimbabwe. *Hydrological Sciences Journal* **49** (4), 703-715.

Mazvimavi, D., 2006. Assessment of Surface Water Resources of Zimbabwe and Guidelines for Planning, Zimbabwe National Water Authority.

McKenzie, R.S. and Craig, A.R., 2001. Evaluations of river losses from the Orange River using hydraulic modelling. *Journal of Hydrology* **241**, 62-69.

Meijerink, A.M.J., 1996. Remote sensing applications to hydrology: groundwater. *Hydrological Sciences Journal* **41**(4) 549-561.

Meijerink, A. M. J., Bannert, D., Batelaan, O., Lubczynski, M., and Pointet, T., 2007. *Remote sensing applications to groundwater*. IHP-VI, Series on Groundwater No.16, UNESCO.

Melching, C.S., Yen, B.C. and Wenzel, H.G., 1990. A reliability estimation in modelling watershed runoff with uncertainties. *Water Resources Research* **26**(10), 2275-2286.

Meyer, S. and Hill, M., 2013. *Volume C2- Groundwater Assessment: Limpopo River BasinMS-81137945*. Supplementary Report to Final Limpopo River Basin Monograph. Prepared for LIMCOM.

Middleton B.J. and Bailey A.K., 2009. Water Resources of South Africa, 2005 study. Water Research Commission Report Number TT 380/08, Water Research Commission, Pretoria, South Africa.

Midgley, D.C., Pitman, W.V. and Middleton. B.J., 1994. *Surface water resources of South Africa 1990, a user guide plus 6 volumes of data, appendices and map*. Water Research Commission Reports 298/1/94 to 298/6/94. Pretoria, South Africa.

Miles, M.B. and Huberman, A.M., 1994. *Qualitative data analysis: An Expanded Sourcebook*. SAGE Publications, California, United States of America, 338.

Millaresis , G. C. and Argialas, D.P., 2000. Extraction and Delineation of Alluvial Fans from digital Elevation Models and LandSat Thematic Mapper Images. *Photogrammetric Engineering and Remote Sensing* **66** (9), 1093-1101.

Miller, S. N., Guertin, D. P., and Goodrich, D. C. Deriving stream channel morphology using GIS-based watershed analysis: in Lyon, J.G. (Ed.) 2003. GIS for Water Resources and Watershed Management. Taylor and Francis, New York, 2003.

Mockler, E.M., O'Loughlin, F.E. and Bruen, M., 2016. Understanding hydrological flow paths in conceptual catchment models using uncertainty and sensitivity analysis. *Computers & Geosciences* **90**, 66-77.

Mohamed, A.E. 2014. Comparing Africa's Shared River Basins – The Limpopo, Orange, Juba and Shabelle Basins. *Universal Journal of Geoscience* **2** (7), 200-211.

Moore, A.E., 1988. Plant distribution and the evolution of the major river systems in southern Africa. *South African Journal of Geology* **91**(3), 346-349.

Morgan, C.S., 1996. The Application of Digital Terrain Models and a Geographical Information System in the Modelling of Flooding in the Nyl River Floodplain. *Unpublished MSc dissertation*, University of the Witwatersrand, Johannesburg, South Africa.

Moriasi, D.N., Arnold, J.G., Van Liew, M.W., bingner, R.L., Hamel, R.D. and Veith, T.L., 2007. Model Evaluation Guidelines for Systematic Quantification of Accuracy in Watershed Simulations. *Transactions of the American Society of Agricultural and Biological Engineers* **50**(3), 885-900.

Morin, E., Grodek, T., Dahan, O., Benito, G., Kulls, C., Jacoby, Y., Van Langenhove, G., Seely, M. and Enzel, Y., 2009. Flood routing and alluvial aquifer recharge along the ephemeral arid Kuiseb River, Nambia. *Journal of Hydrology* **368**, 262-275.

Mostert, A.C., McKenzie, R.S. and Crerar, S.E., 1993. A rainfall/runoff model for ephemeral rivers in an arid or semi-arid environment. *Proceedings of the 6th South African National Hydrological Symposium*, Pietermaritzburg, 219-224.

Moyce, W., Mangeya, P., Owen, R. and Love, D., 2006. Alluvial aquifers in the Mzingwane catchment: Their distribution, properties, current usage and potential expansion. *Physics and Chemistry of the Earth, Parts A/B/C* **31**(15), 988-994.

Mul, M. L., 2009. *Understanding Hydrological Processes in an Ungauged Catchment in sub-Saharan Africa*. PhD Dissertation, Delft University of Technology, The Netherlands. CRC Press/Balkema,

Mwelwa, E. M., 2004. The application of the monthly time step Pitman rainfall-runoff model to the Kafue River basin of Zambia. *Unpublished MSc Dissertation*, Rhodes University, Grahamstown, South Africa.

Mwenge Kahinda, J., Kapangaziwiri, E., Engelbrecht, F.A., Meissner, R. and Ashton, P.J., 2012. Implementing Integrated Catchment Management in the Limpopo River basin Phase 1: Situational assessment. *4th CSIR Biennial Conference: Real problems, relevant solutions, CSIR, Pretoria, 9-10 October 2012*.

Mwenge Kahinda, J., Meissner, R. and Engelbrecht, F.A., 2016. Implementing Integrated Catchment Management in the upper Limpopo River basin: A situational assessment. *Physics and Chemistry of the Earth, Parts A/B/C,* **93**, 104-118.

Nepal, S., 2012. *Evaluating Upstream-Downstream Linkages of Hydrological Dynamics in the Himalayan Region*. *Unpublished PhD Dissertation*, Friedrich Schiller University, Jena.

Nepal, S., Flügen, W. and Shrestha, A., 2014. Upstream-downstream linkages of hydrological processes in the Himalayan region. *Ecological Processes* **3** (19), 1-16.

Nord, M., 1985. *Sand rivers of Botswana, Phase 2*. Department of Water Affairs, Government of Botswana.

Osterkamp, W. R., and Lane, L. J., 2003. Ground-water recharge estimates in arid areas using channel morphology and a simulation model. *Elsevier: Amsterdam* **50**, 281-286.

Owen, R.J.S., Rydzewski, J. and Windram, A., 1989. *The Use of Shallow Alluvial Aquifers for Small Scale Irrigation: with reference to Zimbabwe*. Final Report of ODA Project R4239.

Owen, R.J.S., 1994. Water Resources for Small-scale Irrigation from Shallow Alluvial Aquifers in the Communal Lands of Zimbabwe. *Unpublished MPhil Thesis*. University of Zimbabwe.

Owen, R. and Dahlin, T., 2005. Alluvial aquifers at geological boundaries: geophysical investigations and groundwater resources. In Bocanegra, E., Hernandez, M and

Usunoff, E. (Eds.): *Groundwater and Human Development*. AA Balkema Publishers, 233-246.

Owen, R., Madari, N., 2009. Baseline Report on the Hydrogeology of the Limpopo Basin: Country Studies from Mozambique, South Africa and Zimbabwe. WaterNet Working Paper 7. WaterNet, Harare. Accessed from http://www.waternetonline.ihe.nl on 12 July 2015.

Owen, R. and Madari, N., 2010. *Hydrogeology of the Limpopo Basin: Country studies from Mozambique, South Africa and Zimbabwe*. WaterNet Working Paper 12.

Pafuri Rivercamp, 2009. Accessed from www.pafuri.co.za/knp_self_drive.php on 27 August 2017.

Parsons, A.J., Wainwright, J., Stone, P.M. and Abrahams, A.D., 1999. Transmission losses in rills on dryland. *Hydrological Processes* **13**, 2897-2905.

Parsons, R., 2004. *Surface water – groundwater interaction in a Southern African context*. Water Research Commission, Report No TT 218/03.

Pitman, W.V., 1973. A mathematical model for generating monthly river flows from meteorological data in South Africa. Johannesburg, South Africa: Hydrological Research Unit, University of the Witwatersrand, Report no. 2/73.

Pitman, W.V. and Kaakebeeke, J.P., 1991. WRSM90, Water Resources Simulation Model, User's Guide. Stewart Scott Inc., Sandton.

Prucha, R.H., Graham, D., Watson, M., Avenant, M.F., Esterhuyse, S., Joubert, A., Kemp, M., King, J., Le Roux, P., Redelinghuys, N., Rossouw, L., Rowntree, K., Seaman, M., Sokolic, F., Van Rensburg, L., Van der Waal, B., Van Tol, J. and Vos, T., 2016. MIKE-SHE integrated groundwater and surface water model used to simulate scenario hydrology for input to DRIFT-ARID: the Mokolo River case study. *Water SA* **42** (3), 384–398.

Reichert, P. and Borsuk, M.E., 2005. Does high forecast uncertainty preclude effective decision support? *Environmental Modelling Software* **20**, 991-1001.

Renard, K. G., 1970. *The hydrology of semiarid rangeland watersheds*. Report ARS-41-162, Agricultural Research Service, US Department of Agriculture, Washington, D.C.

Renard, K.G., Nichols, M.H., Woolhiser, D.A. and Osborn, H.B., 2008. A brief background on the U.S. Department of Agriculture. Agricultural Research Service Walnut Gulch Experimental Watershed. Water Resources, 44 (W05S02).

Renard, B., Kavetski, D., Kuczera, G., Thyer, M. and Franks, S.W., 2010. Understanding predictive uncertainty in hydrologic modelling: The challenge of identifying input and structural errors. *Water Resources Research* **46** (W05521).

RHP (River Health Programme), 2006. *State-of-Rivers Report: The Mokolo River System*. Department of Environmental Affairs and Tourism, Pretoria.

Robinson, S., 2006. Conceptual Modeling for Simulation: Issues and Research Requirements. *Proceedings of the 2006 Winter Simulation Conference*, 792-800.

SADC (Southern African Development Community), 2005. Regional Water Policy. Accessed from http://www.sadc.int/documents-publications/show/823 on 20 August 2015.

Sami, K., 1992. Recharge mechanisms and geochemical processes in a semi-arid sedimentary basin, Eastern Cape, South Africa. *Journal of Hydrology* **139** (1-4), 27-48.

Sami, K., 2006. *Technical documentation for surface-groundwater interaction for use in system models*. Draft report prepared for the Department of Water Affairs and Forestry, Pretoria, South Africa.

SARDC-ZERO (South African Research and Documentation Centre and Zimbabwe Regional Environmental Organisation), 2002. *Rapid Environmental Appraisal of the Limpopo River Basin*. Technical Report prepared for the SADC Water Sector, Zimbabwe.

Sawunyama, T., 2008. Evaluating uncertainty in water resources estimation in southern Africa: A case study of South Africa. *Unpublished PhD Dissertation*, Rhodes University, Grahamstown, South Africa.

Schulze, R.E., 2000. Modelling Hydrological Responses to Land Use and Climate Change: A Southern African Perspective. *Ambio* **29**(1), 12-22.

Sharma K. D. and Murthy J. S. R., 1994. Estimating transmission losses in an arid region. *Journal of Arid Environments* **26**, 209-219.

Sharp, A.L. and Saxton, K.E., 1962. Transmission Losses in Natural Stream Valleys. *Journal of the Hydraulics Division* **88** (5), 121-142.

Shentsis I., Meirovich L., Ben-Zvi A. and Rosenthal E., 1999. Assessment of transmission losses and groundwater recharge from runoff events in a wadi under shortage of data on lateral inflow, Negev, Israel. *Hydrological Processes* **13**, 1649-1663.

Shanafield, M. and Cook, P.G., 2014. Transmission losses, infiltration and groundwater recharge through ephemeral and intermittent streambeds: A review of applied methods. *Journal of Hydrology* **511**, 518-529.

Siebert, S., Burke, J., Faures, J. M., Frenken, K., Hoogeveen, J., Döll, P., and Portmann, F. T., 2010. Groundwater use for irrigation – a global inventory. *Hydrology and Earth Systems Sciences* **14**, 1863-1880.

Simmers, I., 2005. Hydrological Processes and Water Resource Management in Simmers, I. (Ed). 2005. *Understanding Water in a Dry Environment: Hydrological Processes in Arid and Semi-Arid Zones*. A.A. Balkema Publishers, 1-14.

Simmons, D.L. and Reynolds, R.J., 1982. Effects of Urbanization on base flow of selected south-shore streams, Long Island, New York. *Journal of the American Water Resources Association* **18**(5), 797-805.

Smakhtin, V.Y., 2001. Low-Flow Hydrology: A Review. *Journal of Hydrology* **240**, 147-186.

Smakhtin, V.Y. and Watkins, D.A., 1997. *Low-flow Estimation in South Africa*. Water Research Commission Report 494/1/97. Pretoria, South Africa

Sorman, A. U. and Abdulrazzak, M. J., 1993. Flood hydrograph estimation for ungaged wadis in Saudi Arabia. *Journal of Water Resources Planning and Management* **119**(1), 45-63.

Spatial Vision Innovations, 2015. Interaction between groundwater and surface water. Accessed from: http://gwhub.srw.com.au/how-does-groundwater-interact-environment-0 on 09 May 2016.

Stephenson, G.R. and Freeze, R.A., 1974. Mathematical simulation of subsurface flow contributions to snowmelt runoff, Reynolds Creek watershed, Idaho. *Water Resources Research* **10**(2), 284-294.

Tanner, J.L., 2013. Understanding and Modelling of Surface and Groundwater Interactions. *Unpublished PhD Dissertation*, Rhodes University, Grahamstown, South Africa.

Tanner, J.L. and Hughes, D.A., 2015. Surface water–groundwater interactions in catchment scale water resources assessments—understanding and hypothesis testing with a hydrological model, *Hydrological Sciences Journal* **60**(11), 1880-1895.

Telvari, A., 1997. Transmission losses in upstream catchments of arid zones. Proceedings of the 8th International Conference on Rainwater Catchment Systems, International Rainwater Catchment Systems Association, Tehran Iran, April 1997. Accessed from http://www.eng.warwick.ac.uk/ircsa/pdf/8th/0809_telvari.pdf on 4 November 2017.

Titus, R. and Rossouw, T., 2008. *Groundwater Reserve Determination Study for Mokolo (A42) Catchment*. Water Geosciences Consulting, Pretoria, South Africa.

Tshimanga, R.M., Hughes, D.A. and Kapangaziwiri, E., 2011. Initial calibration of a semi-distributed rainfall runoff model for the Congo River basin. *Physics and Chemistry of the Earth, Parts A/B/C* **36** (14), 761-774.

Tshimanga, R. M., 2012. Hydrological uncertainty analysis and scenario-based streamflow modelling for the Congo River Basin. *Unpublished PhD Dissertation*, Rhodes University, Grahamstown, South Africa.

Tumbo, M.H., 2014. Uncertainties in modelling hydrological responses in gauged and ungauged sub-basins. *Unpublished PhD Dissertation*, Rhodes University, Grahamstown, South Africa.

UN (United Nations)., 2015. World Economic Situation and Prospects 2015: Statistical Annex. United Nations, New York, 140.

USGS (United States Geological Survey)., 2015. LandSat 8 OLI Images collected between September 2015 and March 2016 from United States Geological Society (USGS) Global Visualization Viewer (GloVis) (https://glovis.usgs.gov/)

USGS (United States Geological Survey), 2016. Landsat 8 OLI (operational Land Imager) and TIRS (Thermal Infrared Sensor). Accessed from https://lta.cr.usgs.gov/L8 on 11 January 2017.

Vandas, S.J., Winter, T.C. and Battaglin, W.A., 2002. *Water and the Environment*. American Geological Institute in cooperation with Bureau of Reclamation, National Park Service, U.S. Army Corps of Engineers, USDA Forest Service, U.S. Geological Survey, ISBN: 0-922152-63-2.

Vaze, J., Jordan, P., Beecham, R., Frost, A. and Summerell, G., 2012. *Guidelines for rainfall-runoff modelling: towards best practice model application*. eWater CRC Ltd., Australia, 47pp.

Vivarelli, R. and Perera, B.J.C., 2002. *Transmission Losses in Natural Rivers and Streams – A Review. River Symposium Papers and Presentations*. River Festival Brisbane Pty Ltd, South Brisbane, Australia.

Vrugt, J.A., Gupta, H.V., Bouten, W. and Sorooshian, S., 2003. A Shuffled complex Evolution metropolis algorithm for optimization and uncertainty assessment of hydrological model parameters. *Water Resources Research* **39** (8), 1-18.

Walter, G.R., Necsoui, M. and McGinnis, R., 2012. Estimating Aquifer Channel Recharge Using Optical Data Interpretation. *Groundwater* **50** (1), 68-76.

Walters, M.O., 1990. Transmission losses in arid regions. *Journal of Hydraulic Engineering* **116** (1), 129-138.

Warner, R.F., 1984. Man's impact on Australian drainage systems. *Australian Geographer* **16** (2), 133-141.

Wikner, T., 1980. *Sand Rivers of Botswana: A Reconnaissance of the Major Sand Rivers*. Department of Water Affairs, Botswana and Swedish International Development Authority, Sweden.

Winker, R.D, Moore, R.D., Redding, T.E., Spittlehouse, D.L., Carlyle-Moses, D.E. and Smerdon, B.D., 2010. Hydrological Processes and Watershed Response. In Pike, R.G., Redding, T.E. and Moore, R.D., Winker, R.D. and K.D. Bladon (Eds). 2010. *Compendium of forest hydrology and geomorphology in British Columbia*. B.C. Min. For. Range, For. Sci. Prog., Victoria, B.C. and FORREX Forum for Research and Extension in Natural Resources, Kamloops, B.C. Land Management Handbook 66. Accessed at www.for.gov.bc.ca/hfd/pubs/Docs/Lmh/Lmh66.htm on 07 April 2016.

Winter, T.C., 1985. A Conceptual Framework for Assessing Cumulative Impacts on the Hydrology of Nontidal Wetlands. *Environmental Management* **12**(5), 605-620.

Winter, T.C., Harvey, J. W., Franke. O. L., and Alley, W. M., 1998. *Groundwater and surface water - A single resource*. U.S. Geological Survey Circular 1139. Accessed from https://pubs.usgs.gov/circ/circ1139/pdf/circ1139.pdf on 18 August 2017.

Wirkus, L. and Böge, V., 2006. Transboundary water management on Africa's international rivers and lakes: current state and experiences. In Scheumann, W. Neubert, S. (Eds.) *Transboundary Water Management in Africa*. Bonn: German Development Institute, 11-102.

WMO (World Meteorological Organisation)., 2012. *Limpopo River Basin: A Proposal to Improve the Flood Forecasting and Early Warning System*. Accessed from http://www.wmo.int/pages/prog/hwrp/chy/chy14/documents/ms/Limpopo_Report.pdf on 26 August 2015.

Xu, C., 2002. *Textbook of Hydrological Models*. Uppsala University, Sweden. Accessed from http://www.soil.tu-bs.de/lehre/Master.Unsicherheiten/2012/Lit/Hydrology_textbook.pdf on 13 April 2016.

Zhu, T. and Ringler, C., 2010. *Climate Change Implications for Water Resources in the Limpopo River Basin*. IFPRI Discussion Paper 00961.